VAPOR-LIQUID EQUILIBRIA IN BINARY HYDROCARBON-WATER SYSTEMS

By

Riki Kobayashi

A dissertation submitted in partial fulfillment
of the requirements for the degree of
Doctor of Philosophy in the
University of Michigan
1951

Committee in charge:

Professor D.L. Katz, Chairman
Professor R.R. White
Associate Professor L.O. Case
Associate Professor G.B. Williams
Assistant Professor C.M. Sliepcevich

Acknowledgment

I wish to gratefully acknowledge all those who so generously aided in the course of this investigation, especially to express my appreciation to:

Professor D.L. Katz, the Chairman of this doctoral committee, for his guidance in the work.

Professor Cedomir M. Sliepcevich for his assistance in the thermodynamic analysis of the data and the purchase of equipment.

Professor L.O. Case for his assistance in developing an understanding of the Phase Rule as applied to hydrocarbon-water systems.

Professor R.R. White and Professor G.B. Williams for their participation as members of this doctoral committee.

Mr. George A. Foster, Mr. Cleatis Bolen, and Mr. William E. Hines for their continual aid in solving the mechanical difficulties encountered.

Professor J.J. McKetta of the University of Texas for the use of unpublished data on the methane-water and ethane-water systems.

Dr. H.J. Aroyan, my laboratory partner.

The Stanolind Oil and Gas Company of Tulsa, Oklahoma for their generous fellowship grants in the years, 1947-1949.

The Phillips Petroleum Company of Bartlesville, Oklahoma for furnishing the propane.

Mrs. Ruth Lesko for handling the purchase of experimental materials and equipment.

Mrs. Kathyrn Michael and Miss Joanne Meredith for their help in the preparation of the manuscript.

My Family for their patience, encouragement, and financial assistance through the years.

TABLE OF CONTENTS

Subject	Page
Title Page	i
Acknowledgement	ii
Table of Contents	iv
List of Tables	vii
Table of Figures	ix
Statement of Problem	xii
Summary	xiii
Part I Vapor-Liquid Equilibria in Binary Hydrocarbon-Water Systems	
Introduction	1
Phase Rule and Its Relation to Experimental Procedure	4
Experimental Method	7
Presentation of Data	10
Phase Rule Analysis of the Propane-Water System	33
The Saturated Water Content of Hydrocarbon Gases and Liquids	43
Thermodynamic Analyis of the Solubility of Pure Light Hydrocarbons in Water at High Pressures and the Extrapolation of the Propane-Water Data to 10,000 Psi	52
Calculation of the Effect of Dissolved Hydrocarbon Gases on the Density of Water at High Pressures	74

TABLE OF CONTENTS (Cont.)

Subject	Page
Part I (cont.)	
The Interrelation of Minimum Solubility, Henry's Law, and the Volumetric Behavior of the Solute-Rich Phase ...	80
Part II Experimental Equipment, Procedures, and Techniques for the Determination of Propane-Water Vapor-Liquid Equilibria Relationships	
Experimental Equipment	86
Vapor-Liquid Equilibria Apparatus..	86
Analytical Train for the Propane-Rich Phases	88
Apparatus for the Analysis of the Water-Rich Phase	89
Pressurizing and Pressure Maintenance Unit	90
Experimental Measurements	96
Temperature Control and Measurement	96
Pressure Control and Measurement...	96
Analytical Weighings	97
Chemicals Used	98
Propane	98
Distilled Water	98
Mercury	98
Experimental Procedure	100
Charging and Equilibrating	100
Sampling and Analysis of the Propane-Rich Phases	101

TABLE OF CONTENTS (Cont.)

Subject	Page
Part II (Cont.)	
Sampling and Analysis of the Water-Rich Phase	107
Part III Appendix	
Laboratory Data and Sample Calculations ..	109
Propane-Rich Phases	109
Water-Rich Phase	111
Calibrations	117
Bibliography	123

LIST OF TABLES

Table No.	Subject	Page
I	Experimental Data in the 3-Phase Region: Concentration of Water in the Vapor Phase	14
II	Experimental Data in the 3-Phase Region: Concentration of Water in the Propane-Rich Liquid Phase	15
III	Experimental Data in the 3-Phase Region: Concentration of Propane in the Water-Rich Phase	16
IV	Smoothed Data in the 3-Phase Region for all Three Phases.	17
V	Experimental Data in the 2-Phase Region: Concentration of Water in the Propane-Rich Phases	18
VI	Experimental Data in the 2-Phase Region: Concentration of Propane in the Water-Rich Liquid Phase	20
VII	Graphically Smoothed Data in the 2-Phase Region: Concentration of Water in the Propane-Rich Phases	22
VIII	Graphically Smoothed Data in the 2-Phase Region: Concentration of Propane in the Water-Rich Phases	23
IX	Solubility of Methane in Water: Comparison of Graphically Smoothed Data with Thermodynamically Smoothed Values	63
X	Solubility of Ethane in Water: Comparison of Graphically Smoothed Data with Thermodynamically Smoothed Values	64
XI	Solubility of Propane in Water: Comparison of Graphically Smoothed Data with Thermodynamically Smoothed Values	65

LIST OF TABLES (Cont.)

Table No.	Subject	Page
XII	Modified Henry's Law Constants and Partial Molal Volumes of Dissolved Gases	67
XIII	(A): Composition of Natural Gas A	77
	(B): Solubility of Natural Gas A in Water	77
	(C): Comparison of Experimental and Calculated Densities of Water Saturated with Natural Gas A	77

TABLE OF FIGURES

Figure No.	Subject	Page
1	Vapor Pressure of the Propane-Water System in the 3-Phase Region	24
2	Concentration of Water in the Propane-Rich Phases in the 3-Phase Region	25
3	Concentration of Propane in the Water-Rich Liquid Phase in the 3-Phase Region	26
4	Concentration of Water in the Propane-Rich Phases in the 2-Phase Region Showing the Experimental Points Along Isotherms	27
5	Concentration of Propane in the Water-Rich Liquid Phase in the 2-Phase Region Showing Experimental Points Along Isotherms	28
6	Smoothed Plot of the Concentration of Water in the Propane-Rich Phases in the 2-Phase Region Along Isobars	29
7	Smoothed Plot of the Concentration of Propane in the Water-Rich Liquid Phase in the 2-Phase Region Along Isobars	30
8	Smoothed Plot of the Concentration of Propane in the Water-Rich Liquid Phase in the 2-Phase Region at Low Pressure	31
9	Equilibrium Vaporization Constants Between the Hydrocarbon-Rich Phases in the 3-Phase Region	32
10	Pressure-Temperature Projection for the Propane-Water System	39

TABLE OF FIGURES (Cont.)

Figure No.	Subject	Page
11	Temperature-Composition Diagrams for the Propane Water System at Several Pressures	40,41
12	An Isometric Drawing of the Pressure-Temperature-Composition Relations for the Propane-Water System	42
13	Water Content of Light Hydrocarbon Vapors and Liquids as a Function of Molal Volume along Isotherms (Calculated Points Shown)	49
14	Water Content of Light Hydrocarbon Vapors and Liquids as a Function of Molal Volume along Isotherms (For Even Values of Molecular Weight)	50
15	Composition of the Hydrocarbon-Rich Phase at the 3-Phase Critical for Light Hydrocarbon-Water Systems as a Function of the 3-Phase Critical Temperatures	51
16	Plots for the Determination of Constants in the Thermodynamic Equation for the Solubility of Methane in Water	68
17	Plots for the Determination of Constants in the Thermodynamic Equation for the Solubility of Ethane in Water	69
18, 18B	Plots for the Determination of Constants in the Thermodynamic Equation for the Solubility of Propane in Water	70,71
19	Modified Henry's Law Constants as a Function of Temperature for Pure Light Hydrocarbons, Hydrogen, and Nitrogen Dissolved in Water	72

TABLE OF FIGURES (Cont.)

Figure No.	Subject	Page
20	Partial Molal Volumes of Pure Light Hydrocarbons, Hydrogen, and Nitrogen Dissolved in Water	73
21	Experimental and Calculated Densities of Water Saturated with a Natural Gas	79
22	Minimum and Maximum Solubility for Henry's Law Constant Decreasing with Temperature	83
23	Minimum and Maximum Solubility for Henry's Law Constant Increasing with Temperature	84
24	Minimum Solubility for the Temperature Region of Maximum Henry's Law Constant	85
25	Flow Sheet of the Vapor-Liquid Equilibria Apparatus	92
26	Analytical Train for the Analysis of the Hydrocarbon-Rich Phases	93
27	Apparatus for the Analysis of the Water-Rich Liquid Phase	94
28	Pressurizing and Pressure Maintenance Unit	95
29	Compressibility Factor for Propane at Room Temperature Below Atmospheric Pressure	115
30	Henry's Law Constants for the Solubility of Propane in Water	116
31	Calibration Curve for the Copper-Constantan Thermocouples	120
32	Calibration Curve for the Upper Section of the Gas-Water Burette	121
33	Calibration Curve for the Lower Section of the Gas-Water Burette	122

STATEMENT OF PROBLEM

The objects of this investigation were:

(1) To obtain experimental vapor-liquid equilibria data for the binary system propane-water from the hydrate region to 300 deg. F. and pressures up to 3000 psi.

(2) To make a study of the phase relations for the propane-water system through the application of the experimental data and the phase rule.

(3) To study and correlate the available vapor-liquid equilibria data on hydrocarbon-water systems using the thermodynamic data of pure hydrocarbons wherever possible.

SUMMARY

Vapor-liquid equilibria data were obtained in the two and three-phase regions for the system Propane-Water at temperatures from 54 deg. F to 300 deg. F and pressures from 100 to 2800 psia. The system was studied with relative thoroughness, especially in the region surrounding 205.7 deg. F and 637 psia, the conditions at which the vapor phase and the propane-rich liquid phase become continuously identical.

Experimental data on the solubility of water in the propane-rich phases were obtained for the three-phase envelope, and in the two-phase region for isotherms of 100, 150, 190, 205.7, 230, 260, and 300 deg. F up to 2800 psia. The solubility of propane in water was determined experimentally in the three-phase region, and in the two-phase region for isotherms of 54, 100, 133, 190, 205.7, 230, 260, and 300 deg. F up to 2800 psia. The experimental data are presented graphically using pressure, temperature, and composition as variables. The graphical representation of the data illustrate clearly the relation of the volumetric properties of propane on the mutual solubilities of propane and water. Excepting at low pressures and high temperatures, the solubility of water

in propane is very low. The concentrations encountered were generally less than 5 mol per cent water in propane. The solubility of propane in liquid water was extremely low, never exceeding 0.07 mol per cent propane over the range of conditions covered in this experimental investigation.

A qualitative analysis of the phase relations for the complete propane-water system based on the Phase Rule of Willard Gibbs and the experimental data has been made.

A correlation showing the solubility of water in light hydrocarbon liquids and vapors as a function of temperature, molal volume, and the molecular weight to a lesser extent, has been developed. For complex hydrocarbon mixtures the water content can be predicted successfully in the vapor phase, in the hydrocarbon-rich liquid phase in the three-phase region at low pressures, and in the compressed hydrocarbon fluid phase. The limitations of this correlation, when applied to complex hydrocarbon-water systems, are discussed and are illustrated graphically.

A thermodynamic equation relating the solubility of a pure hydrocarbon in water to the partial volumetric properties of that hydrocarbon in the coexisting phases and the Henry's Law constant has been applied to the methane-water, ethane-water, and the propane-water systems.

The solubility of propane in water has been calculated from 3000 to 10,000 psi by the application of this equation to the experimental vapor-liquid equilibria data of the propane-water system below 3000 psi and the volumetric data of pure propane from 0 to 10,000 psi. The validity of the extrapolation is supported by the conclusions drawn from the thermodynamic study of the methane-water and the ethane-water systems. The partial molal volumes of the dissolved hydrocarbons obtained from this study have been applied to estimate the effect of dissolved hydrocarbons on the density of water.

Minimum and maximum isobaric solubilities of gases in water at high pressures are discussed qualitatively in relation to Henry's Law and the volumetric behavior of the solute-rich phase.

A detailed discussion of the experimental equipment, procedures, and techniques used in the determination of the propane-water vapor-liquid equilibria relationships is given.

PART I

VAPOR-LIQUID EQUILIBRIA IN BINARY HYDROCARBON-WATER SYSTEM

INTRODUCTION

The general purpose of this study is to contribute to the fundamental understanding of the subject of hydrocarbon-water vapor-liquid equilibria. The appearance of water with hydrocarbons in nature and in commercial processes is quite common. New processes and refinements in natural gas transmission and in petroleum production methods have increased the need for a thorough understanding of hydrocarbon-water systems.

Work on hydrocarbon-water phase relations was initiated by Scheffer in 1913. Studies were then made of the hexane-water (40) and the pentane-water (41) systems up to their respective 3-phase critical conditions. Hydrocarbon-water systems have been investigated more extensively in regard to the formation of gas hydrates (6), (17), (18), (34), (44), (48) than in regard to vapor-liquid equilibria. Lauhlere and Briscoe (24) and Deaton and Frost (13) determined the concentration of water in natural gas up to 100 deg. F and 600 psi in connection with natural gas dehydration processes. These data have been supplemented by those of Russell, Thompson, Vance, and Huntington (35) up to 2000 psi.

Sage, Lacey and co-workers have determined the dew-point compositions of the methane-water (30) and the

ethane-water (32) systems over a wide range of temperatures up to 10,000 psi. Sage and Lacey (33) have also determined the composition of water in the n-butane-water system in the butane-rich phases in the 3-phase region. Data on the water content of a natural gas saturated with water, and the solubility of a natural gas in water and in brine solutions up to 250 deg. F and 5000 psi have been presented by Dodson and Standing (14).

McKetta and Katz (28), (29) made an extensive study of the methane-n-butane-water system and developed general plots for the estimation of the solubility of water in hydrocarbon gases and liquids (28). Culberson, Horn, and McKetta (9) reported data on the solubility of ethane in water up to 1200 psi and for methane in water at 77 deg. F up to 10,000 psi. Culberson and McKetta (10) (11) have recently extended their data on the solubility of methane and ethane in water in the temperature range from 100 deg. F to 340 deg. F and up to 10,000 psi for both systems.

After a consideration of the existing data, a binary system, propane-water, was chosen so that fundamental studies and observations could be made on the behavior of hydrocarbon-water mixtures. The location of the 3-phase vapor-liquid-liquid region for the propane-water system along the

temperature scale, relative to other binary hydrocarbon systems, allows it to be studied much more completely.

This part covers the general subject of vapor-liquid equilibria in binary hydrocarbon systems, which includes the presentation and analysis of the experimental data obtained in this work. Part II is a detailed discussion of the experimental equipment, procedures, and techniques used in the determination of the propane-water vapor-liquid equilibria relationships. The laboratory data taken and the sample calculations are discussed in the Appendix, Part III.

PHASE RULE AND ITS RELATION TO EXPERIMENTAL PROCEDURE

The selection of the dependent and independent variables which are required to completely define an equilibrium system must be made in accordance with the requirements of the Phase Rule of Willard Gibbs. Within this limitation, the choice of dependent and independent variables are selected in relation to the information desired and to experimental convenience.

The Phase Rule of Willard Gibbs is simply stated as:

$$V = C - P + 2 \qquad (1)$$

where V = the degrees of freedom or the number of independent variables required to express the phase equilibria,

C = the number of components, propane and water in the present case,

P = the number of coexisting equilibrium phases.

For a binary system with 3 coexisting phases V = 1. It follows then that the dependent variables concerning vapor-liquid equilibria may be expressed uniquely in terms of a single independent variable. If T is chosen as the independent variable, the following functions suffice to describe the system completely, as far as vapor-liquid equilibria are concerned:

$$P = f_1(T) \qquad (2)$$

$$x_2 = f_2(T) \qquad (3)$$

$$y_1 = f_3(T) \qquad (4)$$

$$z_1 = f_4(T) \qquad (5)$$

in which T = temperature,

P = pressure,

x_2 = mol fraction hydrocarbon in the water-rich liquid phase,

y_1 = mol fraction of water in the vapor phase, and

z_1 = mol fraction of water in the propane-rich or lighter liquid phase.

Thus, setting the temperature of the cell, injecting propane and water into it in quantities that will produce 3-phases, and agitating the mixture until equilibrium is reached will produce unique values of pressure and phase concentrations. The latter are determined by sampling and analyzing the phases. The 3-phase region terminates at the 3-phase critical where the vapor phase and the propane-rich liquid phase become continuously identical.

For the coexistence of 2 phases, since $V = 2$, the variables in which we are interested may be expressed by:

$$x_2 = f_5(T,P) \qquad (6)$$

$$y_1 = f_6(T,P) \qquad (7)$$

$$z_1 = f_7(T,P) \qquad (8)$$

where the variables are defined as before, realizing that $y_1 = f_6(T,P)$ is continuous with $z_1 = f_7(T,P)$ along isotherms for T greater than the 3-phase critical temperature, 205.7 deg. F, and along isobars for P greater than the 3-phase critical pressure, 637 psia. To determine the compositions experimentally, the cell temperature was set

at a selected isotherm, the cell charged with water, and propane added to the desired pressure with the existence of two phases. The mixture was then equilibrated, and the coexisting phases sampled and analyzed to give the equilibrium relationship. In this case, the cell pressure, as well as the temperature, must be controlled by adding the proper amount of propane and water.

EXPERIMENTAL METHOD

This vapor-liquid equilibria study was conducted using a batch operation. Propane and water were placed in a pressure cell surrounded by a thermostatically controlled bath and brought to phase equilibrium by mechanical agitation. The resulting equilibrium phases were sampled under equilibrium conditions. Mercury was injected into the cell to maintain the equilibrium within the cell during the sampling of all phases except the vapor phase in the three-phase region. In the three-phase region, the vapor phase was sampled from the cell with the stirrer running, but without mercury injection. The cell was equipped with a glass window which was used to detect the number and quantities of the coexisting phases.

The samples were transferred directly from the cell to the analytical apparatus through small diameter steel tubing. High pressure pycnometers were used for the first few runs in an attempt to obtain the phase densities as well as the phase compositions. Their use was discarded in order to obtain more accurate analytical results and to permit adjustment of sample sizes with varying conditions. Since the mutual solubilities of propane and water are generally very small, the phase densities must be observed by more refined techniques than high pressure pycnometers will permit, to be of any value.



The use of pycnometers to determine the phase densities of the hydrocarbon-rich phases in binary hydrocarbon-water systems in the three-phase region is entirely impossible because of the similarity of the behavior of these phases in the three-phase region to that of the saturated liquids and vapors of the pure hydrocarbons.

In the sampling operation each phase was sampled through a different port, appropriately located in the own phase, in order to avoid contamination of the sample lines by a second phase. The vapor sample lines were heated above the equilibrium temperature to prevent the condensation of the vapor in the sample lines and the resulting loss of water from the sample during the transfer through the lines.

The hydrocarbon-rich phases were analyzed by absorbing the water from the expanded gas with Dehydrite (magnesium perchlorate) and measuring the corresponding amount of dehydrated gaseous propane. The necessary precautions for the handling and weighing of the U-tubes were observed. The compressibility factors of propane gas at atmospheric and lower pressures were applied in the calculation of the final phase compositions.

The water-rich liquid phase was analyzed by measuring the volumes of liquid and gas formed by an equilibrium flash expansion conducted at substantially room temperature and at one atmosphere. The dissolved propane remaining

in the flash liquid was computed using the solubility data of propane in water at atmospheric pressure (25) and the Henry's Law Constants obtained from the thermodynamic calculations on the propane-water system, pp. 57. The vapor pressure data of water was used to correct for the water vapor present in the equilibrium flash vapor. A material balance of the propane and water made on the overall sample yielded the final composition of the sample.

For any given isotherm, the pressures at which the runs were made were determined from the trend suggested by previously obtained data.

The detailed discussion of the experimental equipment, procedures and techniques used in this vapor-liquid equilibria study are presented in Part II and the sample calculations are presented in Part III, the Appendix.

PRESENTATION OF EXPERIMENTAL DATA

Experimental vapor-liquid equilibria data for the propane-water system are presented in the 3-phase region from 54 deg. F to the 3-phase critical of 205.7 deg. F and 637 psia in Tables 1, 2, 3 and Figures 1, 2, 3. Vapor-liquid equilibria data in the 2-phase region from 100 to 2800 psia are presented at isotherms of 100, 150, 190, 205.7, 230, 260, and 300 deg. F for the propane-rich phases in Table 5 and Figure 4, and at isotherms of 54, 100, 133, 190, 205.7, 230, 260, and 300 deg. F for the water-rich phase in Table 6 and Figure 5.

The Solubility of Water in the Hydrocarbon-Rich Phases

In the 3-phase region, the solubility of water in the propane-rich phase and in the vapor phase describes a continuous envelope, Figure 2, which closes at the 3-phase critical conditions where the composition and the other intensive properties of the two phases become continuously identical. In this region, both the solubility of water in the propane-rich phase and the volumetric properties of that phase are very sensitive functions of pressure and temperature.

In the 3-phase region, the highest equilibrium ratio, K, of the concentration of water in the vapor to the concentration of water in the equilibrium propane-rich liquid, Figure 9, occurs at the lowest temperature.

The ratio becomes 1.0 at the 3-phase critical condition of 205.7 deg. F and 637 psia.

A study of Figure 4 combined with an understanding of the volumetric behavior of pure constituents in their critical regions indicate that the solubility of water in the propane-rich phases is related to the temperature and the volumetric behavior of the propane-rich phases. Thus, the isotherms of the propane-rich phase relating solubility to pressure and the isotherms relating the volumetric behavior of the same phase to pressure are both discontinuous below 205.7 deg. F, but continuous at that and higher temperatures.

Raoult's Law (26) predicts the isotherm on a log concentration versus log pressure plot at a given temperature to be a line of slope -1 passing through the point representing the vapor pressure of pure water at that temperature. The dotted lines, Figure 4, indicate portions of the ideal isotherms predicted by Raoult's Law. These ideal isotherms have been used whenever appropriate to aid in drawing the "best curve" through the experimental points and to extrapolate the data. The data indicates both positive and negative deviations from the law, both in the vapor and propane-rich liquid phases.

Figure 6 shows a plot of water concentration as a function of temperature along several isobars ranging from 100 psia to 3000 psia. The vapor pressure data for pure

water has been used to develop Figure 6 from Figure 4. The greatest inaccuracies in the cross-plot, Figure 6, are expected to occur in the 3-phase critical region where the concentration change with respect to pressure and temperature is greater than for other regions.

The Solubility of Propane in Water

Figure 5 presents the data on the solubility of propane in water. The isotherms are shown from 54 to 300 deg. F. The solubility of propane in water in the 3-phase region is shown as a concaved curve, showing a minimum at about 250 psia, on which the discontinuities of the isotherms below 205.7 deg. F occur. The 3-phase solubility locus terminates at that temperature, the 3-phase critical temperature. The solubility isotherms are continuous functions of pressure at and above 205.7 while the solubility isobars, Figure 7, are continuous functions of temperature at and above 637 psia, the 3-phase critical pressure.

As in the case of the solubility of water in the propane-rich phases, the solubility of propane in the water-rich phase is associated with the volumetric properties of the propane-rich phase. Thus, the continuity and discontinuity in the isothermal and isobaric solubility curves above and below the 3-phase critical condition are related to the continuity and discontinuity

of the volumetric behavior of the propane-rich phases along the corresponding isotherms and isobars. The effect of pressure upon the solubility of propane in water is directly related to the effect of pressure on the volumetric behavior of the coexisting propane-rich phase. If the compressibility of the propane-rich phase is high, e.g., that of a gas, the effect of the pressure on the solubility of propane in water is high. A low compressibility, e.g., that of a liquid, is marked by a small effect of pressure on the solubility. These relations are quantitatively revealed in the section entitled "Thermodynamic Analysis of the Solubility of Hydrocarbon in Water at High Pressures," pp 52 .

To preserve the clarity of Figure 5, some of the isotherms for temperatures greater than 170°F at low pressures have been ommitted. An expanded plot of this region, Figure 8, has been prepared to present all the isotherms determined experimentally in this region.



TABLE I

Experimental Data in the 3-Phase Region:
Concentration of Water in the Vapor Phase

Temperature °F	Pressure psia	Composition of the Vapor Phase Mol Fraction Water
63.0	113.8	.002322
64.1	114.6	.002370
83.1	151.8	.003582
87.0	159.7	.003708
102.5	195.0	.004855
111.6	220	.00552
111.8	220	.00549
127.7	270	.00696
128.2	271	.00696
144.1	328	.00854
144.1	328	.00863
170.0	437	.01097
179.0	488	.01175
179.2	487	.01177
187.6	529	.01263
188.6	535	.01278
190.3	540	.01282
192.8	561	.01282
193.0	562	.01270
201.6	613	.01212
201.7	612	.01208

TABLE II

Experimental Data in the 3-Phase Region: Concentration of Water in the Propane-Rich Liquid Phase

Temperature °F	Pressure psia	Composition of the Propane-Rich Liquid Phase Mol Fraction Water
58.4	107.1	.0001368
78.5	142.5	.0003340
78.7	142.5	.0003403
101.9	195.0	.000614
101.9	195.6	.000626
128.5	272	.001368
128.8	271	.001378
144.6	330	.001995
170.0	438	.003555
171.0	443	.003682
188.6	535	.00542
191.4	551	.00605
191.6	549	.00544
195.6	572	.00659
201.7	611	.00764
202.1	612	.00769
* 205.4	633	.01001
* 206.1	638	.00995

* Critical Region

TABLE III

Experimental Data in the 3-Phase Region: Concentration of Propane in the Water-Rich Liquid Phase

Temperature °F	Pressure psia	Composition of the Water-Rich Liquid Phase Mol Fraction Propane
* 42.3	82.2	.000366
53.9	101	.0002913
78.1	142	.0002208
79.1	143	.0002208
100.2	191	.00002045
100.6	191	.0002001
132.9	284	.0002046
137.7	300	.0002003
154.2	366	.0002063
160.3	391	.0002107
172.2	446	.0002298
179.7	482	.0002360
189.6	538	.0002495
191.1	543	.0002489
201.7	608	.0002638
205.4	632	.0002726

* Quadruple point by extrapolation.

TABLE IV

Smoothed Data in the 3-Phase Region
for all Three Phases

Temperature	Pressure	Composition		
°F	psia	M.F. Water in the Vapor Phase	M.F. Water in the Propane-Rich Liquid Phase	M.F. Propane in the Water-Rich Liquid Phase
42.3	82.2	.00140	.000105	.000366
60.0	108.5	.00218	.000187	.000264
80.0	146.0	.00335	.000344	.000219
100.0	191.5	.00465	.000615	.000203
120	246	.00625	.00109	.000199
140	311	.00813	.00184	.000202
160	389	.01002	.00291	.000212
170	432	.01097	.00358	.000223
180	483	.01191	.00446	.000236
190	538	.01280	.00558	.000250
195	568	.01278	.00632	.000256
200	602	.01237	.00723	.000264
* 205.7	637	.00998	.00998	.000272

* 3-Phase Critical.

TABLE V

Experimental Data in the 2-Phase Region: Concentration of Water in the Propane-Rich Phases

Temperature °F	Pressure psia	Composition of the Propane-Rich Phase, Mol Fraction Water
100	102	.00954
100	141	.00696
100	533	.00492
100	818	.000587
100	1015	.000673
100	2018	.000540
100	2023	.000643
100	2798	.000591
100	2798	.000623
150	146	.02649
150	217	.01702
150	289	.01200
150	856	.002328
150	1564	.002224
150	2484	.002060
150	2803	.002046
190	190	.04967
190	309	.02910
190	465	.01722
190	1342	.00502
190	2003	.00475
190	2803	.00463
205.7	207	.0637
205.7	445	.02639
205.7	603	.01568
205.7	637	.00998
205.7	696	.00813
205.7	755	.00779
205.7	1217	.00726
205.7	2023	.00674
205.7	2803	.00640

TABLE V (Con't)

Experimental Data in the 2-Phase Region: Concentration of Water in the Propane-Rich Phases

Temperature °F	Pressure psia	Composition of the Propane-Rich Phases, Mol Fraction Water
230	252	.08094
230	446	.04325
230	630	.02659
230	718	.02028
230	823	.01366
230	1530	.01033
230	2023	.00959
230	2704	.00919
260	439	.07856
260	675	.04660
260	812	.03599
260	996	.02499
260	1411	.01843
260	2023	.01646
260	2023	.01649
260	2755	.01490
300	622	.10146
300	928	.06350
300	1217	.04496
300	1441	.03875
300	2023	.03105
300	2803	.02684

TABLE VI

Experimental Data in the 2-Phase Region: Concentration of Propane in the Water-Rich Liquid Phase

Temperature °F	Pressure psia	Composition of the Water-Rich Liquid Phase Mol Fraction Propane
54.0	617	.0002963
54.0	617	.0003029
54.0	1222	.0002906
54.0	1988	.0002948
100	72	.0000863
100	117	.0001552
100	428	.0002046
100	622	.0002175
100	1531	.0002151
100	2012	.0002239
100	2687	.0002304
133.0	188	.0001499
133.0	1199	.0002249
133.0	1810	.0002267
133.0	2787	.0002364
170	181	.0001146
170	307	.0001763
190	131	.0000796
190	224	.0001330
190	359	.0001960
190	990	.0002580
190	1523	.0002703
190	2012	.0002745
190	2787	.0002880

TABLE VI (cont'd)

Experimental Data in the 2-Phase Region:
Concentration of Propane in the Water-Rich
Liquid Phase

Temperature °F	Pressure psia	Composition of the Water-Rich Liquid Phase Mol Fraction Propane
205.7	230	.0001261
205.7	400	.0002162
205.7	478	.0002449
205.7	910	.0002842
205.7	1810	.0003008
205.7	2787	.0003134
230	222	.0001301
230	504	.0002633
230	810	.0003243
230	1128	.0003415
230	1810	.0003542
230	2787	.0003765
260	170	.0001001
260	332	.0001964
260	511	.0002892
260	751	.0003665
260	1232	.0004197
260	1810	.0004393
260	2787	.0004766
300	265	.0001666
300	471	.0003031
300	694	.0004130
300	987	.0004876
300	1565	.0005801
300	1810	.0006078
300	2787	.0006861

TABLE VII

Graphically Smoothed Data in the 2-Phase Region: Concentration of Water in the Propane-Rich Phases

Pressure psia	Temperature °F								
	100	130	160	190	205.7	220	250	280	310
	Mol Fraction Water in the Propane-Rich Phases								
100	.00979	.02360	.0505	.0962	.1330	.1742	.2999	.4920	.7727
200	.000605	.01104	.02382	.04678	.0647	.0853	.1489	.2449	.3837
300	.000605	.00139	.01500	.03034	.04246	.0562	.0984	.1618	.2547
400	.000604	.001380	.002911	.02123	.03034	.04083	.0726	.1205	.1892
500	.000604	.001374	.002877	.01503	.02218	.03041	.0552	.0931	.1489
600	.000604	.001365	.002838	.005507	.01563	.02254	.04935	.0764	.1222
637	.000603	.001361	.002829	.00547	.00998	.01941	.04065	.0711	.1146
700	.000603	.001358	.002819	.00542	.00815	.01486	.03622	.0637	.1030
800	.000602	.001355	.002799	.00535	.00782	.01124	.02898	.0540	.0887
900	.000601	.001352	.002773	.00527	.00767	.01001	.02323	.04581	.0778
1000	.000600	.001349	.002760	.00521	.00752	.00964	.01897	.03917	.0687
1250	.000598	.001340	.002729	.00509	.00705	.00933	.01563	.02992	.0515
1500	.000597	.001327	.002698	.004978	.00703	.00895	.01455	.02642	.04405
2000	.000596	.001321	.002655	.004809	.00665	.00845	.01370	.02280	.03642
3000	.000594	.001315	.002600	.004571	.00619	.00787	.01265	.02009	.03112

TABLE VIII

Graphically Smoothed Data in the 2-Phase Region:
Concentration of Propane in the Water-Rich
Phase

Pressure psia	Temperature °F									
	60	100	130	160	190	205.7	220	250	280	310
	Mol Fraction Propane in the Water-Rich Phase									
100	.0002573	.0001273	.0000876	.0000698	.0000609	.0000582	.0000562	.000513	.0000415	.0000220
200	.0002670	.0002045	.0001603	.0001303	.0001197	.0001172	.0001180	.0001170	.0001160	.0001147
300	.0002679	.0002060	.0002003	.0001782	.0001700	.0001696	.0001708	.0001768	.0001857	.0001923
400	.0002687	.0002076	.0002043	.0002138	.0002107	.0002132	.0002173	.0002307	.0002480	.0002677
500	.0002696	.0002091	.0002075	.0002210	.0002400	.0002468	.0002550	.0002757	.0003000	.0003277
600	.0002703	.0002106	.0002090	.0002261	.0002530	.0002680	.0002798	.0003107	.0003453	.0003803
637	.0002706	.0002112	.0002108	.0002271	.0002550	.0002723	.0002878	.0003222	.0003602	.0004007
700	.0002711	.0002122	.0002124	.0002295	.0002578	.0002767	.0002952	.0003375	.0003825	.0004290
800	.0002717	.0002137	.0002145	.0002319	.0002602	.0002815	.0003053	.0003562	.0004087	.0004627
900	.0002722	.0002152	.0002164	.0002341	.0002623	.0002846	.0003115	.0003695	.0004287	.0004886
1000	.0002728	.0002166	.0002182	.0002358	.0002642	.0002865	.0003155	.0003787	.0004444	.0005133
1500	.0002748	.0002221	.0002228	.0002415	.0002715	.0002957	.0003257	.0003995	.0004927	.0006160
2000	.0002760	.0002264	.0002276	.0002462	.0002783	.0003043	.0003357	.0004144	.0005246	.0006858
2500	.0002768	.0002287	.0002307	.0002507	.0002835	.0003116	.0003445	.0004293	.0005502	.0007332
3000	.0002775	.0002302	.0002355	.0002542	.0002877	.0003160	.0003525	.0004442	.0005753	.0007703

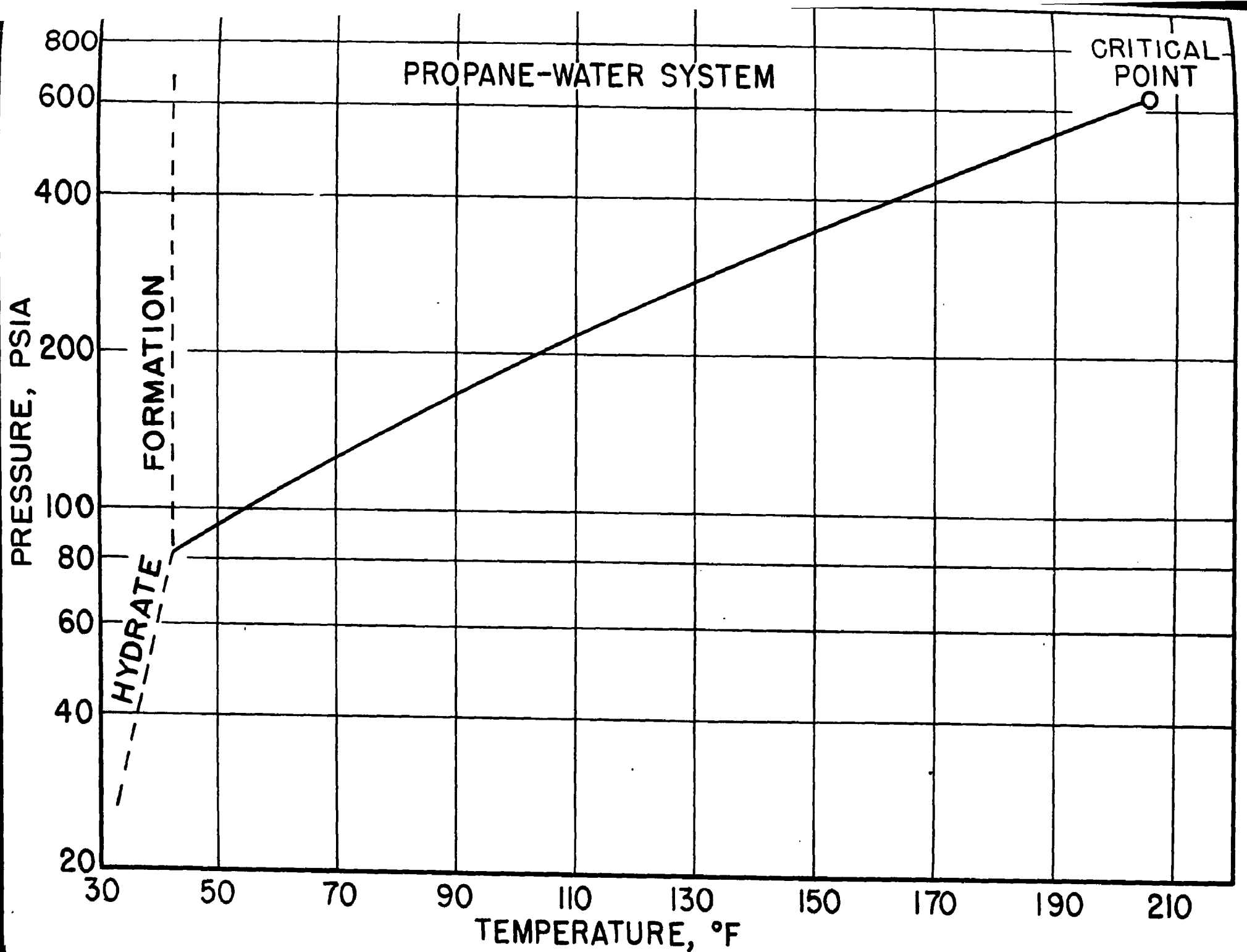


FIGURE 1 VAPOR PRESSURE OF THE PROPANE-WATER SYSTEM IN THE 3-PHASE REGION

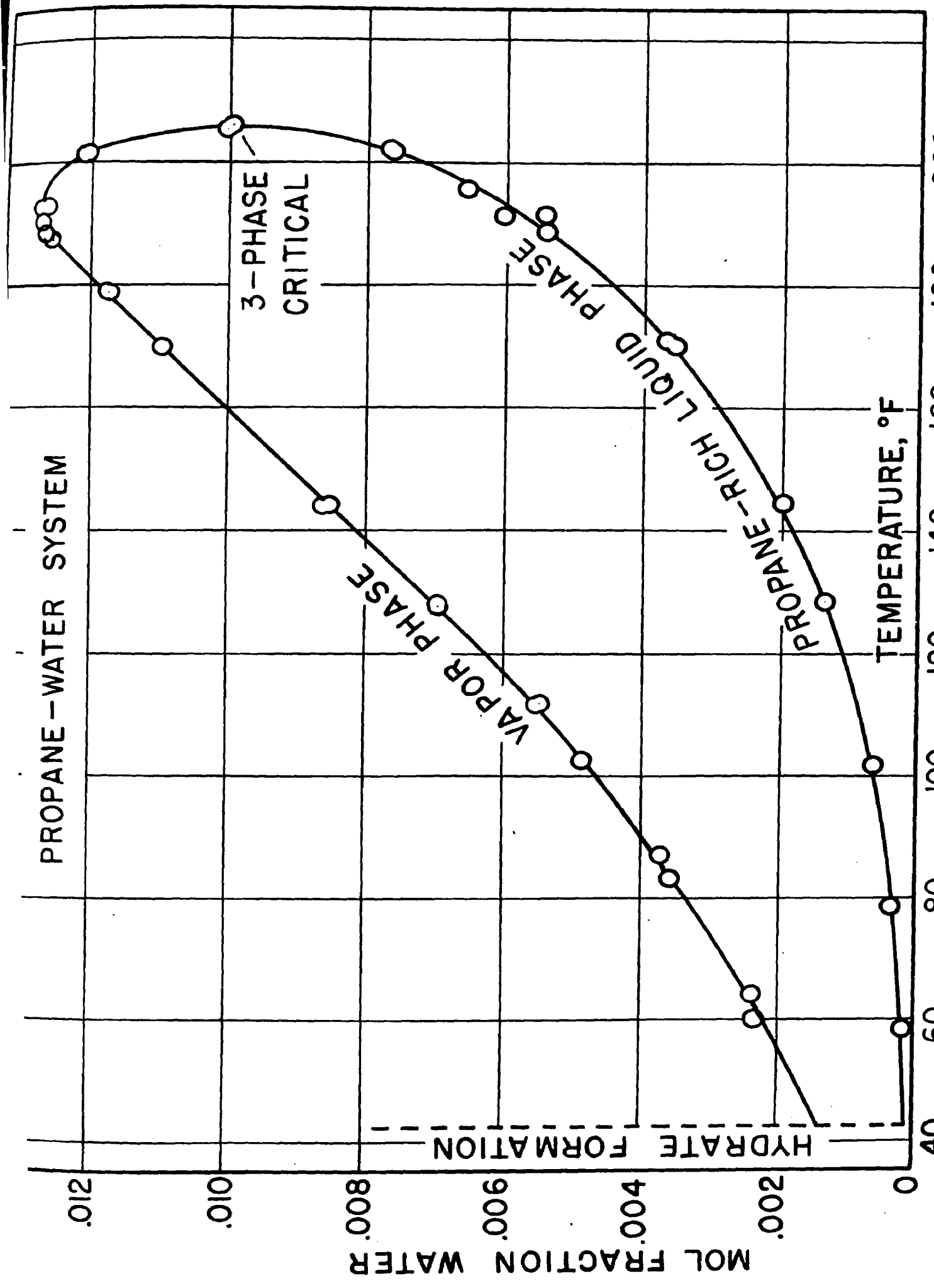


FIGURE 2 CONCENTRATION OF WATER IN THE PROPANE–RICH PHASES IN THE 3–PHASE REGION

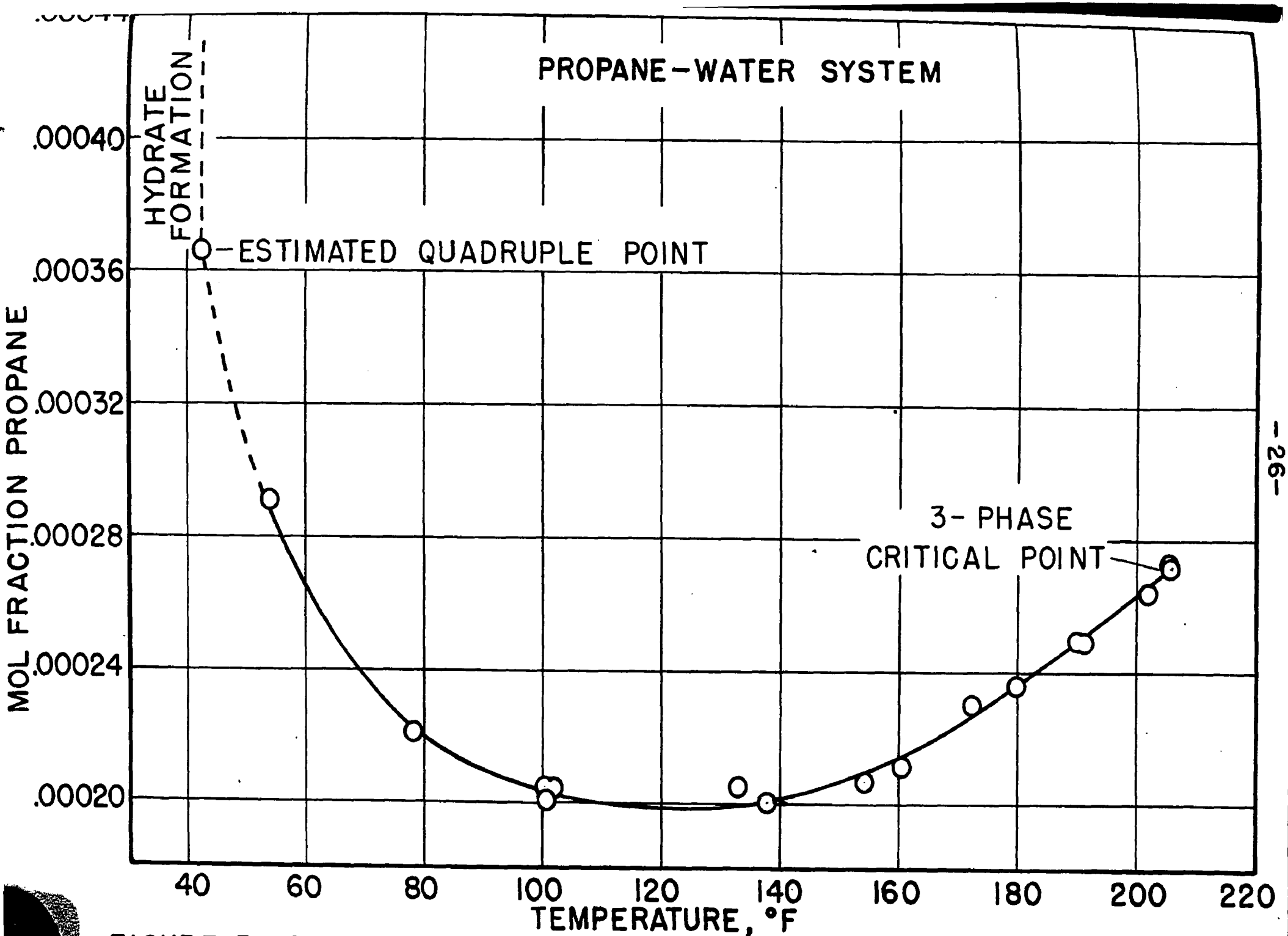


FIGURE 3 THE CONCENTRATION OF PROPANE IN THE WATER-RICH PHASE IN THE 3-PHASE REGION

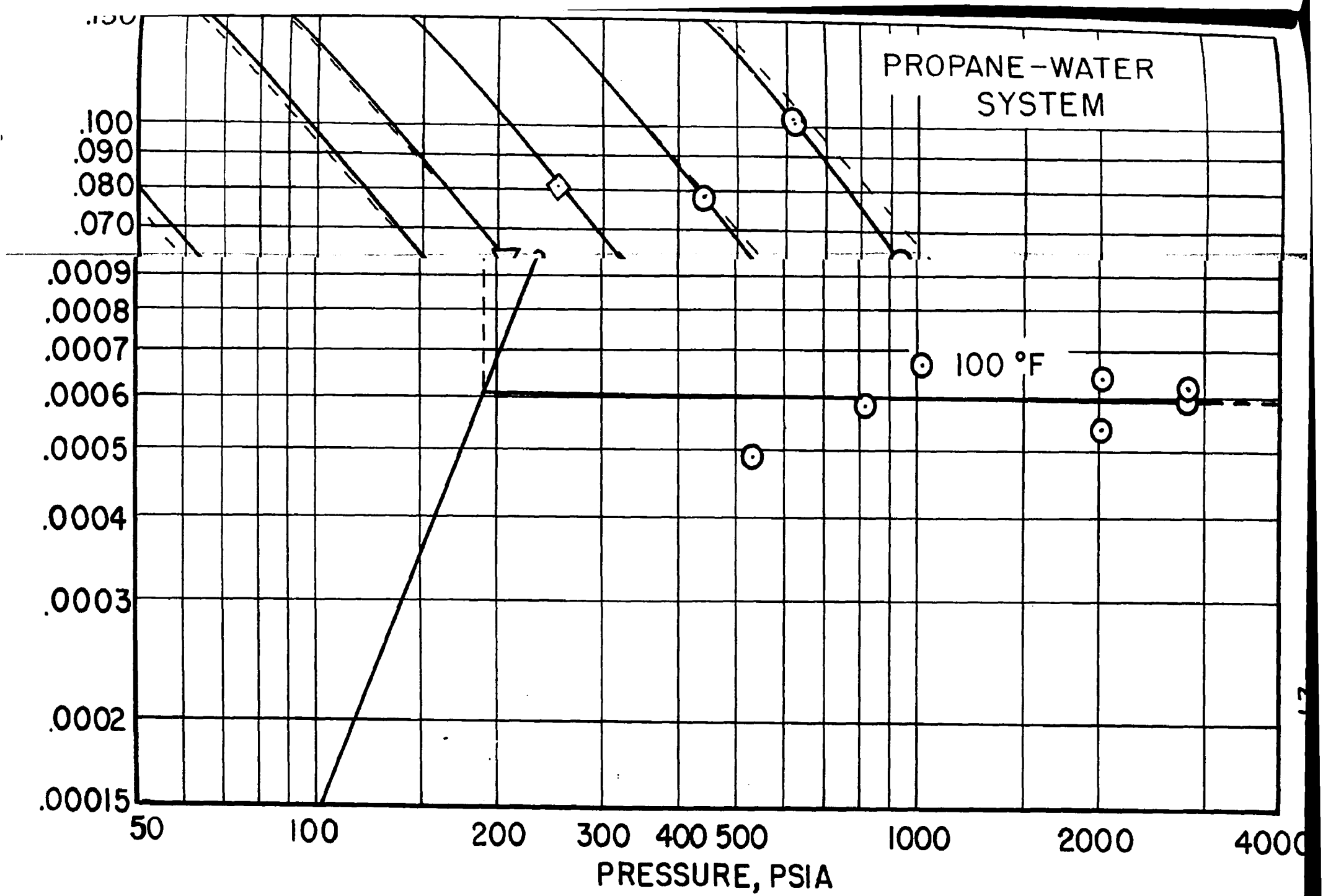


FIGURE 4 CONCENTRATION OF WATER IN THE PROPANE-RICH PHASES IN THE 2-PHASE REGION

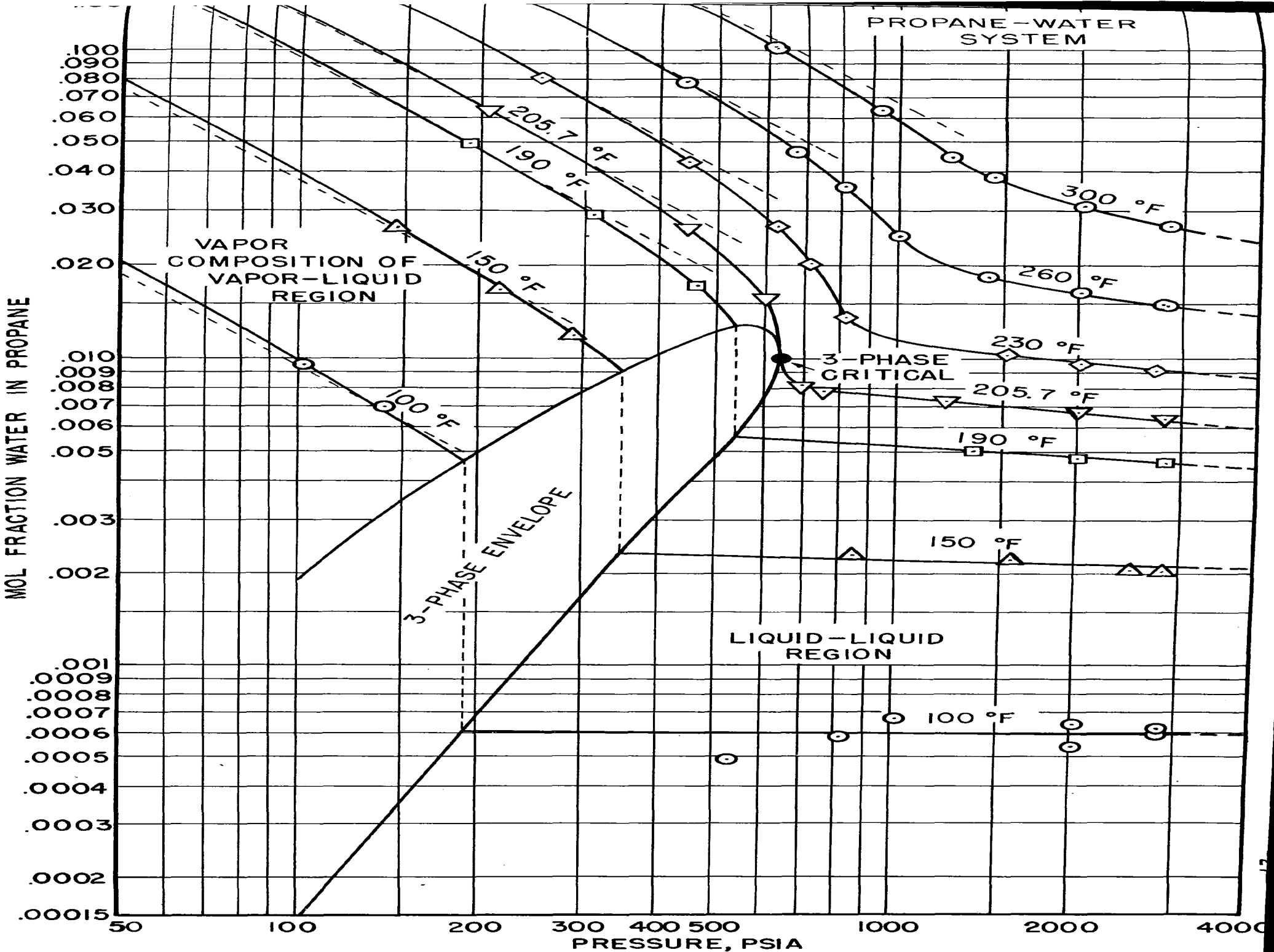


FIGURE 4 CONCENTRATION OF WATER IN THE PROPANE–RICH PHASES IN THE 2–PHASE REGION

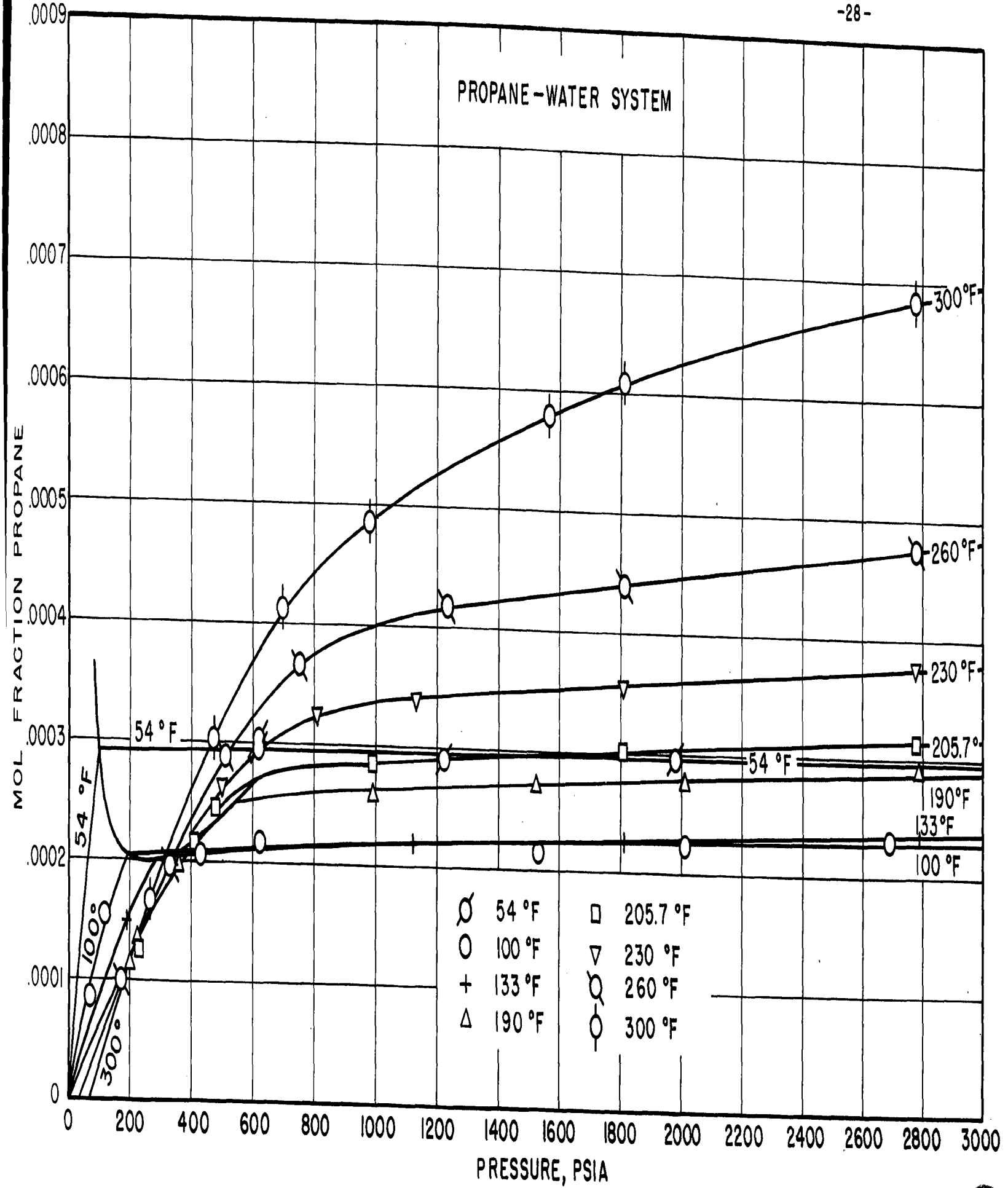


FIGURE 5 CONCENTRATION OF PROPANE IN THE WATER-RICH LIQUID PHASE IN THE 2-PHASE REGION

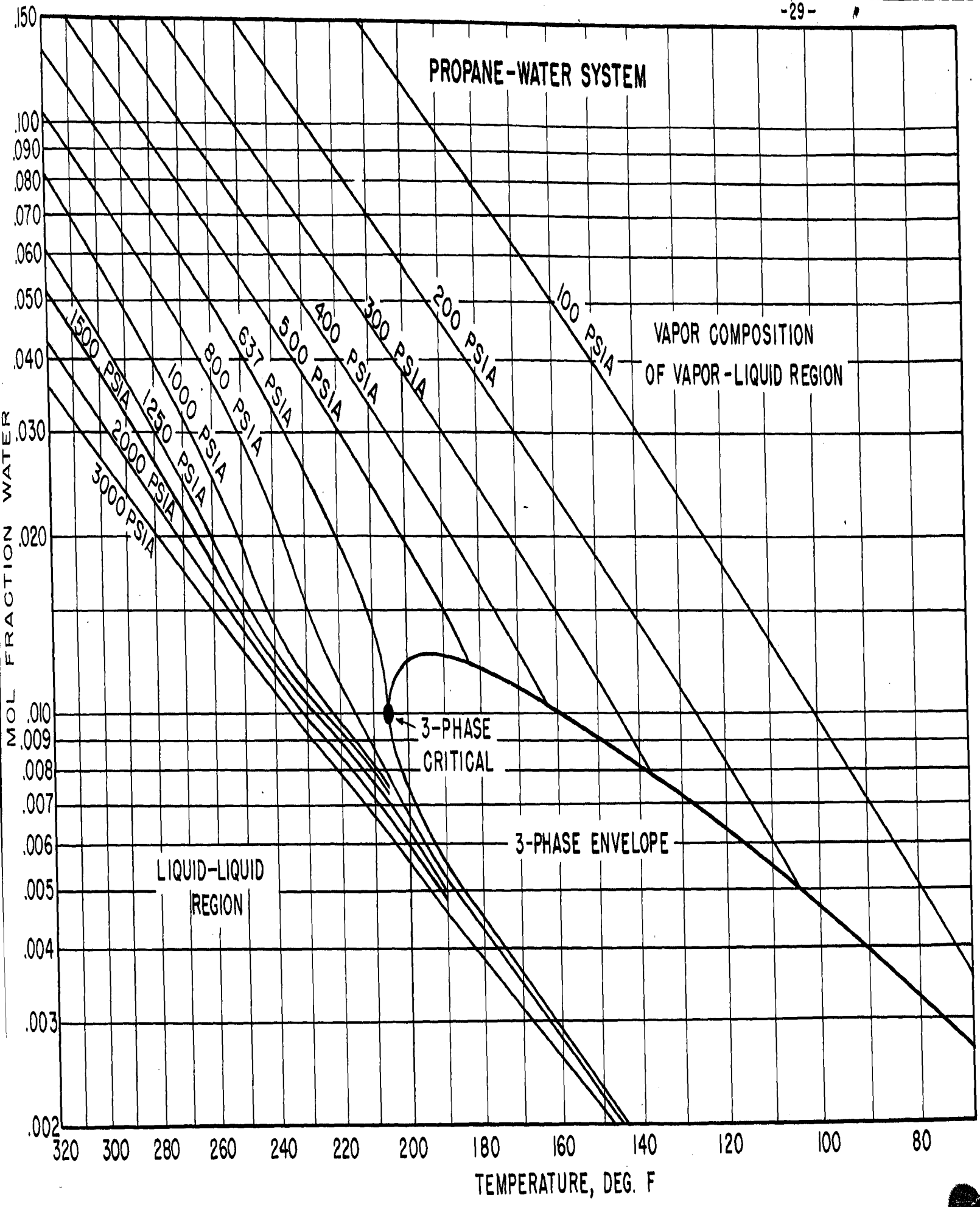


FIGURE 6 CONCENTRATION OF WATER IN THE PROPANE-RICH PHASES IN THE 2-PHASE REGION

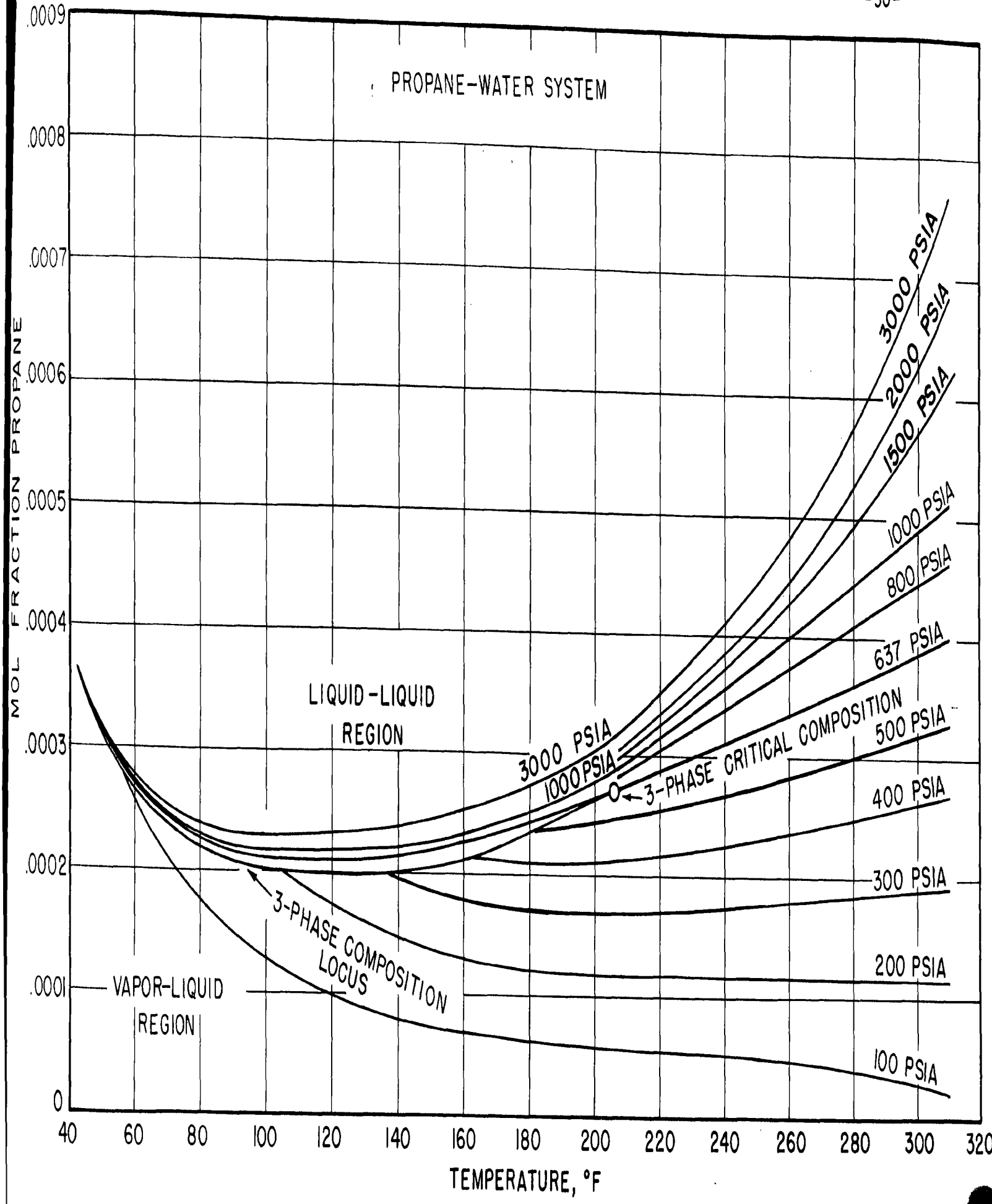


FIGURE 7 CONCENTRATION OF PROPANE IN THE WATER-RICH LIQUID PHASE IN THE 2-PHASE REGION ALONG ISOBARS

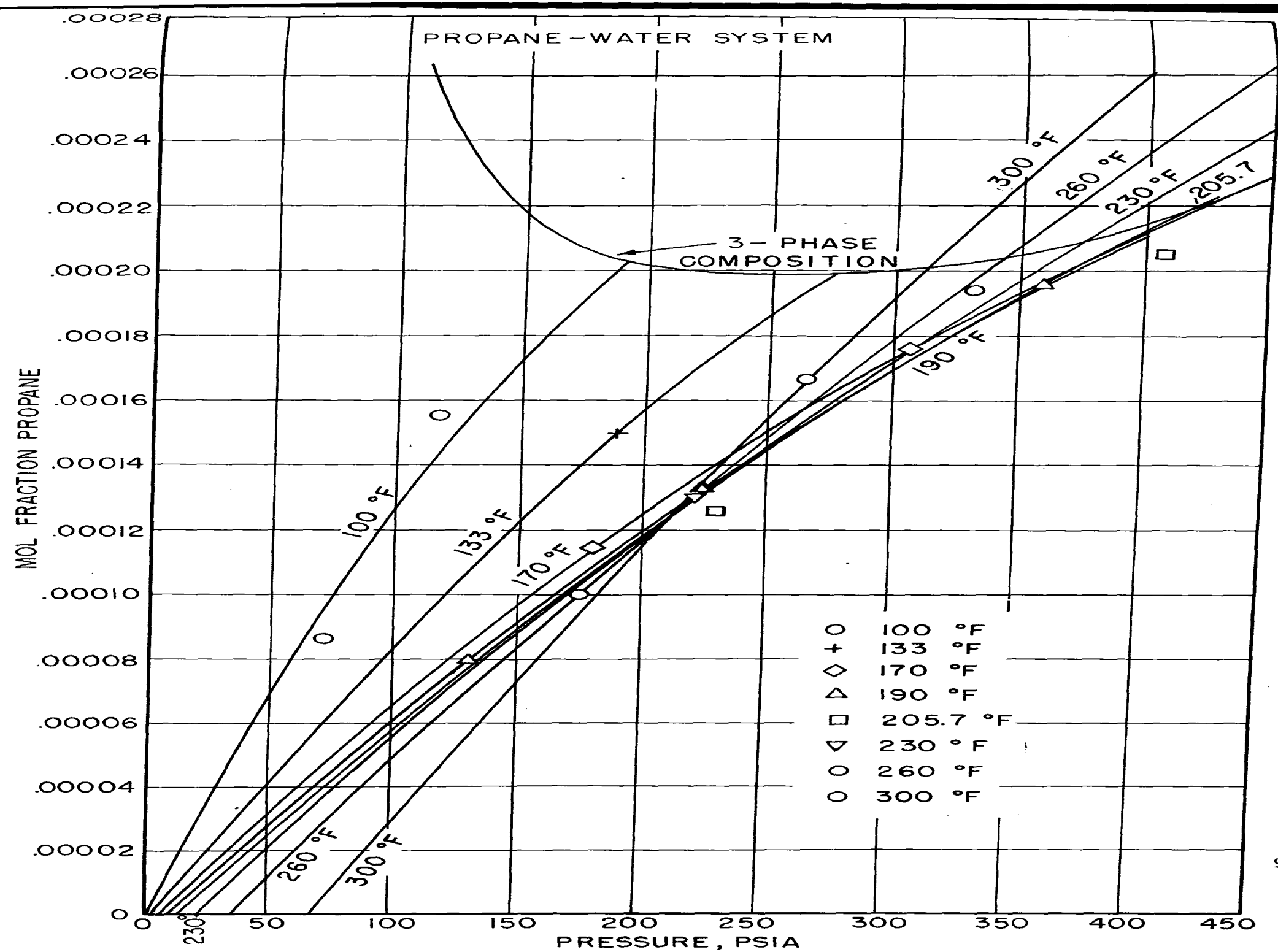


FIGURE 8 CONCENTRATION OF PROPANE IN THE WATER–RICH LIQUID PHASE IN THE 2–PHASE REGION AT LOW PRESSURES

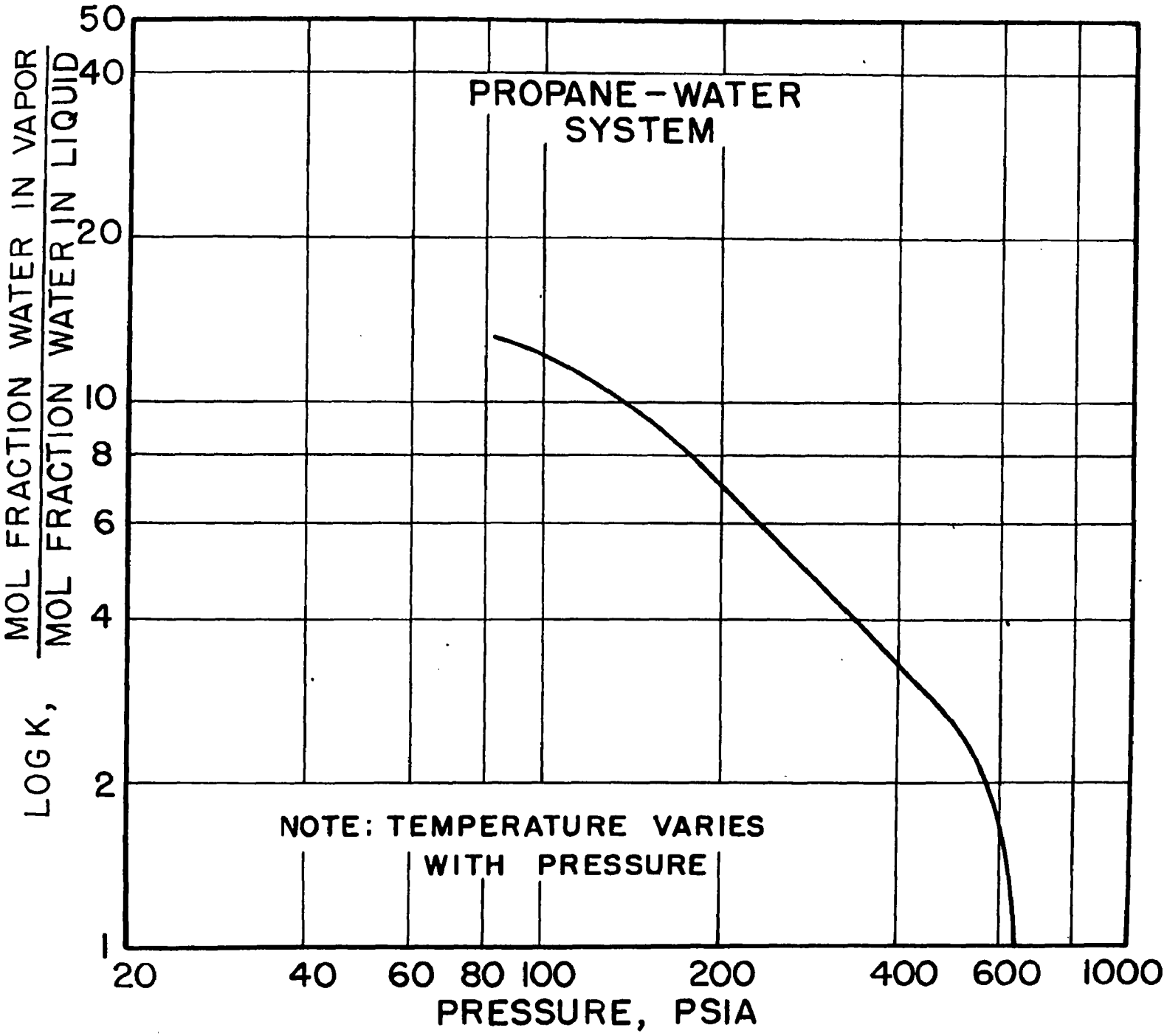


FIGURE 9 EQUILIBRIUM VAPORIZATION CONSTANTS FOR THE HYDROCARBON-RICH PHASES IN THE 3-PHASE REGION

PHASE RULE ANALYSIS OF THE PROPANE-WATER SYSTEM

A general understanding of the phase relations of the propane-water system may be developed through the application of the phase rule to the existing data on the binary propane-water system, including the data of the pure components propane and water. The emphasis on such a study are qualitative relationships expressing phase rule principles rather than on quantitative ones. The implications of the phase rule certainly extend beyond the scope of the data, but the qualitative relationships thereby expressed are no longer actual but logical relationships.

The variables which are required to express 2-phase and 3-phase vapor-liquid equilibria has been discussed under "Phase Rule and Its Relation to Experimental Procedure" on pp 4 to 6 . Also listed in the section are the functions, Equation (2) through Equation (8), which are necessary to describe 3-phase and 2-phase vapor-liquid equilibria completely. Since all the compositions of a binary system may be expressed along a common axis, the variables pressure, temperature, and compositions may be represented for all conceivable phase equilibria with a Pressure-Temperature-Composition Diagram (P-T-X diagram).

Two-phase equilibria are represented by a pair of surfaces, one for each phase. Three-phase equilibria are

represented by three space curves, each formed by the intersection of two surfaces. The condition of the uniformity of pressure and temperature for an equilibrium system requires that the space curves for all 3-phases yield the same projection on the pressure-temperature (P-T) plane.

Further, 4-phase equilibria are represented as four unique points in space at their respective phase compositions, which fall on a straight line perpendicular to the P-T plane. From each of such points, there must radiate three space curves. The 12 space curves originating from the 4-phase equilibria points appear as four 3-phase curves emanating from an invariant 4-phase point or quadruple point, when projected on the P-T plane. For the pure components, 2-phase equilibria appear as lines in the pure component planes of the P-T-X figure.

The termination of a 3-phase locus for a 2-component system may occur in the three following ways if the appearance of solid-solid solubilities is rejected:

(1) by the addition of another phase to give an invariant quadruple point,

(2) by the loss of a component in which the end point is identified as an invariant triple point of the other pure component, and

(3) by critical behavior in which any two of the coexisting liquid or vapor phases become continuously identical.

All the above implications of the phase rule are to be followed in the development of the phase rule analysis.

The development of the analysis is initiated by drawing the P-T projection, Figure 10, for the propane-water system, including that for the pure constituents propane and water.

Throughout this discussion, the following phase designations are used:

H for hydrate,

L_1 for the water-rich liquid phase,

L_2 for the hydrocarbon-rich liquid phase,

I for ice,

V for the vapor phase, and

P for solid propane

The appearance of only one hydrate of propane and the absence of solid-solid solubilities is assumed in the foregoing treatment. No attempt has been made to keep an exact scale in the diagrams utilized in this discussion because many of the lines shown would coincide indistinguishably with others. The concentrations are, in most cases, so small that they could not be illustrated clearly unless exaggerated. On the other hand, the correct or logically correct relative positions of the lines and the phase compositions have been maintained.

Figure 11 shows a series of T-X diagrams taken at seven different pressures which were considered pertinent to the development of the phase rule analysis and to the

construction of Figure 12. Figure 12 is an isometric drawing of the propane-water system representing its pressure-temperature-composition relationships. Thus, the seven T-X diagrams of Figure 11 reappear on Figure 12 in isometric positions.

The P-T projection prove to be of considerable aid in drawing the T-X diagrams of Figure 11. The intersection of the constant pressure planes, shown as dotted lines on Figure 10, with a line of the P-T projection define a temperature at which the phase compositions are to be located on the T-X diagrams of Figure 11. Empirical data are used to determine the relative location of the phase compositions at that temperature. These phase compositions represent the terminal points of the lines relating temperature and composition on the T-X diagrams.

Some of the constant pressure planes were chosen for their distinctive features:

P_1 for the existence of the triple point $I\text{-}L_1\text{-}V$,

P_4 for the existence of the quadruple point $H\text{-}L_1\text{-}L_2\text{-}V$,

P_5 for the existence of the 3-phase critical at which L_2 and V become continuously identical, and

P_6 for the existence of the 2-phase critical of water, the initial point of the critical loci for the binary in which L_1 and V become continuously identical.

A method of designating the space curves in Figure 12 and in the discussion has been devised. As an example,

for the 3-phase equilibria L_1-H-V the three space curves are designated in Figure 12 by L_1 (L_1-H-V), H(L_1-H-V), and V(L_1-H-V). The letter or letters before the parenthesis designate the phase whose composition is defined by the space curve, and the letters within the parenthesis designate the coexisting equilibrium phases for that equilibria. Thus, 2-component 2-phase vapor and liquid equilibria lines, which appear on the T-X planes of Figure 12, are designated by L_1(L_1-V) for the liquid phase and V(L_1-V) for the vapor phase.

The vapor pressure curve of water is designated by L_1,V(L_1-V) and terminates at the critical point B. The vapor pressure curve for propane is labelled L_2,V(L_2-V) and terminates at its critical E. The critical loci involving the water-rich liquid phase and the vapor phase is labelled L_1 = V,(L_1-V) and the critical loci involving the propane-rich liquid phase and the vapor phase is defined by the line DE.

The equilibria (L_1-V-L_2), which exists between P_4 and P_5, are designated L_1(L_1-V-L_2), V(L_1-V-L_2), and L_2(L_1-V-L_2). The experimental data, it may be recalled, of these loci are plotted on Figures 2 and 3. At P_4, 4 phases are in equilibrium, phase H disappearing immediately as the pressure is increased along L_1(L_1-V-L_2). V(L_1-V-L_2), and L_2(L_1-V-L_2).

The surface through the traces labelled L_1 (L_1-V) represent the liquid compositions in equilibrium with the vapor compositions on the surface through the traces labelled V(L_1-V). Lines at constant pressure and temperature pierce the respective surfaces at the vapor and liquid compositions in equilibrium. The experimental work of this study has been to determine these two surfaces precisely.

Also of practical interest are the space curves for the equilibria involving gas hydrates. Of these the most important are the ones involving the (L_1-H-L_2), (L_1-H-V), and the (H-V-L_2) equilibria. Their space curves may be traced in Figure 12. Other equilibria may be followed on Figure 12 by following the general designations used and through the use of Figures 10 and 11.

The presentation of complete phase relationships immediately becomes much more complex when a third component is added, in fact, three dimensions are then needed to represent a single isotherm or a single isobar. An understanding of simple binary systems can be applied to special cases approaching binary systems and indirectly applied to the understanding of complex systems. Quite frequently, the application of the phase rule and phase equilibria principles to a limited amount of data will enable predictions to be made intelligently for conditions not covered by experiment.

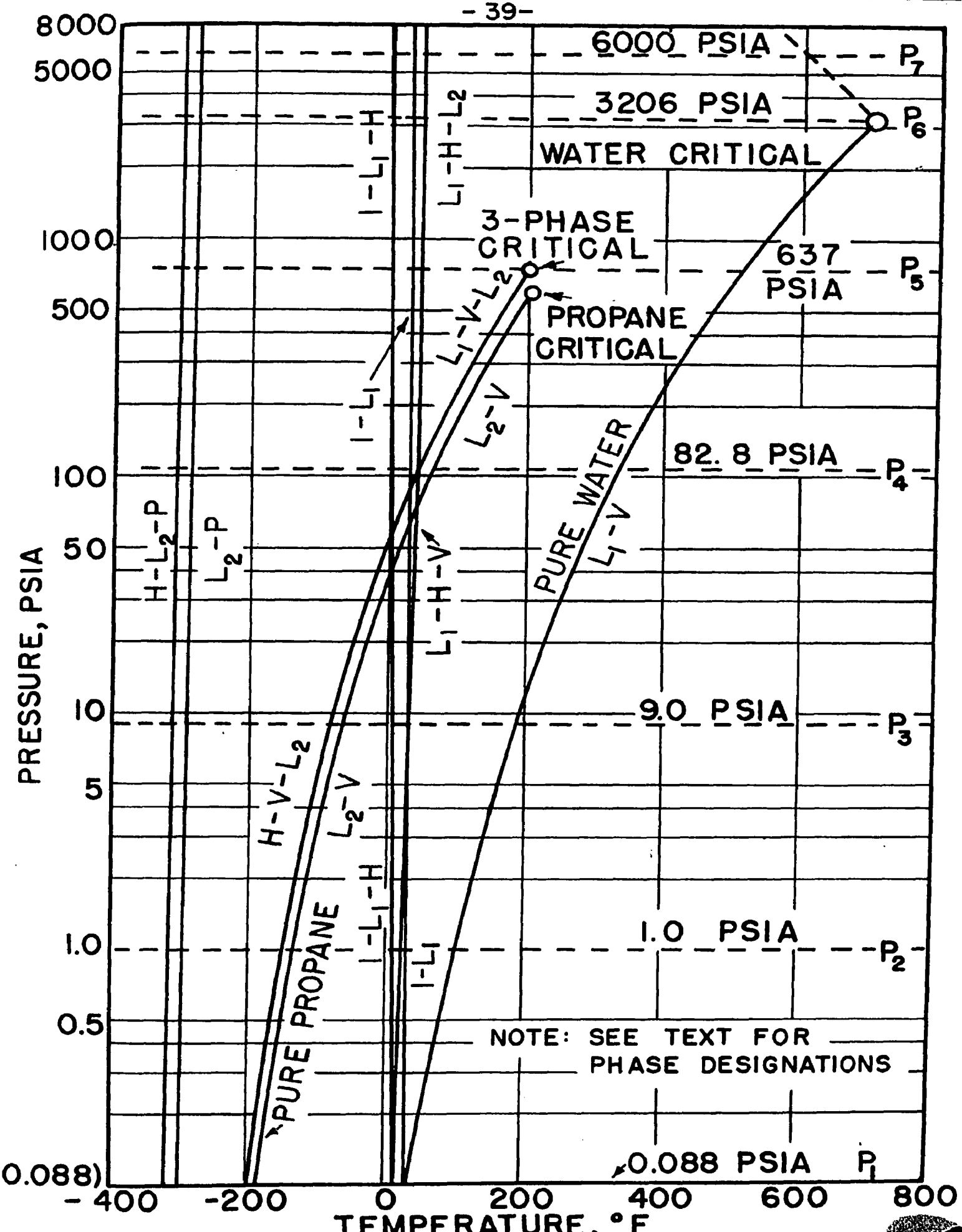


FIGURE 10 PRESSURE-TEMPERATURE PROJECTION FOR THE PROPANE - WATER SYSTEM

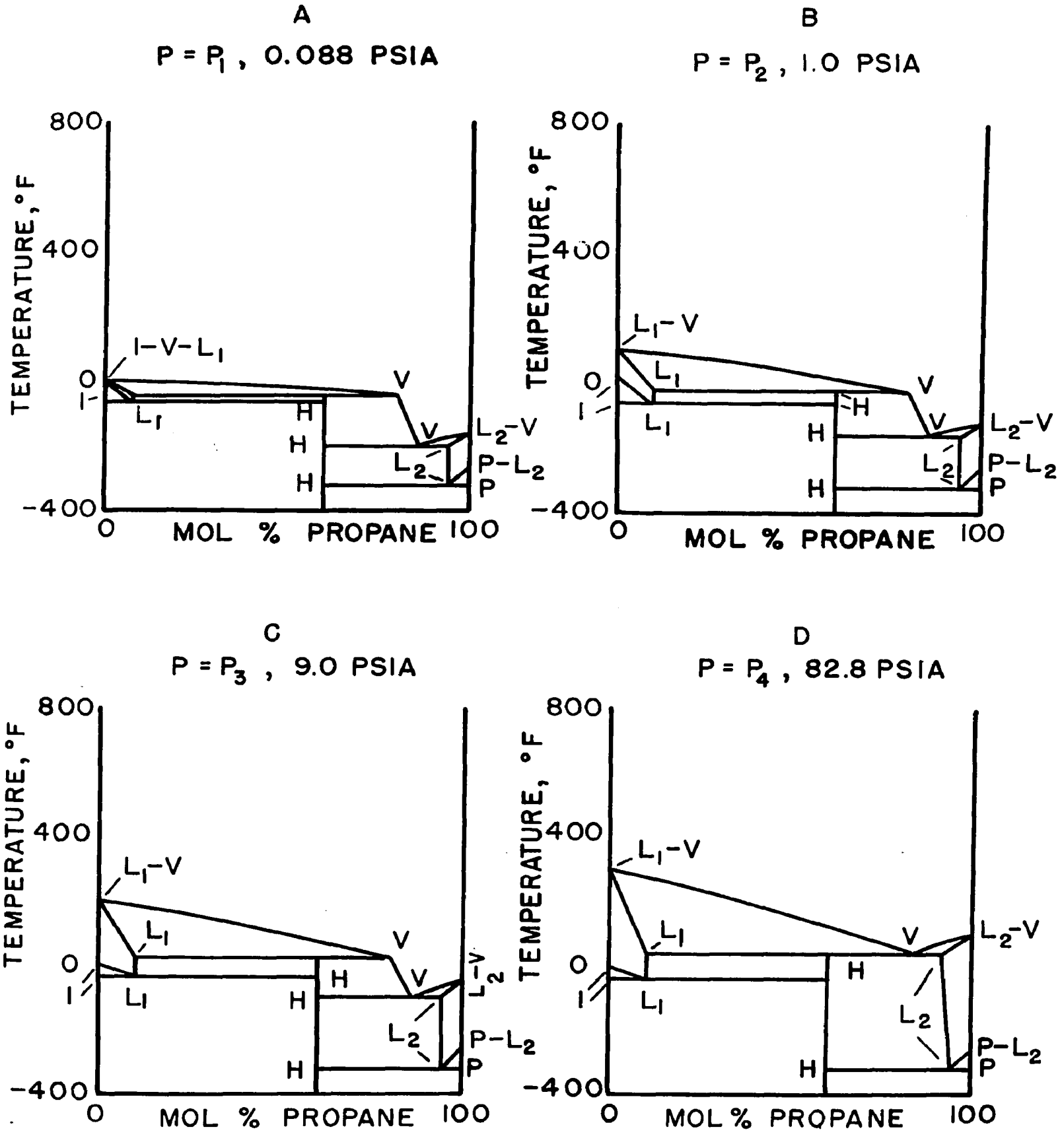


FIGURE II TEMPERATURE-COMPOSITION DIAGRAMS FOR THE PROPANE-WATER SYSTEM AT SEVERAL PRESSURES

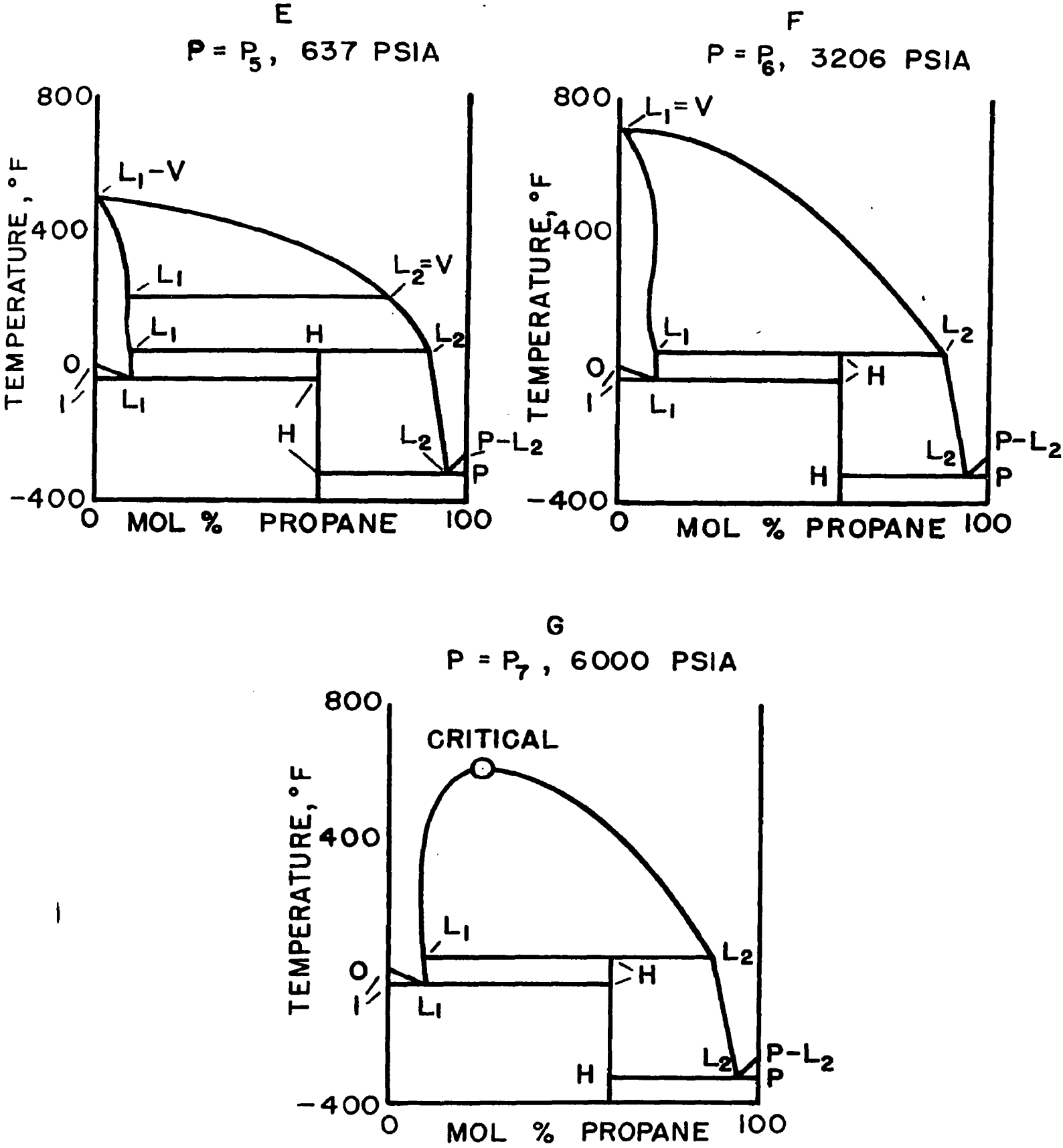


FIGURE 11 TEMPERATURE-COMPOSITION DIAGRAMS FOR THE PROPANE-WATER SYSTEM AT SEVERAL PRESSURES

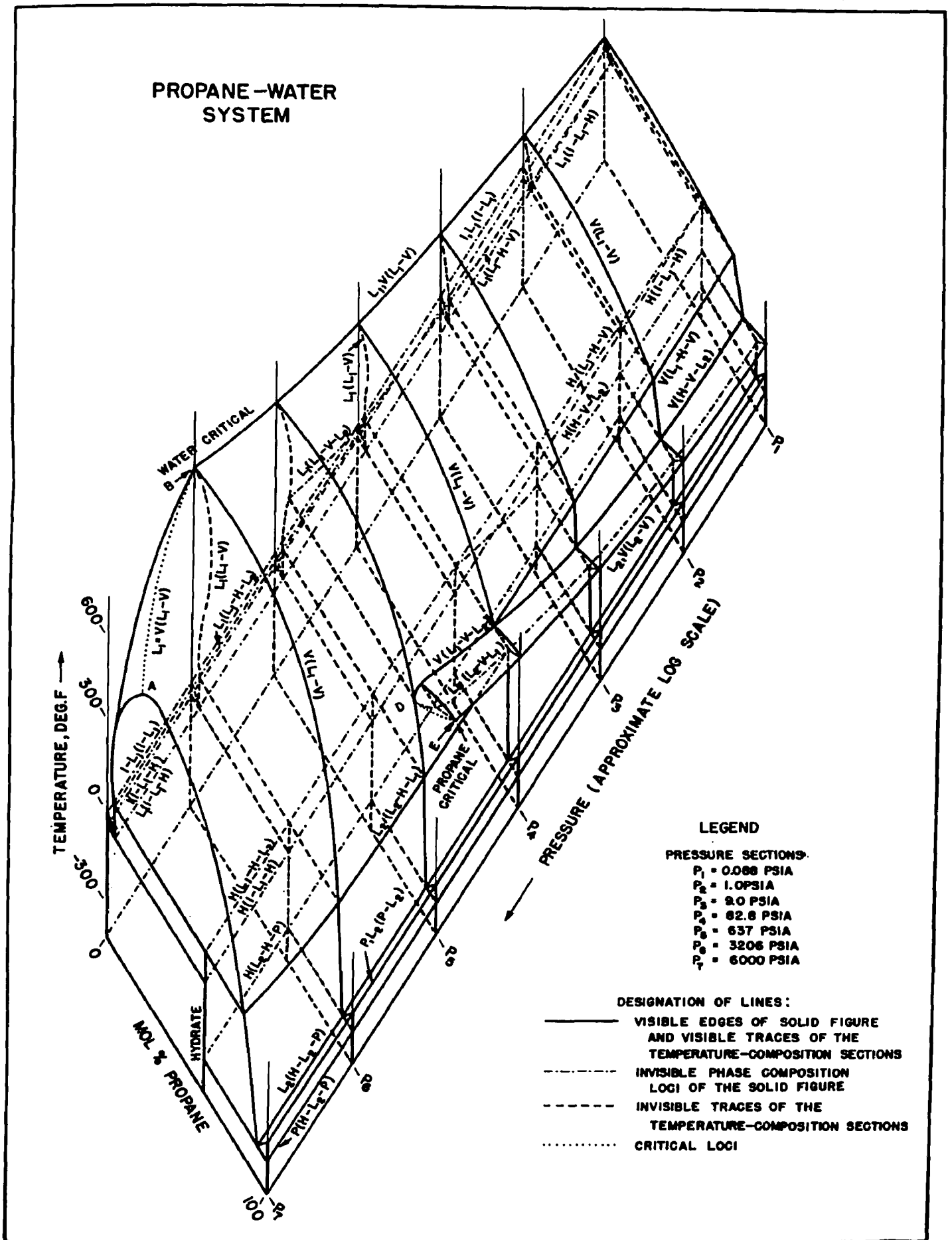


FIGURE 12 ISOMETRIC DRAWING OF PROPANE-WATER SYSTEM

THE SATURATED WATER CONTENT OF HYDROCARBON GASES AND LIQUIDS

Several investigations have been made to calculate or correlate the saturated water content at high pressures of "non-polar gases" such as nitrogen, hydrogen, methane, ethane, and natural gases (3), (28), (30), (32).

The simplest relation expressing the saturated water concentration in the vapor-phase, which is generally valid at low pressures for the non-polar gases is that

$$y = \frac{p^\circ}{P} \qquad (9)$$

where y = mol fraction of water in the vapor at the temperature of the system.

p° = vapor pressure of water at the temperature of the system, and

P = the total pressure of the system.

Equation (9) results from the use of Dalton's Law of partial pressure and Raoult's Law (26), and the fact that the liquid phase is substantially pure water.

Saddington and Krase (36) have found that at high pressures, the water content of nitrogen greatly exceeds the theoretical value as predicted from the application of Poynting's Relationship (26). This may be interpreted to mean that the effect of increased pressure on the vapor pressure of water is greater than predicted from Poynting's Relation which is stated as follows:

$$\frac{dp}{dP} = \frac{V}{v} \qquad (10)$$

where p = the vapor pressure of water at the temperature T,

P = the total pressure on the system,

V = the specific volume of the liquid at T, and

v = the specific volume of the vapor at T

Equation (10) is integrated over a finite pressure range to obtain the corresponding change in the vapor pressure of water.

That the Poynting effect cannot explain the increased volatility of water with increased pressure at a given temperature, indicates that the non-polar gases actually have a solvent effect upon the water molecules at high pressures. It is evident that the same attractive and intermolecular forces come to play at high pressures in the "solubility of a liquid in a gas" as for the solubility of a gas in a liquid.

Figure 4 and the discussion of the data in the section entitled "Experimental Data" show that the volumetric behavior of the hydrocarbon-rich phases is related to the solubility of water in them. This suggests a correlation which is based upon the volumetric behavior of the hydrocarbon-rich phases.

An empirical correlation in which the mol fraction of water in the hydrocarbon-rich phases is plotted against the anhydrous molal volume of those phases for several

isotherms is presented on Figure 13 and Figure 14. The molal volume is expressed in cc/gm. mol and is obtained from

$$V_m = \frac{M}{d} \qquad (11)$$

where V_m = the molal volume of the anhydrous hydrocarbon,

M = the anhydrous molecular weight of the phase, gms/gm. mol.

d = the density of the phase, gms/cc.

The effect of molecular weight on the isotherms is almost non-existent at high molal volumes (low pressures), but become appreciable as the molal volumes approach those of normal light hydrocarbon liquids.

All the experimental data used in the development of the correlation are shown on Figure 13. The saturated solubility of water in methane was obtained from the work of Olds, Sage and Lacey (30). The solubility of water in ethane for 220, 280, and 310 deg. F were obtained from the data of Reamer, Olds, Sage, and Lacey (32). The ethane data of the latter for the 100 and 160 deg. isotherms have been readjusted to account for the proximity of those isotherms to the 3-phase critical of the ethane-water system. The data on the water composition of the hydrocarbon-rich phase for the systems propane-water, n-butane-water, n-hexane-water, and methane-n-butane-water have been plotted on Figure 15 to estimate the 3-phase critical composition of the ethane-water system used in the readjustment of the ethane-water data.

The solubility of water in propane was obtained from this work, and the 3-phase data of the n-butane-water system from Reamer, Olds, Sage, and Lacey (33). The methane-n-butane-water data were obtained from the work of McKetta and Katz (29). The 3-phase points of the latter have been distinguished from the 2-phase points in Figure 13. Additional experimental points on the solubility of water in 190 molecular weight kerosene (17) and 95 molecular weight gasoline (8) appear on the correlation. The numbers opposite the methane-n-butane-water points indicate the anhydrous molecular weight of the phase.

Figure 13 has been cross-plotted to locate the position of the curves for even values of molecular weight up to a molecular weight of 70, Figure 14.

Figure 5 shows that the solubility isotherms for propane below the 3-phase critical temperature becomes discontinuous at the 3-phase pressure where two hydrocarbon-rich phases of different water concentrations coexist. This discontinuity does not appear in the isotherms of Figure 13 because the molal volumes of these two co-existing phases differ in the same proportions as their water concentrations. That is to say, that considered on a molal volume basis, there is a continuity in the solubility of water in the hydrocarbon-rich liquid and vapor phases for temperatures below the 3-phase critical as well as for temperatures above. The 230 deg. F iso-

therm for propane on Figure 4 and the 220 deg. F isotherm for propane on Figure 13 may be compared to indicate that the inflection in the former has disappeared in the latter.

The saturated vapor phase water content of complex hydrocarbon-water systems can be estimated from this correlation to pressures very near to the 3-phase critical to within 5% of the total water concentration in that phase. The solubility of water in the 3-phase hydrocarbon-rich liquid phase cannot be predicted with the same degree of success. Here, the maximum error, which is again to be expected in the 3-phase critical region, is about 20% of the total water concentration in that phase. The predicted value for this region is about 20% lower than the actual concentration.

The use of the correlation in predicting the water content of the compressed lighter liquid phase, i.e., well within the 2-phase region, is quite satisfactory as the calculated points on Figure 13 indicate. The water content of saturated hydrocarbons at temperatures other than those plotted on Figure 14 can best be obtained by a cross plot of log composition versus T, or 1/T, holding the molal volume and the molecular weight constant.

The use of Figure 14 presupposes a knowledge of the phase density and the phase molecular weight of the anhydrous hydrocarbon-rich phase under the equilibrium conditions. McKetta (29) has shown the effect of water

on the vapor-liquid equilibria relationship of the methane-n-butane system. Since such data are generally unavailable, the calculation of phase compositions, if there should be two coexisting hydrocarbon-rich phases, should be made by the conventional method (43) for calculating the coexisting phases using suitable equilibrium constants for the system (4), (15), (19), (37).

The vapor phase densities may be calculated by the law of corresponding states (5). The liquid phase densities may be calculated by the method of apparent specific weights (5) or by the method using the partial molal volumes of condensed hydrocarbons (38).

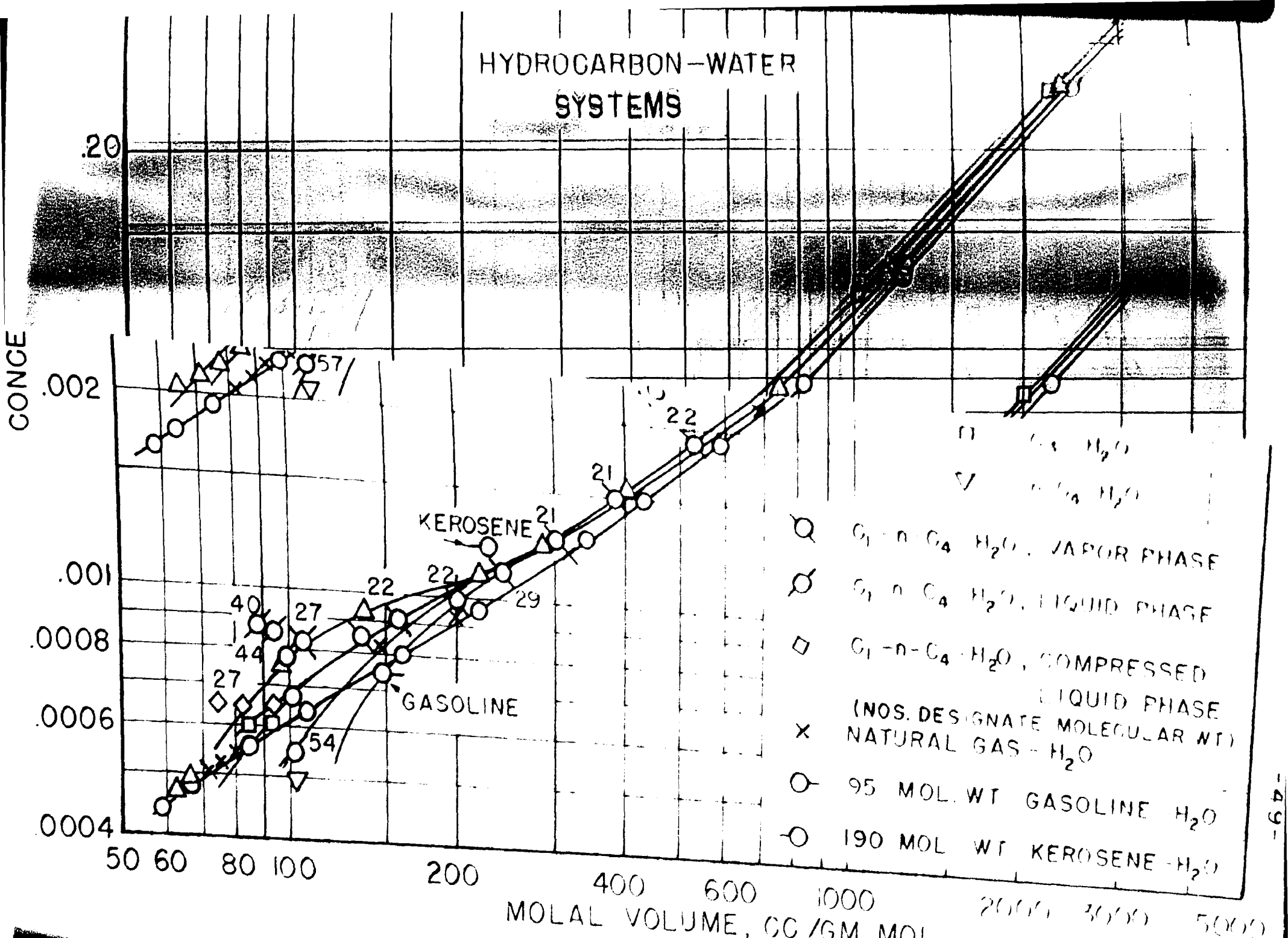


FIGURE 13 WATER CONTENT OF LIGHT HYDROCARBON

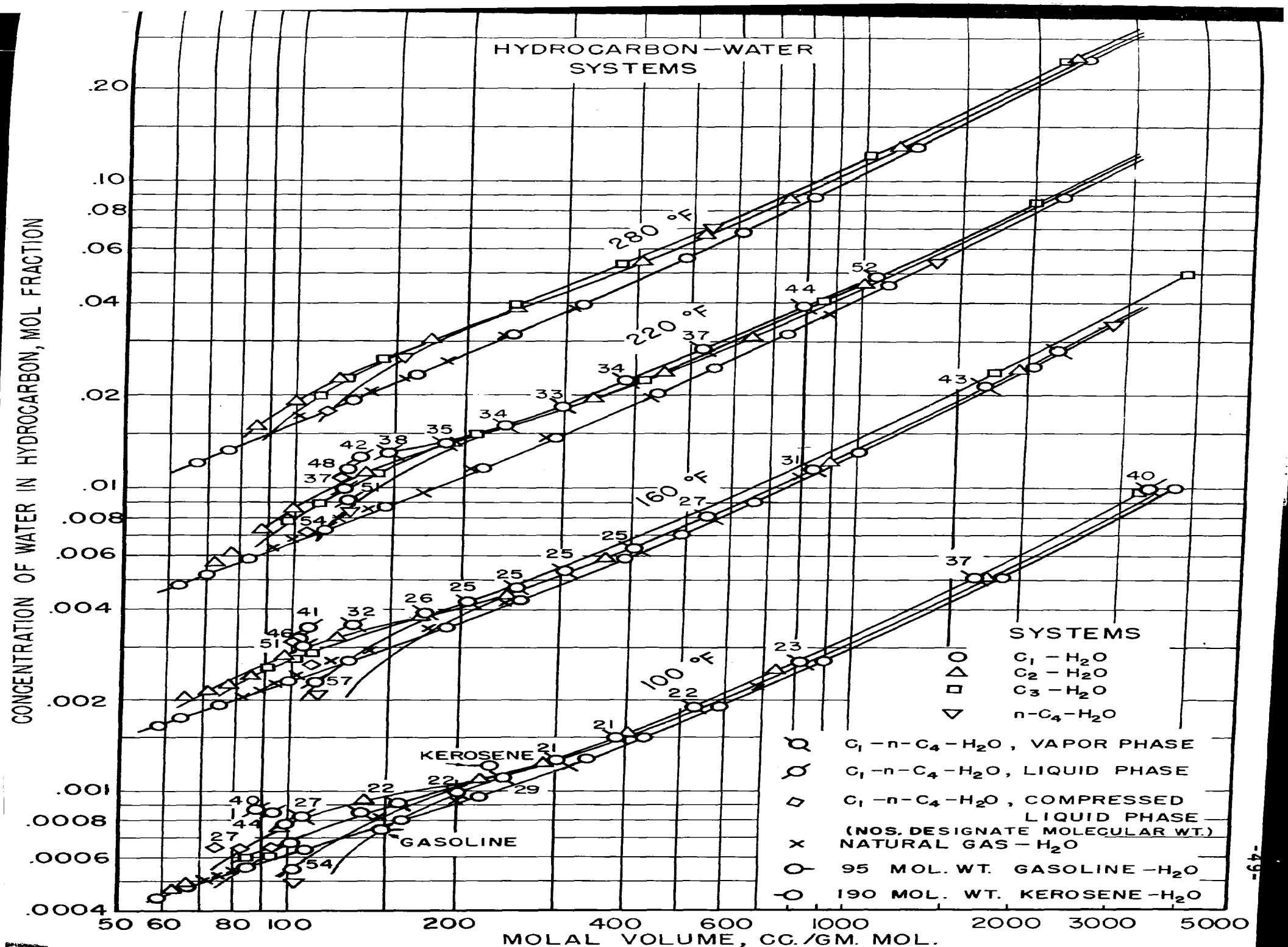


FIGURE 13 WATER CONTENT OF LIGHT HYDROCARBON VAPORS AND LIQUIDS AS A FUNCTION OF MOLAL VOLUME

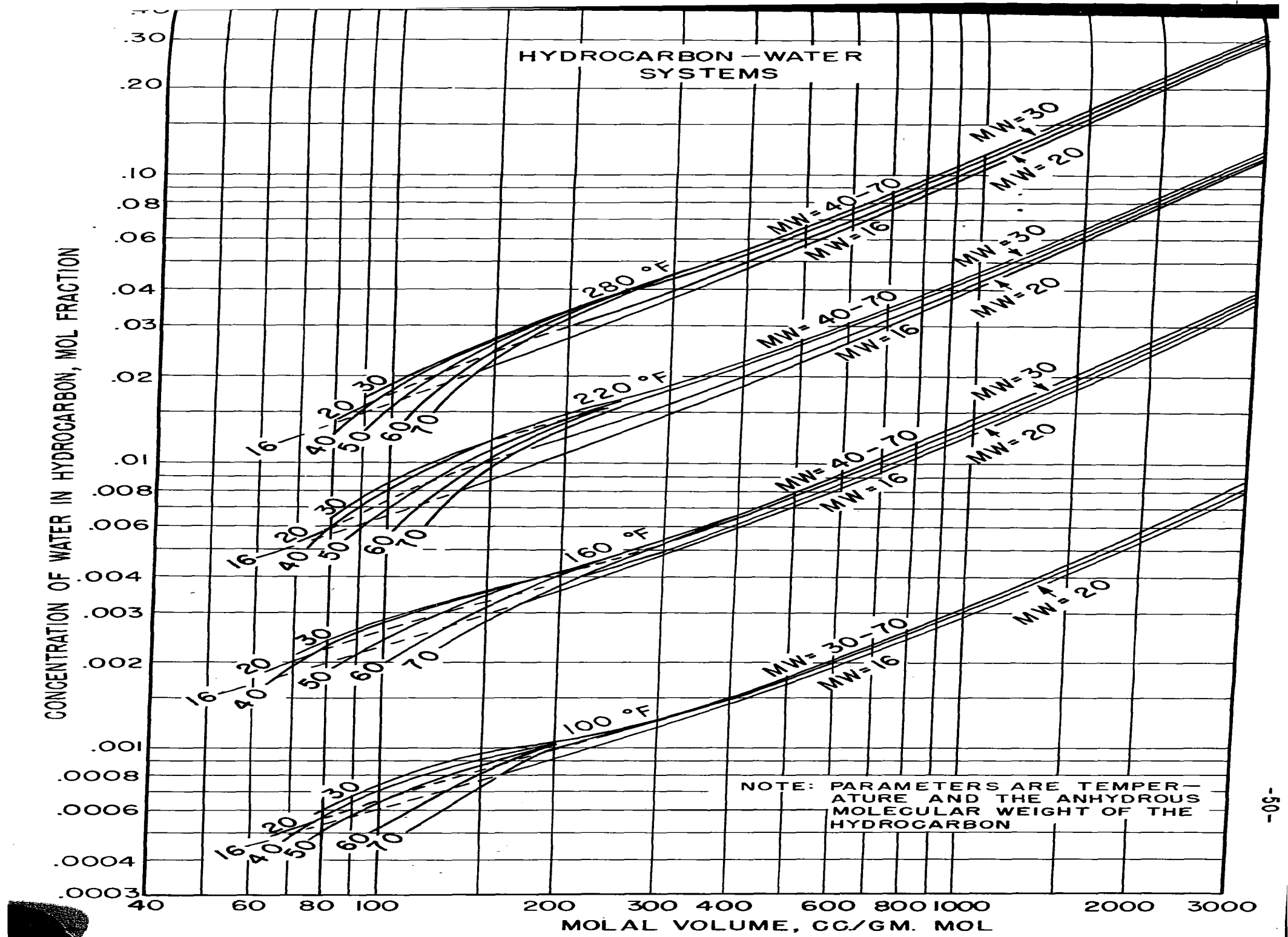


FIGURE 14 WATER CONTENT OF LIGHT HYDROCARBON VAPORS AND LIQUIDS AS A FUNCTION OF MOLAL VOLUME

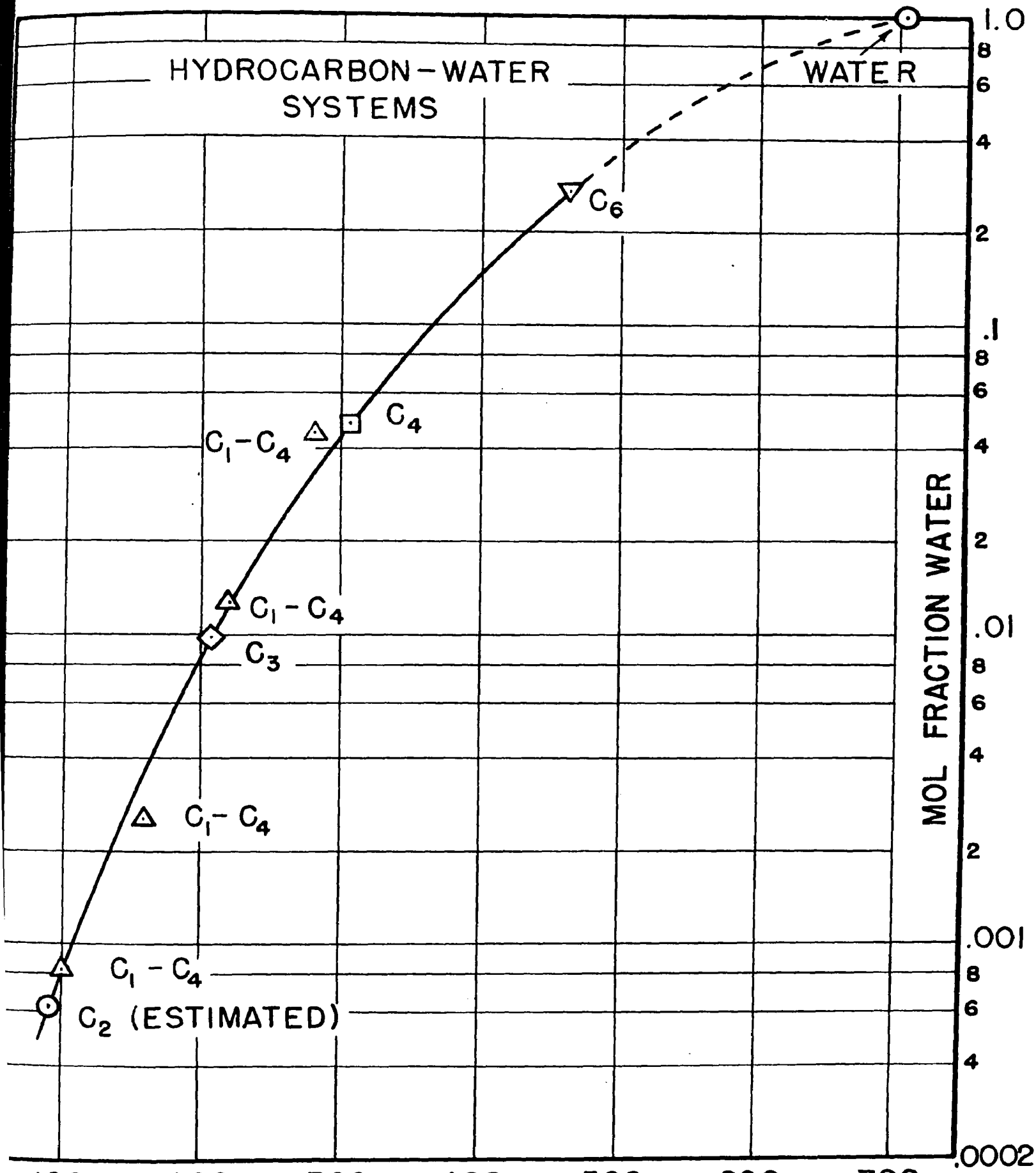


FIGURE 15 COMPOSITION OF THE HYDROCARBON-RICH PHASE AT THE 3-PHASE CRITICAL CONDITIONS

THERMODYNAMIC ANALYSIS OF THE SOLUBILITY OF PURE HYDROCARBONS IN WATER

Successful methods of calculating the solubility of slightly soluble gases in water at high pressure from low pressure solubility data and the thermodynamic data of the pure gas at high pressures have been developed. Krichevsky and Kasarnovsky (20) utilized the fugacity data of compressed nitrogen and the atmospheric solubility data of nitrogen in water to compute its solubility from 25 deg. C to 100 deg. C up to pressures of 1000 atmospheres. The agreement of the calculated values with the experimental is excellent. They repeated the calculations for similar data on hydrogen for several isotherms from 0 deg. C to 100 deg. C up to 1000 atmospheres with equal success.

Wiebe and Gaddy (46), (47) computed the solubility of carbon dioxide in water from 12 deg. C to 100 deg. C for pressures up to 700 atmospheres with fair success, using the thermodynamic data of carbon dioxide over the range of conditions. The equation developed by Krichevsky and Kasarnovsky and the equation used by Wiebe and Gaddy are derived and discussed. The equation in the form presented by Krichevsky and Kasarnovsky is applied to the following study.

Derivation of Wiebe and Gaddy:

Wiebe and Gaddy (46), (47) develop their equation as follows:

The general equation for a binary isothermal system with two phases in equilibrium is given by:

$$\left[\frac{d\bar{F}_2}{dP}\right]_{N_2} dP + \left[\frac{d\bar{F}_2}{dN_2}\right]_P dN_2 = \left[\frac{d\bar{F}_2'}{dP}\right]_{N_2'} dP + \left[\frac{d\bar{F}_2'}{dN_2'}\right]_P dN_2' \qquad (12)$$

where $\bar{F}_2$ and $\bar{F}_2'$ are the partial molal free energies of the carbon dioxide in the liquid and gas phases, respectively.

P, is the pressure, and

N_2 and N_2' are the concentrations of carbon dioxide in the liquid and gas phases, respectively.

Since $$\left[\frac{d\bar{F}_2}{dP}\right]_{T,N} = \bar{v}_2 \qquad (13)$$ Ref. (26)

and by definition $$\left[\frac{d\bar{F}_2}{d \ln \bar{f}_2}\right]_T = RT \qquad (14)$$ Ref. (26)

and $$dN_2 = N_2 d \ln N_2 \qquad (15)$$

equation 12 becomes

$$\bar{v}_2 dP + RT \left[\frac{d \ln \bar{f}_2}{d \ln N_2}\right]_P \frac{dN_2}{N_2} = \bar{v}_2' dP + RT \left[\frac{d \ln \bar{f}_2'}{d \ln N_2'}\right]_P \frac{dN_2'}{N_2'} \qquad (16)$$

where the $\bar{v}$'s and the $\bar{f}$'s are the partial molal volumes and fugacities of carbon dioxide in the two phases.

Since we are dealing with a dilute solution of carbon dioxide in the liquid phase, at constant temperature and pressure

$$d \ln \bar{f}_2 = d \ln N_2 \qquad (17) \text{ Ref. (26)}$$

and since the concentration of carbon dioxide is almost unity, $\frac{dN_2}{N_2'}$ is small relative to $\frac{dN_2}{N_2}$ so that equation 16 reduces to:

$$d \ln N_2 = \frac{(\bar{v}_2' - \bar{v}_2)}{RT} dP \qquad (18)$$

The solubilities of carbon dioxide in water at 25 atmospheres for several temperatures were used as reference points in the integration of equation (18) to compute the solubilities of carbon dioxide in water for several isotherms up to 700 atm. Other data used in the integration of equation (18) were the volumetric properties of carbon dioxide and the molal volume of carbon dioxide dissolved in water at atmospheric conditions. The calculated solubilities for the isotherms at 40, 50, 75, and 100 deg. C were generally lower than the experimental ones by 1 to 4% of the solubility, the greatest deviation occurring at the highest pressure.

Method of Krichevsky and Kasarnovsky:

The final equation derived by Krichevsky and

Kasarnovsky (20) is rederived here in a slightly different manner. Combining equations (13) and (14) gives:

$$RT d \ln \bar{f}_2 = \bar{v}_2 dP \qquad (19)$$

which may be integrated at constant temperature, under the supposition that $\bar{v}_2$ is independent of pressure and is unaffected by the small change in N_2 with pressure.

$$RT \int_{\bar{f}_2^s}^{\bar{f}_2} d \ln \bar{f}_2 = \bar{v}_2 \int_{P^s}^{P} dP \qquad (20)$$

gives $$\ln \frac{\bar{f}_2}{\bar{f}_2^s} = \frac{\bar{v}_2}{RT} (P - P^s)$$

where $\bar{f}_2^s$ is the partial molal fugacity of the solute gas at the saturation pressure of water.

For an infinitely dilute solution Henry's Law (26)

$$\bar{f}_2^s = K N_2 \qquad (22)$$

applies, so that equation (21) becomes

$$\log \frac{\bar{f}_2}{N_2} = \log K + \frac{\bar{v}_2 (P - P^s)}{2.303 RT} \qquad (23)$$

Equation (23) has been rewritten as

$$\log \frac{\bar{f}_2}{N_2} = \log K' + \frac{\bar{v}_2 P}{2.303 RT} \qquad (24)$$

by setting $\log K' = \log K - \frac{\bar{v}_2 P^s}{2.303 RT}$. By combining equations (13) and (14) with equation (18), the latter may be converted into the form of equation (24). Equation (24) was applied to the study on the solubility of pure

hydrocarbons in water. The terms of equation (24) are redefined as follows:

$\bar{f}_2$ = the fugacity of the solute gas, psia,

N_2 = the mol fraction of solute in the water-rich liquid phase,

K' = the modified Henry's Law constant,

$\bar{v}_2$ = the partial molal volume of the solute gas dissolved in the water-rich phase, cu.ft./lb.mol,

P = pressure, psia,

R = gas constant, 10.73, and

T = the absolute temperature, °R

Krichevsky and Kasarnovsky (20) computed the solubilities of nitrogen in water at 25, 50, 75, and 100 deg. C and of hydrogen in water at 0, 25, 50, and 100 deg. C up to 1000 atm. pressure. The agreement of the computed solubilities with the experimental are exceptionally good with the greatest deviations less than 1% of the total solubility, and in most instances the deviations are within the range of accuracy of the experimental measurements.

Application of the Method of Krichevsky and Kasarnovsky to the Systems, Methane-water, Ethane-water, and Propane-water

The partial volumetric properties of dissolved hydrocarbons in water were not available to permit a direct calculation of the solubility of the pure hydrocarbons in water. Therefore, the existing thermodynamic data for the pure components and the vapor-liquid equilibria data for the

binary hydrocarbon-water systems were applied to compute the characteristic isothermal constants, K's and $\bar{v}_2$'s, for the systems methane-water, ethane-water, and propane-water.

Since the concentrations of water in the hydrocarbon-rich phases are quite small, or become large only at relatively low pressures, ideal solutions may be assumed. Then, the fugacity of the hydrocarbon, $\bar{f}_2$, in equation (24) may be estimated from

$$\bar{f}_2 = f_2^o y_2 \qquad (25) \quad \text{Ref. (26)}$$

where f_2^o = the fugacity of the pure hydrocarbon at the equilibrium pressure and temperature, and

y_2 = the mol fraction of hydrocarbon in the hydrocarbon-rich phase.

The concentration of water in the dew point gas for the methane-water system (30) and the ethane-water system (32) were obtained from the data of Sage and Lacey and applied in equation (25). The fugacity data of the pure hydrocarbons methane, ethane, and propane were obtained from the data prepared by Sage and Lacey (39). The concentration of water in the propane-rich phases and the solubility of propane in water were obtained from this investigation. The solubility of methane and ethane in water were obtained from the works of Culberson, Horn, and McKetta (9) and Culberson and McKetta (10), (11).

The modified Henry's Law constant, K', and the partial molal volumes of the dissolved hydrocarbons were

determined by an isothermal plot of "log $\frac{\bar{f}_2}{N_2}$ " against " $\frac{P}{2.303RT}$ ". The plots from which the constants for the three systems were determined are shown on Figure 16, 17, 18A and 18B. For any given isotherm, $\bar{v}_2$, the slope of the isotherm, was found to be substantially constant with some scattering of the points at the lower pressures. The greater inaccuracy of the experimental solubility data at low pressures and the higher water concentrations in the hydrocarbon-rich phase at low pressures may account for the increased deviations. With increased water concentrations in the hydrocarbon-rich phase, the assumption of ideal solutions in that phase probably loses its validity. Equation (24), however, is found to be a very sensitive relationship, and what appears to be serious deviations from a straight line on Figure 16, 17, and 18 are produced by relatively small changes in the values of N_2, the concentration of hydrocarbon in the water-rich phase. The results show that the agreement between the graphically smoothed experimental data and the thermodynamically smoothed data for the solubility of the hydrocarbons in water is surprisingly good, as may be seen from Tables 9, 10, and 11. It should be mentioned that the thermodynamic calculations were made using the graphically smoothed experimental data, so that the thermodynamic smoothing is not an independent operation. In addition, the fugacity of the hydrocarbon

in the solution, $\bar{v}_2$, calculated from equation (25) has been assumed correct in obtaining the smoothed values from equation (24). The application of the same calculations to the original experimental points presents a possible means of smoothing the data independently. In view of the assumptions made in the derivation of the thermodynamic equation, an independent smoothing of the data was not felt to be justified.

The calculated solubilities of propane in water for pressures from 3000 to 10,000 psia are included in Table XI. The validity of the extrapolation is supported by the thermodynamic calculations made on the methane-water and the ethane-water systems up to 10,000 psi. Both of the methane-water and ethane-water show a remarkable isothermal constancy of $\bar{v}_2$ throughout the pressure range from 1000 to 10,000 psi.

Since the isotherms of Figures 17, 18, and 19 yield straight lines, it appears that $\bar{v}_2$, the partial molal volume of the dissolved hydrocarbon, for a given temperature is independent of pressure, at least at high pressures. Though this is mathematically the case, this may not be so as far as the internal constitution of the solution is concerned. It must be remembered that $\bar{v}_2$ was determined by the integration of equation (19) with the supposition that $\bar{v}_2$ was independent of the change in concentration of the dissolved hydrocarbon from zero to the saturated

concentration. Primarily $\bar{v}_2$ is to be considered as a quantity defined in terms of other and directly measurable quantities, and as a quantity of practical importance in thermodynamic calculations. In this respect, a question was raised as to the constancy of $\bar{v}_2$ over the pressure range when an attempt was made to use it to calculate the density of water saturated with hydrocarbons at high pressures in the following section. The assumption of ideal solutions in the water-rich liquid phase may not be valid, so far as the density calculations are concerned.

Figure 19 gives the plots of modified Henry's Law constants, K', as a function of temperature for the solubility of methane, ethane, propane, hydrogen, and nitrogen in water. The partial molal volumes of the same pure constituents dissolved in water are plotted as functions of temperature in Figure 20. In Figure 20, no explanation has been found to explain the trends of the curves for ethane and propane, both of which exhibit maxima. The maxima cannot be associated, even qualitatively, with the criticals of pure ethane, since the maximum for ethane occurs at about 310 deg. F as compared to 200 deg. F for propane. The inability to predict $\bar{v}_2$ for the individual hydrocarbons is not completely discouraging because $\bar{v}_2$ need not be determined with great accuracy for calculations at low and moderate pressures, e. g. up to 2000 psi, for under these

conditions the deviations from Henry's Law which is contributed by the term $\frac{\bar{v}_2 P}{2.303\ RT}$ is generally small.

Sufficient data on the solubility of hydrocarbons in water at low pressures are not available to permit a general relationship for estimating Henry's Law constant. However, the Henry's Law constants presented and discussed here do follow similar trends and indicate their similarity for gases of widely different critical conditions.

The maxima in the curves of Figure 19 are associated with the appearance of the isobaric minimum solubilities discussed on pp 80.

The thermodynamic calculations show that the solubility of pure light hydrocarbons can be predicted from accurate atmospheric solubility data, the partial molal volume of the hydrocarbons dissolved in water, the volumetric behavior of the pure hydrocarbons at the elevated pressure conditions, and the concentration of the hydrocarbon in the solute-rich phase. The latter may be determined accurately through the use of the generalized plot of the water content of saturated hydrocarbon liquids and gases given in Figure 14.

Unfortunately, the partial molal volumes of the hydrocarbons dissolved in water are extremely difficult to determine by direct measurements. There remains, however, the possibility of obtaining the partial molal volumes

indirectly as in the present analysis. A few experimental values of the solubilities of hydrocarbon in water accurately determined at each temperature over a moderate pressure range will provide the necessary information to predict the solubilities at higher pressures. No accurate data on the solubilities of complex light hydrocarbon mixtures in water on which the thermodynamic calculations may be made are available.

These calculations provide a method for smoothing the experimental data thermodynamically. The assumptions which are necessary to make the calculations appear to be most valid at high pressures. The comparison of the experimental data with the thermodynamically smoothed data indicate that graphical smoothing of the data is preferred to the thermodynamic smoothing of the data excepting at high pressures.

TABLE IX

Solubility of Methane in Water: Comparison of Graphically Smoothed Data with Thermodynamically Smoothed Values

Pressure psia	100°F		160°F		220°F		280°F		340°F	
	Mol Fraction Methane in the Water-Rich Phase									
	Graph.	Thermo.	Graph.	Thermo.	Graph.	Thermo.	Graph.	Thermo.	Graph.	Thermo.
500	.000642	.000645	.000503	.000505	.000463	.000484	.000486	.000523	.000567	.000545
1000	.001195	.001173	.000954	.000942	.000937	.000925	.001007	.001048	.001252	.001210
1500	.001620	.001606	.001310	.001325	.001322	.001311	.001500	.001521	.001872	.001819
2000	.001956	.001963	.001612	.001636	.001643	.001655	.001947	.001951	.002428	.002380
3000	.002497	.002519	.002130	.002163	.002218	.002234	.002702	.002688	.003377	.003440
4000	.002955	.002949	.002572	.002582	.002702	.002705	.003304	.003311	.004190	.004223
6000	.003677	.003626	.003254	.003242	.003462	.003452	.004262	.004317	.005533	.005640
8000	.004200	.004204	.003736	.003772	.004037	.004039	.005062	.005120	.006676	.006790
10000	.004650	.004698	.004210	.004221	.004536	.004523	.005787	.005817	.007747	.007761

TABLE X

Solubility of Ethane in Water: Comparison of Graphically Smoothed Data with Thermodynamically Smoothed Values

Pressure psia	100°F		160°F		220°F		280°F		340°F	
	Mol Fraction Ethane in the Water-Rich Phase									
	Graph.	Thermo.	Graph.	Thermo.	Graph.	Thermo.	Graph.	Thermo.	Graph.	Thermo.
400	.000596	.000518	.000356	.000352	.000290	.000332	.000343	.000361	.000345	.000375
600	.000717	.000677	.000491	.000481	.000443	.000469	.000514	.000533	.000593	.000609
800	.000763	.000764	.000573	.000579	.000578	.000584	.000677	.000682	.000836	.000819
1000	.000718	.000786	.000629	.000652	.000677	.000679	.000814	.000812	.001037	.001007
1500	.000817	.000825	.000727	.000748	.000841	.000845	.001068	.001064	.001403	.001400
2000	.000848	.000857	.000792	.000798	.000952	.000944	.001233	.001237	.001681	.001691
3000	.000912	.000913	.000882	.000869	.001091	.001069	.001452	.001458	.002113	.002146
4000	.000971	.000971	.000960	.000934	.00117	.001161	.001587	.001603	.002366	.002383
6000	.001067	.001045	.001061	.001015	.001286	.001300	.001785	.001799	.002689	.002769
8000	.001122	.001118	.001121	.001120	.001398	.001409	.001913	.001934	.003002	.003039
10000	.001133	.001175	.001177	.001193	.001516	.001504	.002012	.002029	.003316	.003241

TABLE XI

Solubility of Propane in Water: Comparison of Graphically Smoothed Data with Thermodynamically Smoothed Values

Pressure psia	100°F		130°F		160°F		190°F	
	Mol Fraction Propane in the Water-Rich Phase							
	Graph.	Thermo.	Graph.	Thermo.	Graph.	Thermo.	Graph.	Thermo.
200	.000204	.000210	.000160	.000166	.000130	.000139	.000120	.000127
400	.000208	.000212	.000204	.000212	.000214	.000228	.000211	.000224
600	.000211	.000214	.000210	.000214	.000226	.000231	.000253	.000256
800	.000214	.000215	.000215	.000216	.000232	.000234	.000260	.000260
1000	.000217	.000217	.000218	.000218	.000236	.000236	.000264	.000264
1500	.000222	.000221	.000223	.000223	.000242	.000241	.000272	.000272
2000	.000226	.000225	.000228	.000227	.000246	.000246	.000278	.000278
2500	.000229	.000227	.000231	.000231	.000251	.000251	.000284	.000284
3000	.000230	.000230	.000236	.000235	.000254	.000254	.000288	.000288
4000		.000235		.000241		.000261		.000296
6000		.000242		.000251		.000269		.000306
8000		.000246		.000257		.000273		.000311
10000		.000248		.000261		.000274		.000312

TABLE XI (cont'd)

Solubility of Propane in Water: Comparison of Graphically Smoothed Data with Thermodynamically Smoothed Data

Pressure psia	220°F		250°F		280°F		310°F	
	Mol Fraction Propane in the Water-Rich Phase							
	Graph.	Thermo.	Graph.	Thermo.	Graph.	Thermo.	Graph.	Thermo.
200	.000118	.000121	.000117	.000119	.000116	.000114	.000115	.000112
400	.000217	.000218	.000231	.000226	.000248	.000238	.000268	.000248
600	.000280	.000281	.000311	.000303	.000345	.000332	.000380	.000364
800	.000305	.000305	.000356	.000351	.000409	.000399	.000463	.000454
1000	.000316	.000313	.000379	.000374	.000444	.000439	.000513	.000520
1500	.000326	.000326	.000400	.000399	.000493	.000494	.000616	.000622
2000	.000336	.000336	.000414	.000416	.000525	.000524	.000686	.000680
2500	.000345	.000345	.000429	.000430	.000550	.000556	.000733	.000728
3000	.000353	.000353	.000444	.000443	.000575	.000577	.000770	.000770
4000		.000366		.000464		.000606		.000849
6000		.000385		.000497		.000665		.000991
8000		.000397		.000520		.000712		.001123
10000		.000403		.000537		.000757		.001249

TABLE XII

Modified Henry's Law Constants and Partial Molal Volumes of Dissolved Gases

Temperature °F	Methane		Ethane		Propane		Hydrogen		Nitrogen	
	Log K' Psia/M.F.	$\bar{v}_2$ Cu Ft/lb mol	Log K' Psia/M.F.	$\bar{v}_2$ Cu Ft/lb mol	Log K' Psia/M.F.	$\bar{v}_2$ Cu Ft/lb mol	Log K' Psia/M.F.	$\bar{v}_2$ Cu Ft/lb mol	Log K' Psia/M.F.	$\bar{v}_2$ Cu Ft/lb mol
32	-	-								
77	-	-	-	-	-	-	6.4291	.3195	-	.519
100	5.841	.570	5.780	.849	5.8522	1.220	6.5232	.3115	6.6055	.526
122	-	-	-	-	-	-	-	-	-	-
130	-	-	-	-	5.9835	1.222	6.5544	.3133	6.7120	.534
160	5.956	.605	5.970	.858	6.0593	1.285	-	-	-	-
167	-	-	-	-	-	-	-	-	-	-
190	-	-	-	-	6.1063	1.317	-	-	6.7509	.545
212	-	-	-	-	-	-	6.5029	.3420	6.7330	.579
220	5.969	.652	5.996	.917	6.1158	1.303	-	-	-	-
250	-	-	-	-	6.1027	1.275	-	-	-	-
280	5.9070	.667	5.931	1.021	6.0714	1.226	-	-	-	-
310	-	-	-	-	6.0320	1.020	-	-	-	-
340	5.815	.677	5.827	1.025	-	-	-	-	-	-

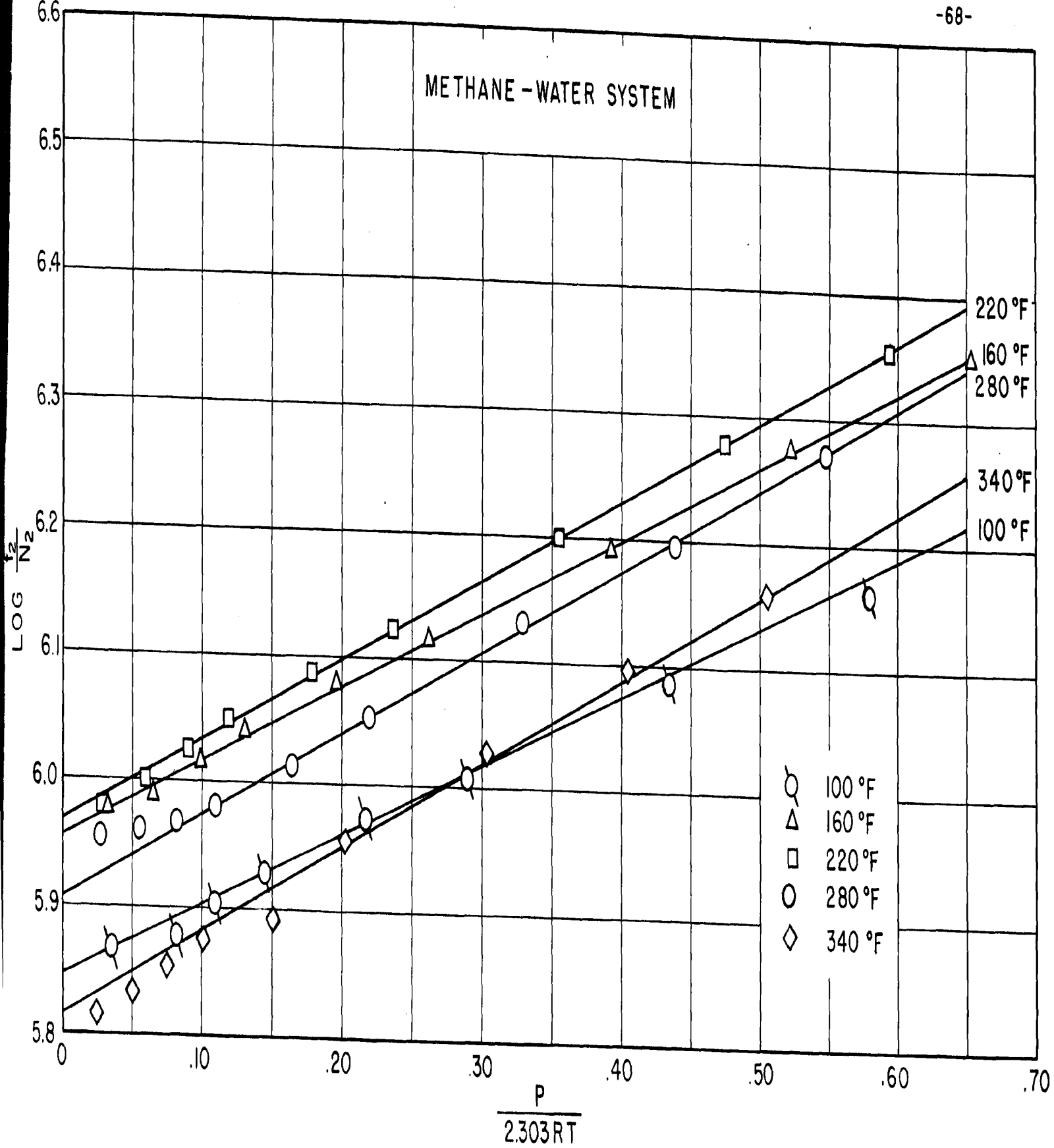


FIGURE 16 PLOTS FOR THE DETERMINATION OF CONSTANTS IN THE THERMODYNAMIC EQUATION FOR THE SOLUBILITY OF METHANE IN WATER

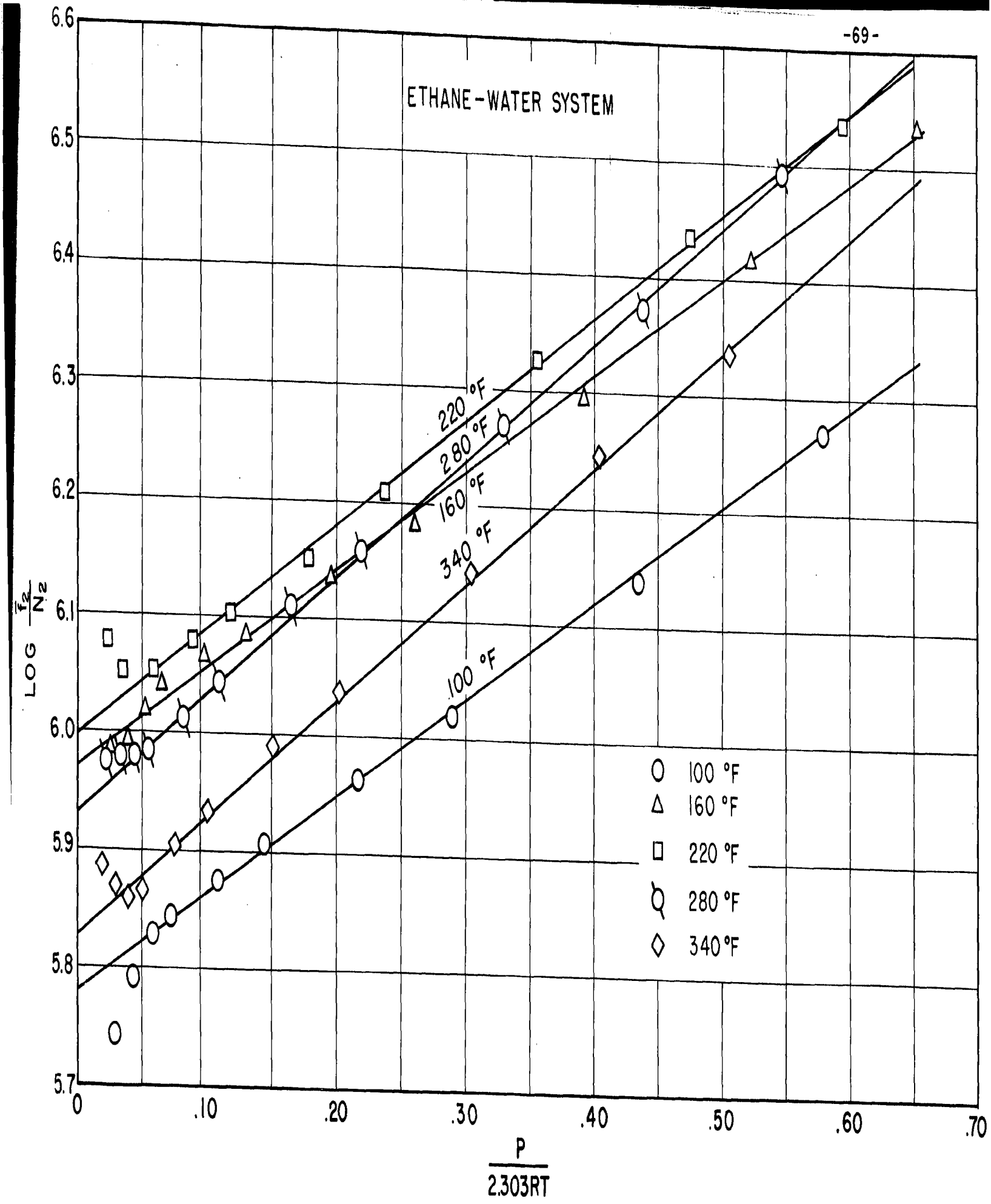


FIGURE 17 PLOTS FOR THE DETERMINATION OF CONSTANTS IN THE THERMODYNAMIC EQUATION FOR THE SOLUBILITY OF ETHANE IN WATER

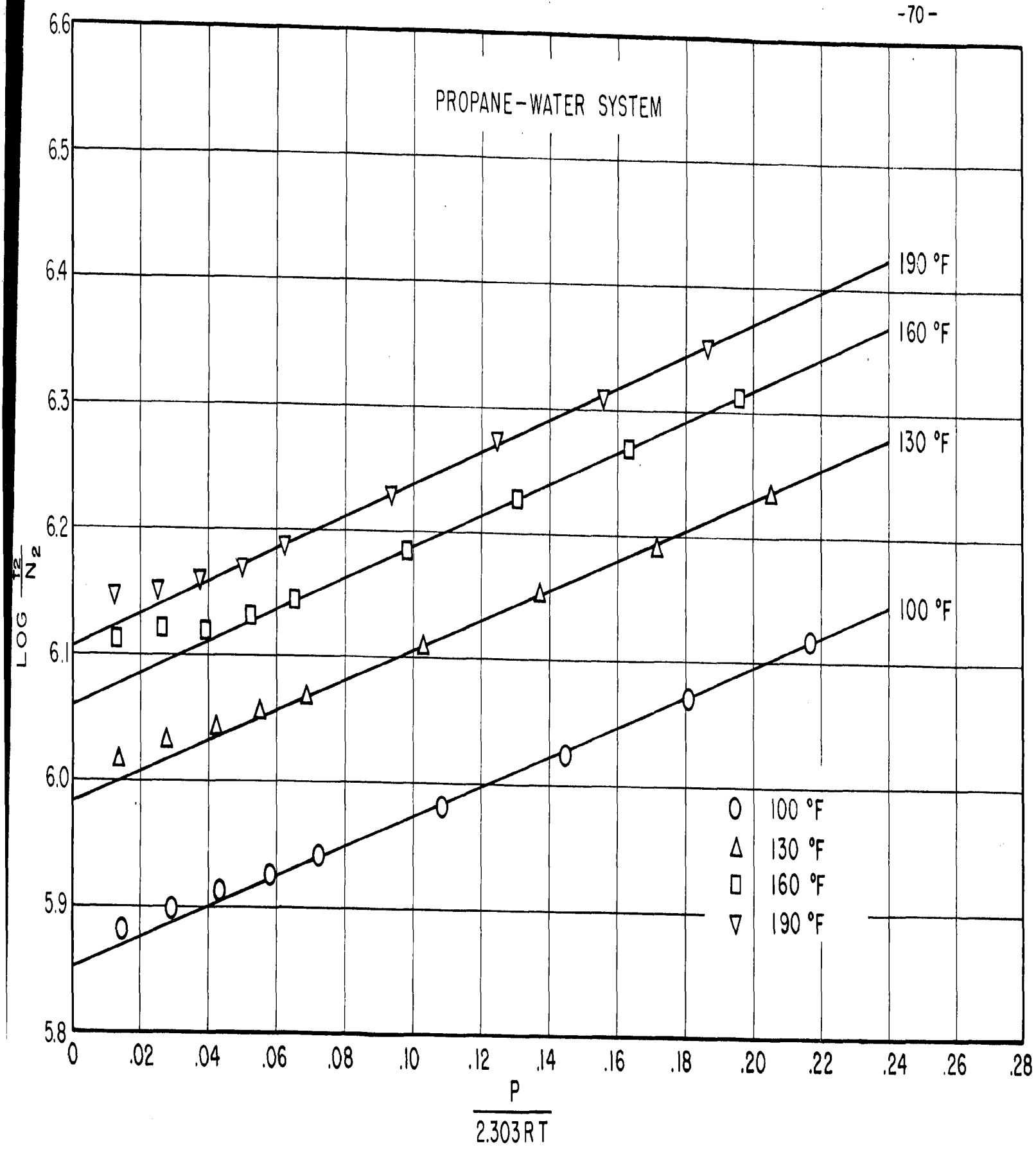


FIGURE 18 A PLOTS FOP THE DETERMINATION OF CONSTANTS IN THE THERMODYNAMIC EQUATION FOR THE SOLUBILITY OF PROPANE IN WATER

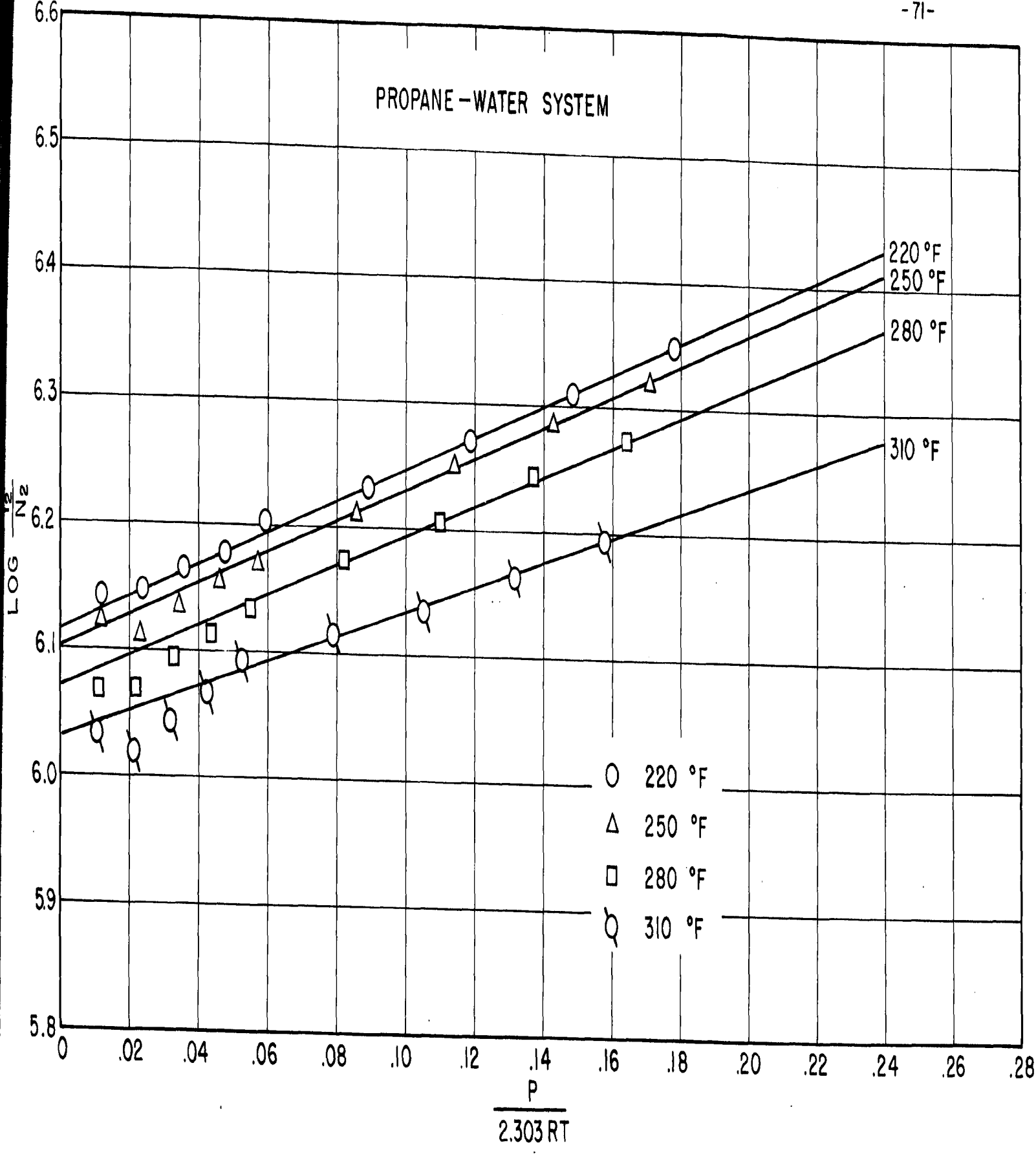


FIGURE 18 B PLOTS FOR THE DETERMINATION OF CONSTANTS IN THE THERMODYNAMIC EQUATION FOR THE SOLUBILITY OF PROPANE IN WATER

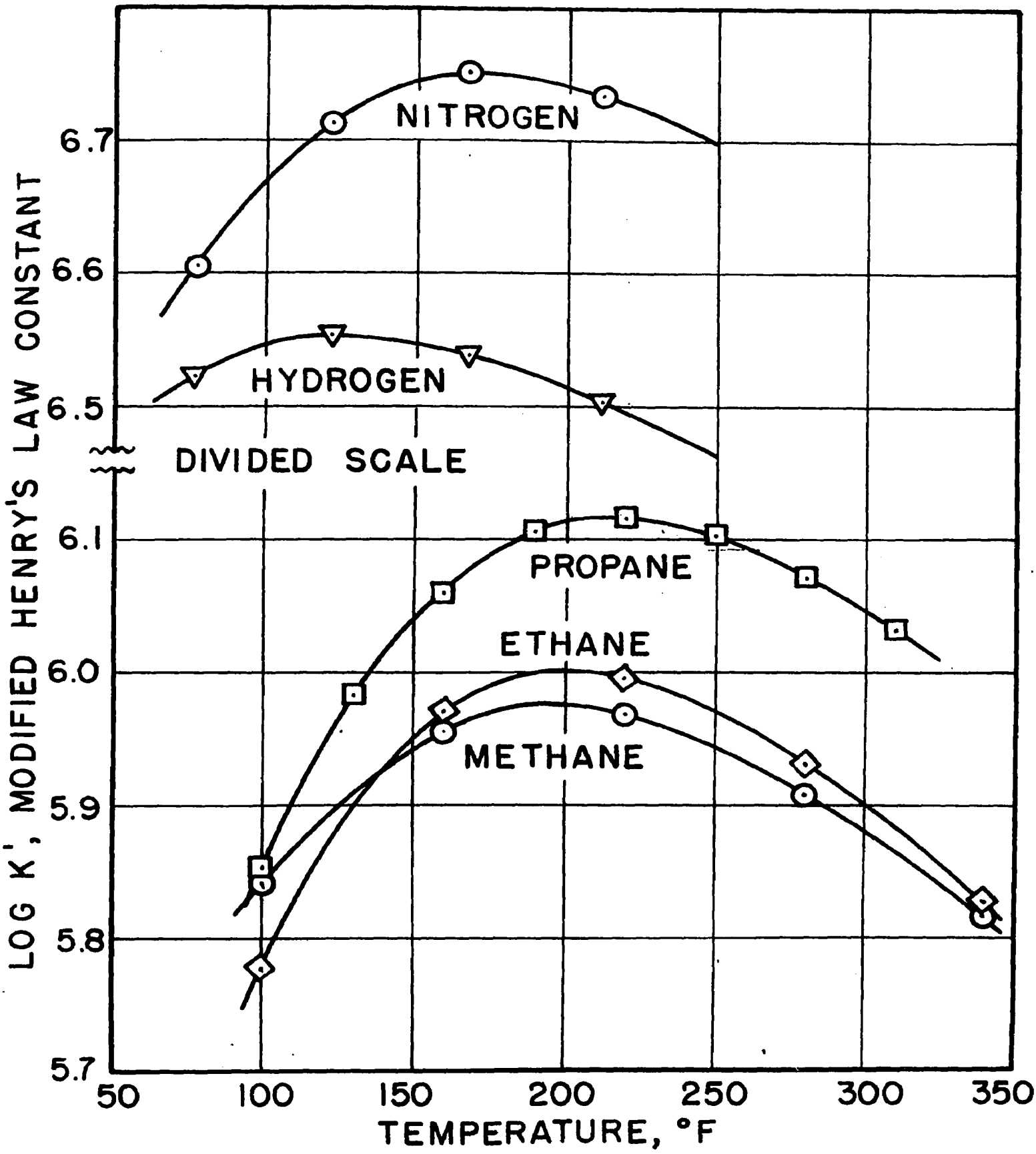


FIGURE 19 MODIFIED HENRY'S LAW CONSTANTS FOR THE SOLUBILITY OF PURE LIGHT HYDROCARBON, HYDROGEN, AND NITROGEN IN WATER

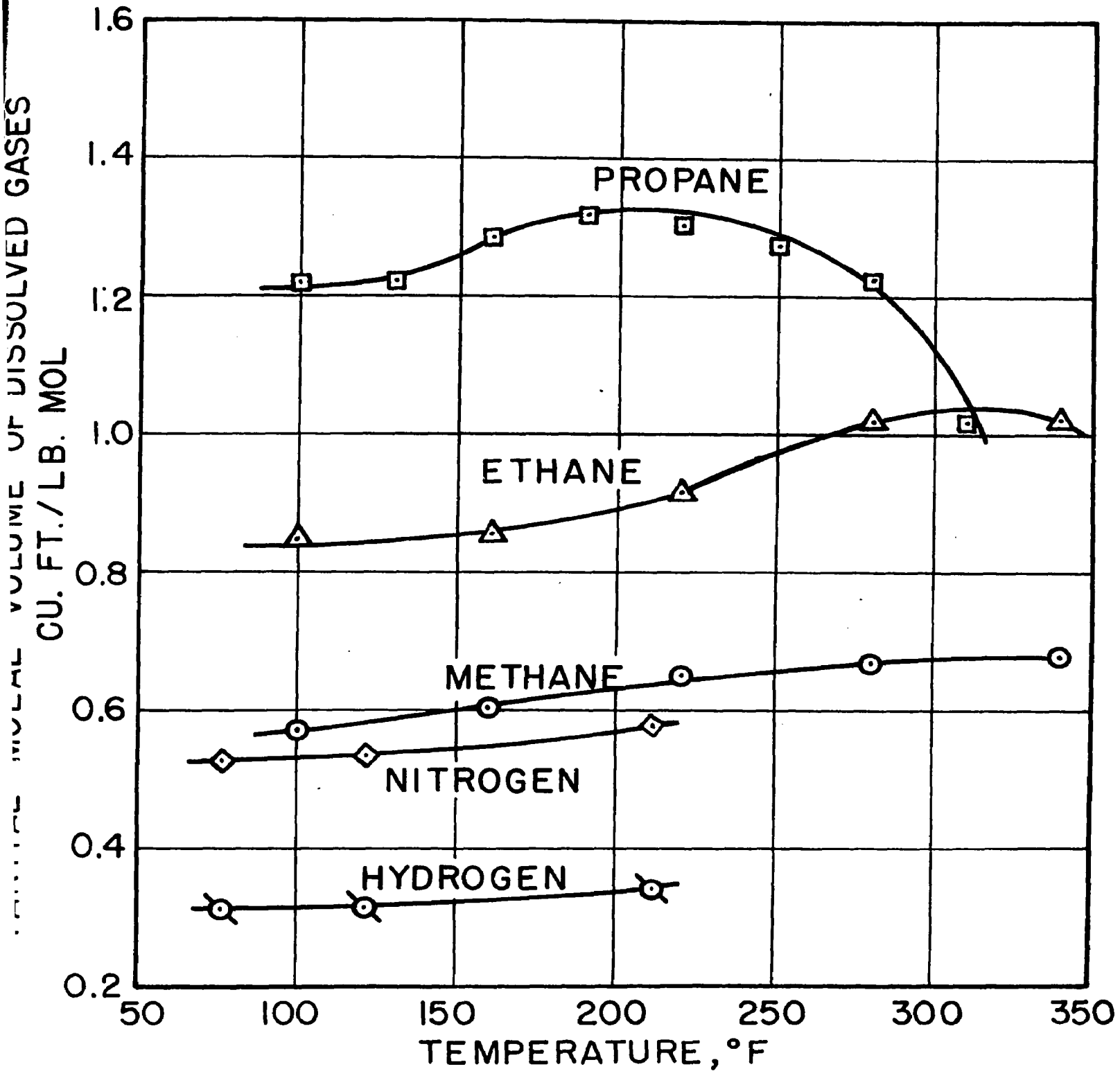


FIGURE 20 PARTIAL MOLAL VOLUMES OF PURE HYDROCARBONS, HYDROGEN, AND NITROGEN DISSOLVED IN WATER

CALCULATIONS OF THE EFFECT OF DISSOLVED HYDROCARBON GASES ON THE DENSITY OF WATER AT HIGH PRESSURES

The partial molal volume of the pure hydrocarbons dissolved in water has been applied to calculate the effect of dissolved hydrocarbons on the density of water. The computed densities have been compared with the experimental densities of water saturated with a natural gas under pressure. These experimental densities were obtained by Dodson and Standing (14) for several isotherms up to 5000 psi. The composition of the natural gas, its solubility in water, the experimental densities and the calculated densities are listed in Table 13.

Dodson and Standing did not determine the phase compositions. Since the natural gas was predominantly methane, the concentration of each constituent in water is taken to be proportional to its concentration in the original gas. By applying the law of additive volumes, the specific volume of the mixture, V, was calculated from the following relationship (27):

$$V = \bar{v}_1 x_1 + \bar{v}_2 x_2 + \bar{v}_3 x_3 + \bar{v}_4 x_4 \qquad (26)$$

where subscripts 1, 2, 3, and 4 designate water, methane, ethane, and propane and heavier molecular weight hydrocarbons, respectively. The $\bar{v}$'s denote the partial molal volumes, and the $\bar{x}$'s denote the concentrations. Since

all the concentrations encountered were less than 0.0004 mol fraction hydrocarbon, $\bar{v}_1$, was taken as the specific volume of pure water at the saturation temperature and pressure.

The computed and experimental densities for the water solutions and the densities for pure water are plotted for isotherms at 100, 150, 200, and 250 deg. F up to 5000 psi in Figure 21. In general, the agreement between the experimental and the computed densities is good up to 3000 psi. With increased pressure the deviation increases until at 5000 psi, the calculations are only able to account for 60% of the density decrease resulting from the solution of the hydrocarbons in the water.

It may be recalled that Figures 16, 17, and 18 show that the slopes of the isothermal curves from which the hydrocarbon $\bar{v}$'s were determined are most representative at high pressures. Contrary to this observation, is the observation that the deviations between the experimental and calculated densities of water saturated with hydrocarbons increase with pressure. Hence, the values of $\bar{v}$'s which describe the vapor-liquid equilibria relationships best, i. e. at the high pressures, are the poorest in describing the volume changes caused by the solution of the hydrocarbons in water.

There is a further point of interest. At high pressures, the deviations between the experimental and calculated densities are in a direction which indicates that the partial molal volumes of the hydrocarbon increase with increasing pressures. Although the present investigation should not be taken as a conclusive evidence of this astonishing fact, because of its limited treatment, the partial molal volumes of some substances have been known to increase with pressure at constant temperature and composition (1). There also remains the likely alternative that the partial molal volume of water, $\bar{v}_1$, undergoes a change under the elevated pressure conditions.

TABLE XIII

Composition of Natural Gas A. Solubility of Natural Gas A in Water, and Comparison of Experimental and Calculated Densities of Water Saturated with Natural Gas A

(A)

Composition of Natural Gas A:

Constituents	Mol Fraction
Methane	0.8851
Ethane	0.0602
Propane	0.0318
Isobutane	0.0046
Normal Butane	0.0085
Isopentanes & Heavier	0.0098
	1.0000

Gravity = 0.655

(B)

Solubility of Natural Gas A in Water:

Pressure	Temperature °F			
	100	150	200	250
psia	Mol Fraction Gas in Liquid			
1000	.00121	.00106	.00100	.00099
2000	.00187	.00162	.00164	.00168
3000	.00238	.00206	.00209	.00219
4000	.00275	.00238	.00244	.00258
5000	.00309	.00262	.00272	.00288

TABLE XIII (cont'd)

(C)

Comparison of Experimental and Calculated Densities of Water Saturated with Natural Gas A:

Pressure psia	100°F			150°F			200°F			250°F		
	Density, gms/cc											
	Pure Water	Expt'l	Calc.	Pure Water	Expt'l	Calc.	Pure Water	Expt'l	Calc.	Pure Water	Expt'l	Calc.
1000	.9965	.9958	.9952	.9839	.9821	.9827	.9666	.9652	.9654	.9460	.9449	.9448
2000	.9995	.9979	.9975	.9867	.9841	.9848	.9695	.9674	.9675	.9493	.9470	.9470
3000	1.0024	.9998	.9999	.9896	.9860	.9873	.9726	.9692	.9700	.9526	.9489	.9499
4000	1.0052	1.0016	1.0021	.9923	.9877	.9895	.9756	.9709	.9726	.9557	.9506	.9525
5000	1.0081	1.0034	1.0047	.9951	.9893	.9921	.9784	.9726	.9750	.9589	.9523	.9552

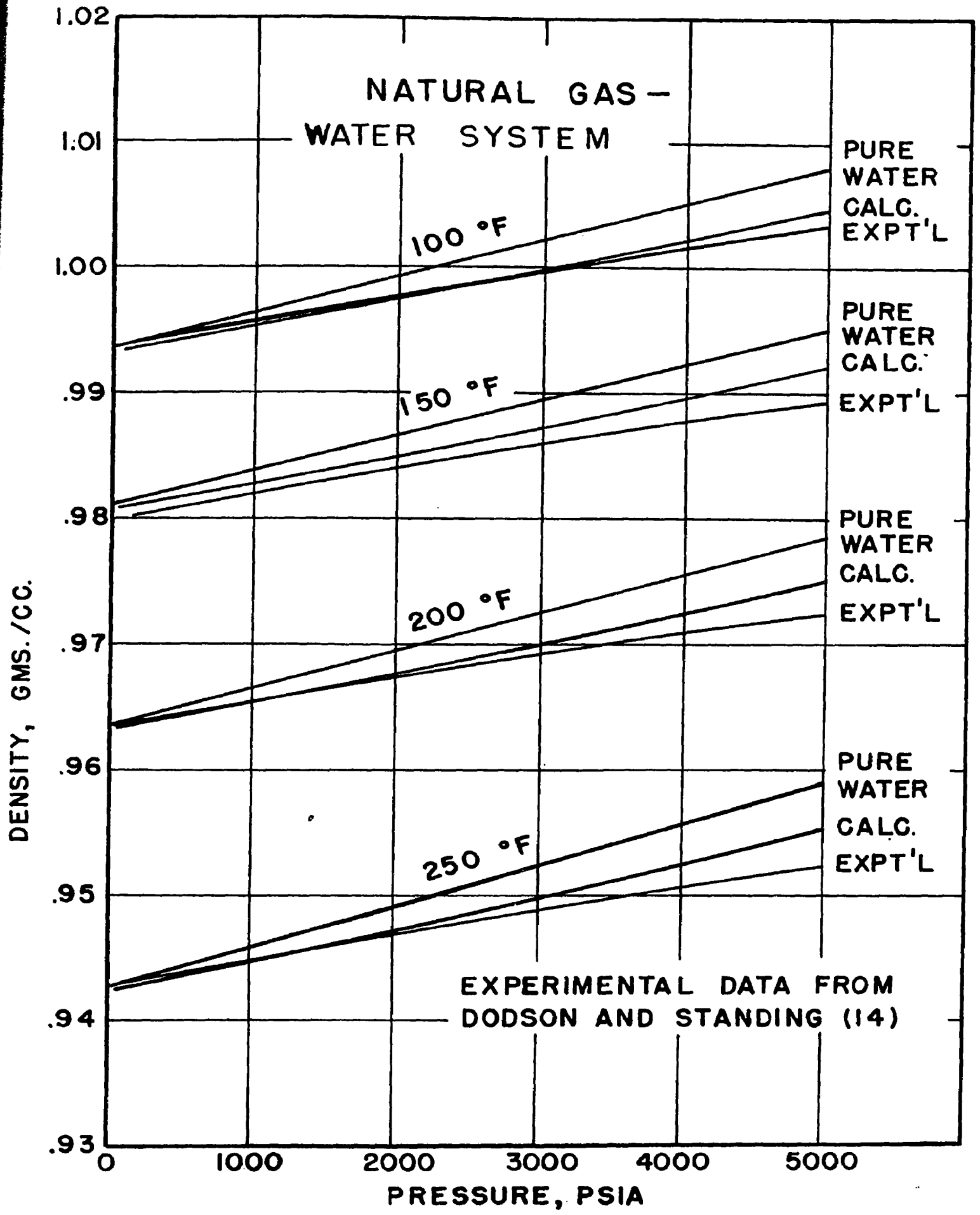


FIGURE 21 EXPERIMENTAL AND CALCULATED
NSITIES OF WATER SATURATED WITH NATURAL GAS A

THE INTERRELATION OF MINIMUM SOLUBILITY, HENRY'S LAW AND THE VOLUMETRIC BEHAVIOR OF THE SOLUTE-RICH PHASE

The phenomenon of minimum isobaric solubility has been widely reported and discussed for various systems by several authors (8), (9), (10), (36), (46), (47). Keunen (21), (22) applied his understanding of the behavior of binary mixtures in the critical retion to predict the existence of a region of minimum solubility.

Aroyan (2) has discussed isobaric minimum solubility on a general basis by interrelating it with reverse solubility, maximum solubility, and isobaric retrograde condensation. Minimum isobaric solubility is said to occur when the concentration of a solute in a solution undergoes a minimum at some temperature. In reverse solubility there is an increase in the solubility of the solute with temperature. Maximum solubility occurs when a relative maximum appears in the isobaric solubility curve at the point where there is a transition from reverse solubility to normal solubility with increased temperature.

Aroyan's conclusions may be summarized as follows:

(1) that reverse solubility always occurs whenever minimum solubility occurs,

(2) that the occurrence of reverse solubility does not necessarily mean that a minimum solubility exists for some lower temperature, (there remaining the possibility that a third phase is encountered before the minimum solubility occurs, as in the hydrogen-n-butane system).

(3) that a maximum in the bubble point corresponds to a minimum solubility, hence reverse solubility and minimum solubility may be expected in certain regions of the phase diagram for all two component systems,

(4) that a minimum in the bubble point curve corresponds to a maximum in the solubility curve,

(5) that the region of reverse solubility is increased as the extent of the bubble-point-dew point envelope in the critical region is increased,

(6) that a region of reverse solubility is a region of isobaric retrograde vaporization.

The phenomenon of minimum solubility may be illustrated geometrically by the way in which the solubility isotherms cross on a pressure-composition diagram for a binary system (2). The same approach may be extended to relate minimum and maximum solubility to Henry's Law and to the volumetric behavior of the solute-rich phase. Figure 19 shows that the Henry's Law constants, K, for pure non polar gases, such as those treated here, increase with increasing temperature, go through a maximum, then decrease. These three sections of the curve are to be discussed in relation to minimum and maximum solubility.

For K decreasing with increasing temperature, either a minimum isobaric solubility, Figure 22A, or a maximum isobaric solubility, Figure 22B, can occur, depending on the manner in which the lines or the isothermal elements of the surface cross. The minimum solubility exhibited

by methane in water at high temperatures and low pressures illustrated in Figure 22A is of this type.

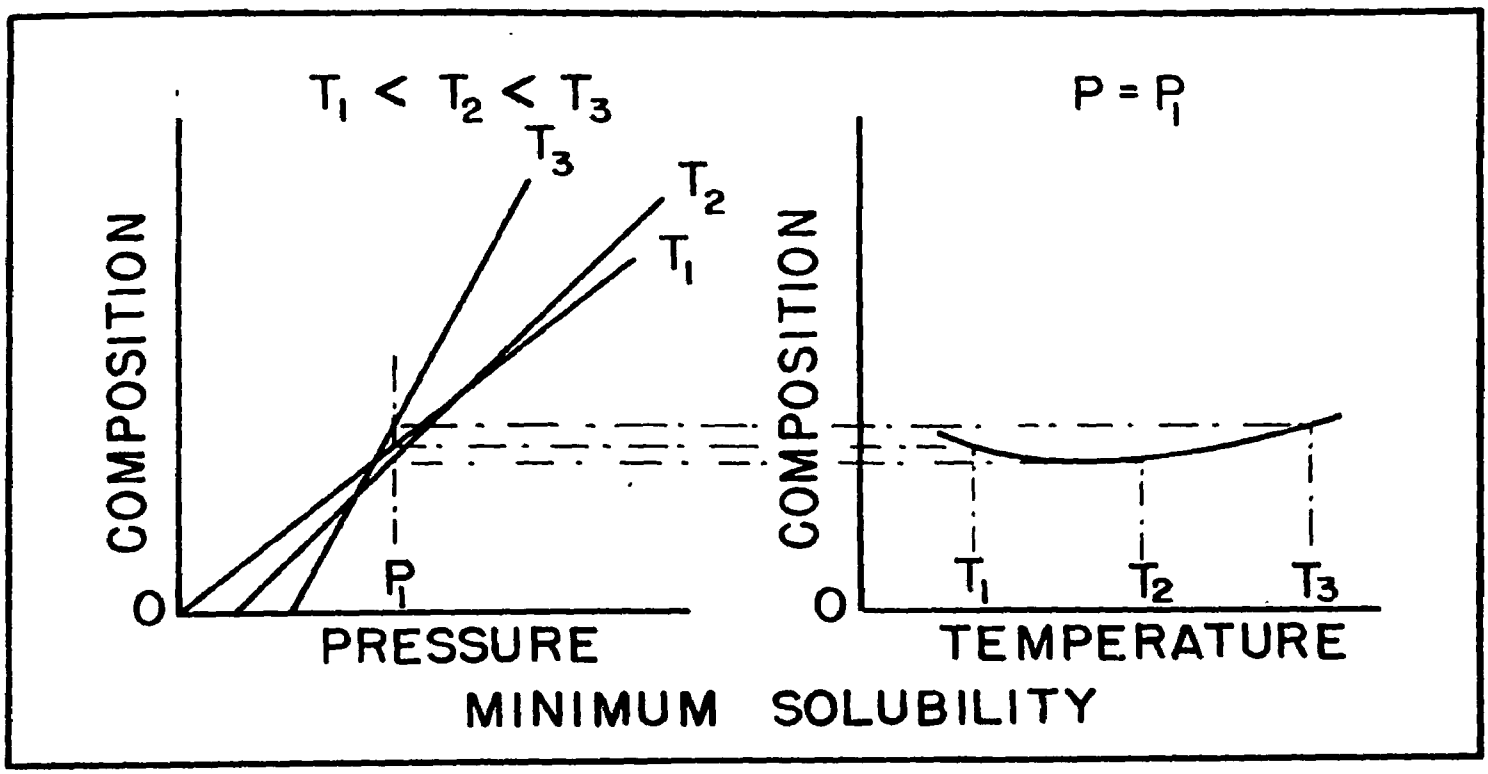
Figure 22A and 22B have been drawn showing the system to obey Henry's Law, however, non-ideal behavior in the solute-rich phase give the same relative crossing of the lines to produce minimum solubility for some temperature and maximum solubility at some higher temperature.

For the region in which K increases with temperature, however, it is necessary that the solute-rich phase behave as a non-ideal gas in order to produce a maximum or minimum solubility as may be seen from Figure 23A and 23B. The effect of non-ideal behavior of the solute-rich phase on the isothermal solubility curves is illustrated most clearly in Figure 5.

Finally, there remains the case in which Henry's Law constants undergo a maximum value. In this case, Figure 24, if ideal gas behavior is assumed in the solute-rich phase, the minimum solubility is produced at the temperature where K undergoes a maximum.

Thus, the existence of maximum solubilities may be predicted qualitatively from the solubility data obtained at atmospheric conditions and the volumetric behavior of the solute-rich phase, which, for the hydrocarbon-water systems can be estimated from the volumetric behavior of the anhydrous solute.

A



B

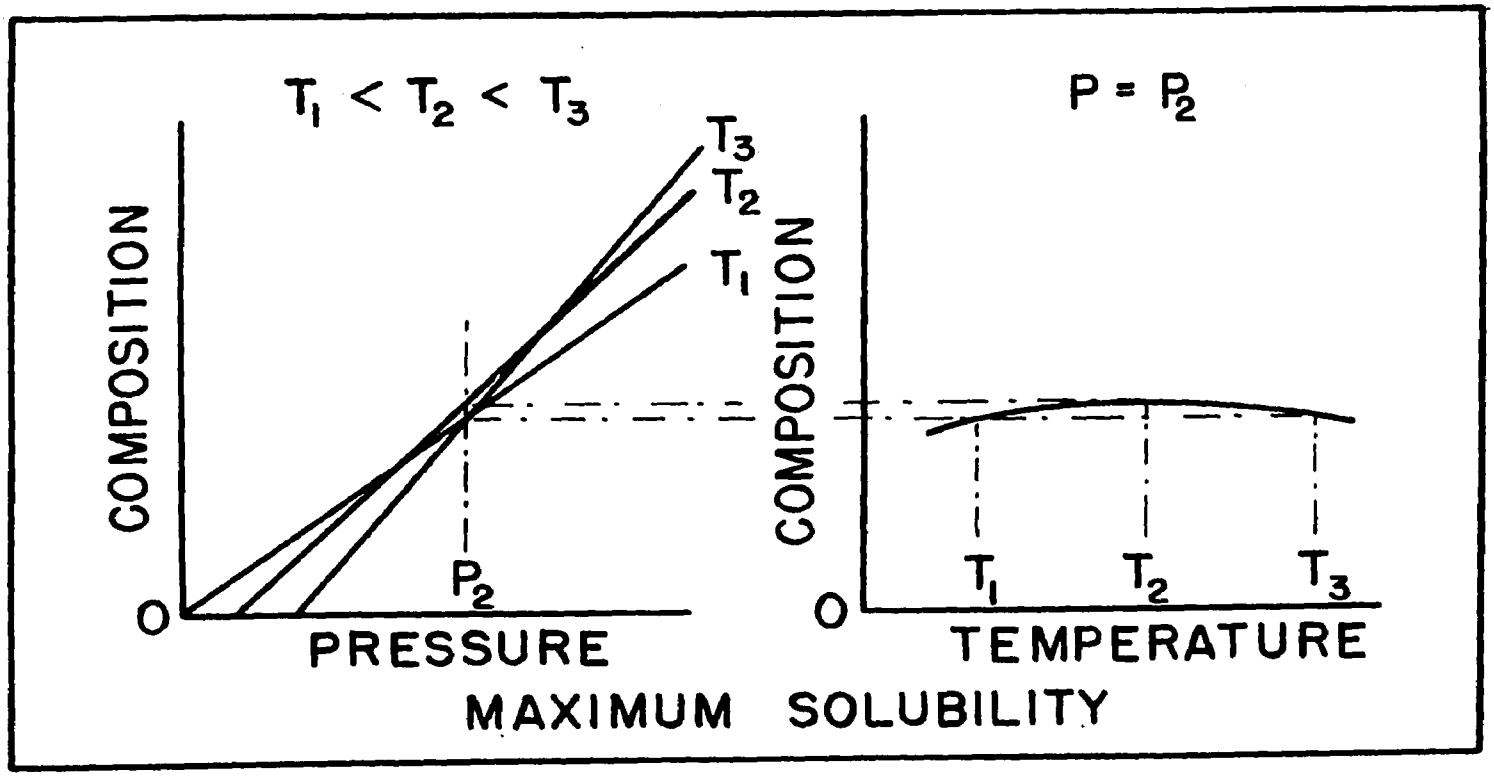


FIGURE 22 MINIMUM AND MAXIMUM SOLUBILITY FOR HENRY'S LAW CONSTANT DECREASING WITH TEMPERATURE

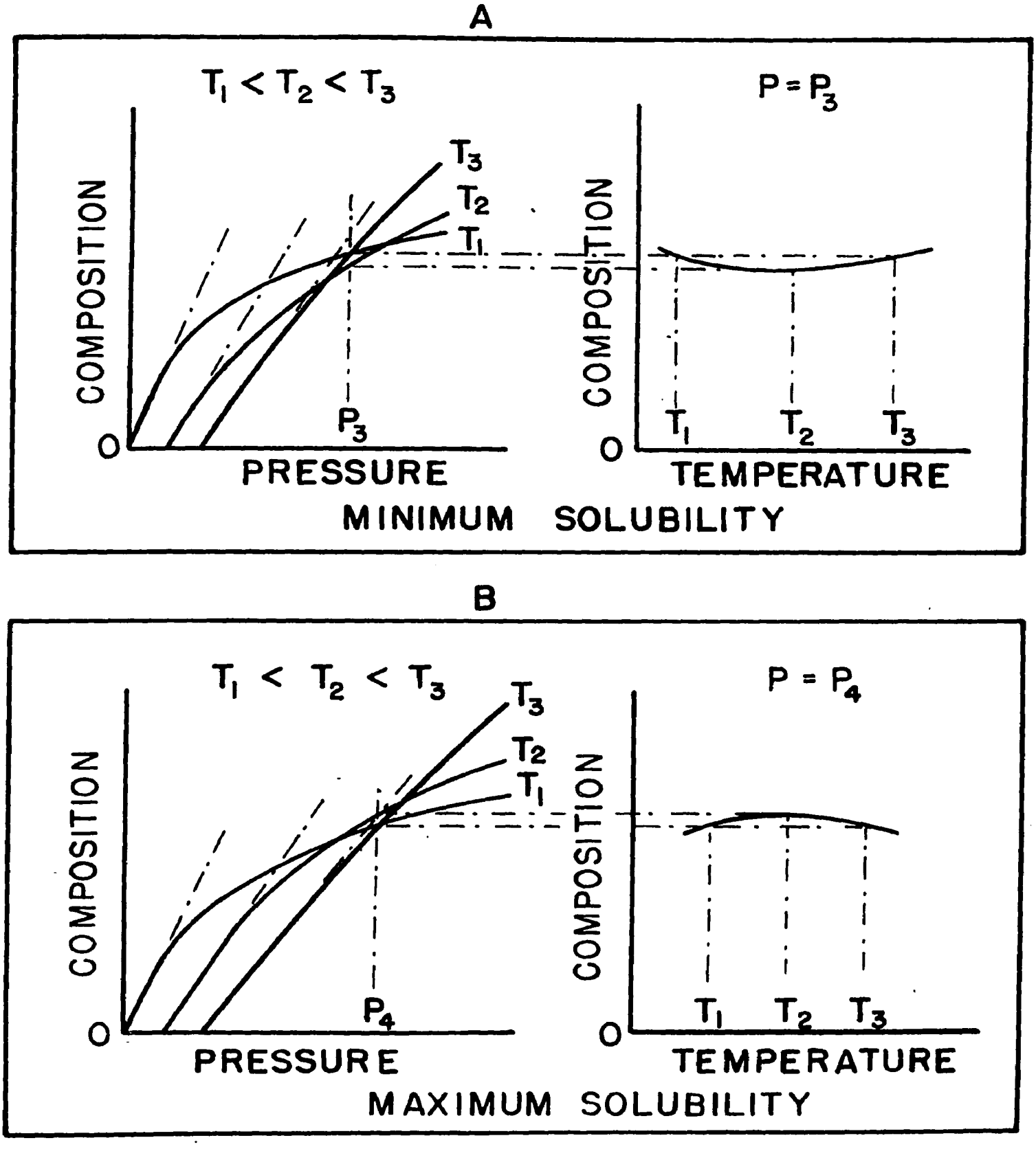


FIGURE 23 MINIMUM AND MAXIMUM SOLUBILITY FOR HENRY'S LAW CONSTANT INCREASING WITH TEMPERATURE

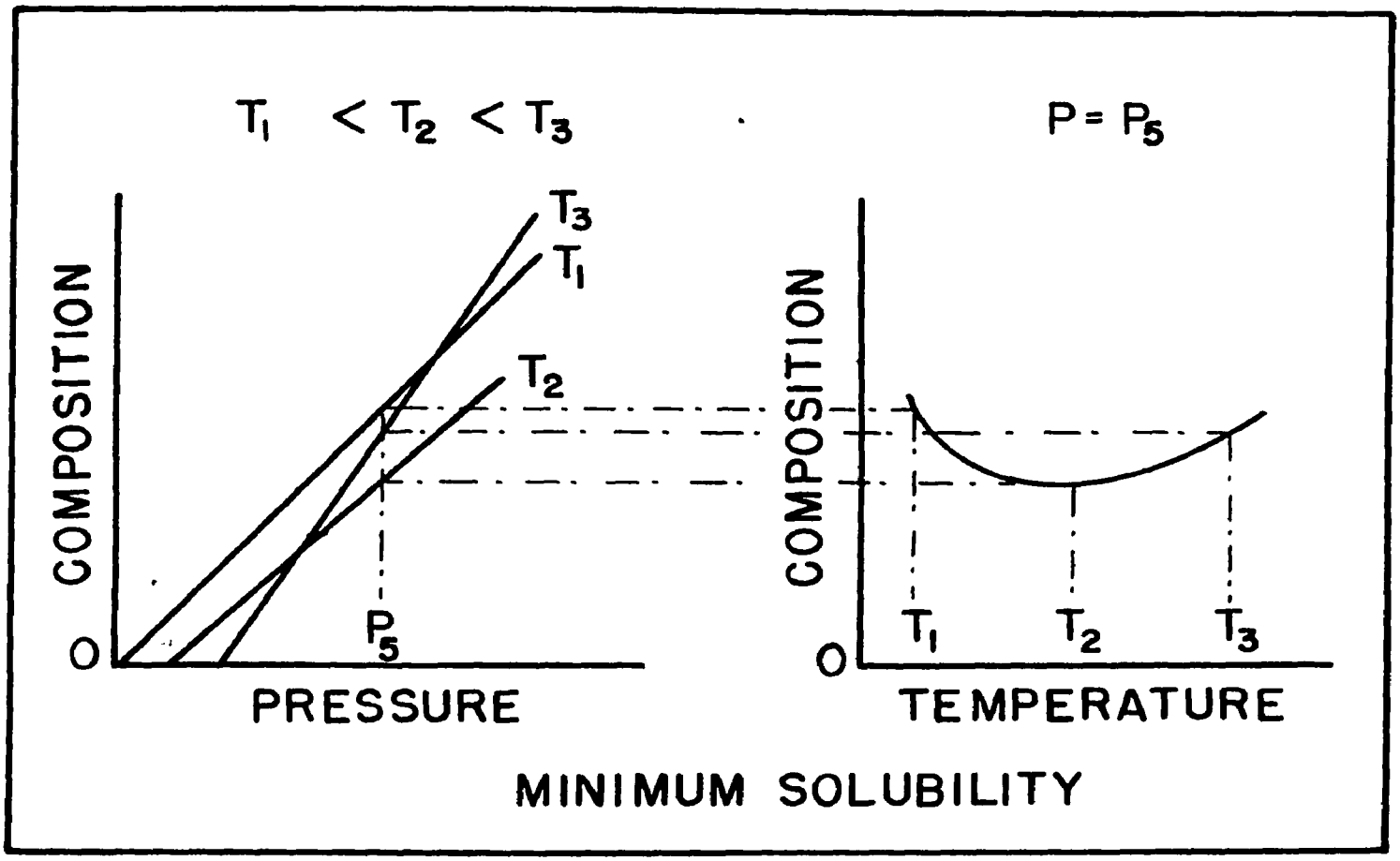


FIGURE 24 MINIMUM SOLUBILITY FOR THE TEMPERATURE REGION OF MAXIMUM HENRY'S LAW CONSTANT

PART II

EXPERIMENTAL EQUIPMENT, PROCEDURES, AND TECHNIQUES FOR THE DETERMINATION OF PROPANE-WATER VAPOR-LIQUID EQUILIBRIA RELATIONSHIPS

EXPERIMENTAL EQUIPMENT

The experimental equipment used in this work consisted of the following basic units:

(1) a high pressure vapor-liquid equilibria apparatus,

(2) an analytical train for the analysis of the hydrocarbon-rich phases,

(3) an apparatus for the analysis of the water-rich phase, and

(4) a source of high pressure mercury used for charging and sampling operations.

Schematic flow diagrams of each unit is presented in Figures 25, 26, 27, and 28, respectively.

Vapor Liquid Equilibria Apparatus:

The high pressure equilibrium cell used in this investigation was constructed by Chaddock (7). The vapor-liquid equilibria apparatus used was constructed by McKetta and has been thoroughly discussed by him (27). Some revisions of the apparatus have been made by the author in order to adapt the equipment to the study of the propane-water system. Only the detailed discussion of the revisions are given here, otherwise the reader is referred to (27) for details.

The cell was machined from a forged steel billet and designed for a pressure of 5000 psi. Its net capacity is approximately 1000 cc. The cell was constructed with a Jerguson-type window so that the relative quantities of

the coexisting phases could be observed. A thermostatically controlled air bath surrounding the cell served to maintain it at thermal equilibrium.

Phase equilibria were accomplished by means of an electrically powered stirrer mounted entirely within the cell. A midget induction motor powers the impeller which rotates within a closely fitting steel confining tube. The heavier liquid phase is lifted in this tube to the top of the cell by the action of the impeller and dropped through the hydrocarbon phase or phases. In order to minimize the localized heating by the induction motor, it was operated intermittently by an electronic on-off timer.

The induction motor used was a KYAB 2115 (10V-60 cycles A.C.) vacuum impregnated motor manufactured by the Barber-Colman Company of Rockford, Illinois. The metallic surface bearings were replaced by the ball bearings in order to minimize the friction. No lubrication was used in the motor during operation. The impeller bearing was machined from a piece of soft Iron Oilite obtained from the Amplex Division of the Chrysler Corporation in Detroit, Michigan. The stirrer arrangement was a source of considerable difficulties.

Ports located at 4 different and appropriate positions in the cell were used for charging, sampling, and discharging the contents of the cell. Figure 25 gives a flow diagram of the apparatus showing the relative positions

of the sampling ports, the auxiliary valves, the gauges, and the flow lines.

The vapor phase sampling line, $V-T_4-16$, was wrapped with a resistance heater in order to superheat the vapor sample leaving the cell. It was especially important that the condensation of the vapor phase be prevented when sampling in the 3-phase region. The heater also hastened the purging of any excess water remaining in the lines from previous runs.

Analytical Train for the Propane-Rich Phases:

The flow diagram for the analytical train used in the analysis of the hydrocarbon-rich phase is shown in Figure 26.. With the exception of the block needle valves A and B and the rubber tubing connections, the entire train was constructed of glass.

A glass case was placed around the dehydrite-filled U-tubes to prevent dust from settling on the tubes. A mercury bubbler placed directly behind the U-tubes served to indicate the sampling rate. The rubber tubing connections preceding the U-tubes were specially prepared to prevent the absorption of water from the atmosphere. No flexible rubber or plastic tubing impervious to the diffusion of water could be found. A satisfactory method of treating rubber to prevent the diffusion of water to lower concentrations has been developed by Pregl (31).

A wooden scale, checked for accuracy by means of a high precision cathetometer, was used to make the manometer readings. A calibrated bottle of 11.56 liter capacity was used as a receiver for the measurement of the quantity of dried propane in the sample. As a safety precaution, a heavy wire guard was placed over the bottle. The temperature of the gas within the bottle was registered on a calibrated thermometer whose bulb was located in the center of bottle M, Figure 26.

Air dried by passage through an ascarite tower and three dehydration towers was used to flush the train and the U-tubes at the beginning and end of each run, just prior to weighing the tubes.

Apparatus for the Analysis of the Water-Rich Phase:

Figure 27 is a flow diagram of the apparatus used for the analysis of the water-rich phase.

The concentric-tube cooler was constructed of 1" I.D. brass tubing 4 ft. long on the outside and a 1/4" O.D. by 3/32" I.D. stainless steel tubing concentric with the brass tubing. The inner tube served to transport the sample through the cooler. Water at substantially room temperature was used as the cooling medium. The sample was expanded to atmospheric pressure through valve S, Figure 27, located at the top of the cooler.

The pressure in the burette was maintained precisely at the barometric value by adjusting the mercury levelling bulb. A scale was fastened to the side of the water jacket so that the water head within the burette could be measured and taken into account in the adjustment of the levelling bulb. The burette was telescoped from a 100 cc gas burette to a 500 cc burette to give flexibility in the selection of sample sizes. A glass pyrex tube equipped with the proper inlets and outlets served as an isothermal jacket for the burette. Air was bled into the bottom of the water jacket to minimize the temperature gradients in the annulus. A thermometer placed in the annulus registered the temperature of the water in the jacket.

Pressurizing and Pressure Maintenance Unit:

The flow diagram of the pressurizing and pressure maintenance equipment is presented in Figure 28. The pressurizing unit, whose boundery is shown by the dotted line in Figure 28, has been discussed at length by Aroyan (2).

The pressurizing unit has been combined with an auxiliary mercury chamber for use in charging and sampling operations. High pressure mercury obtained from the compression unit is accompanied by a trace of oil. By using the pressurizing unit solely for the purpose of compressing

nitrogen gas and combining its use with the auxiliary chamber, absolutely clean mercury could be charged to the cell.

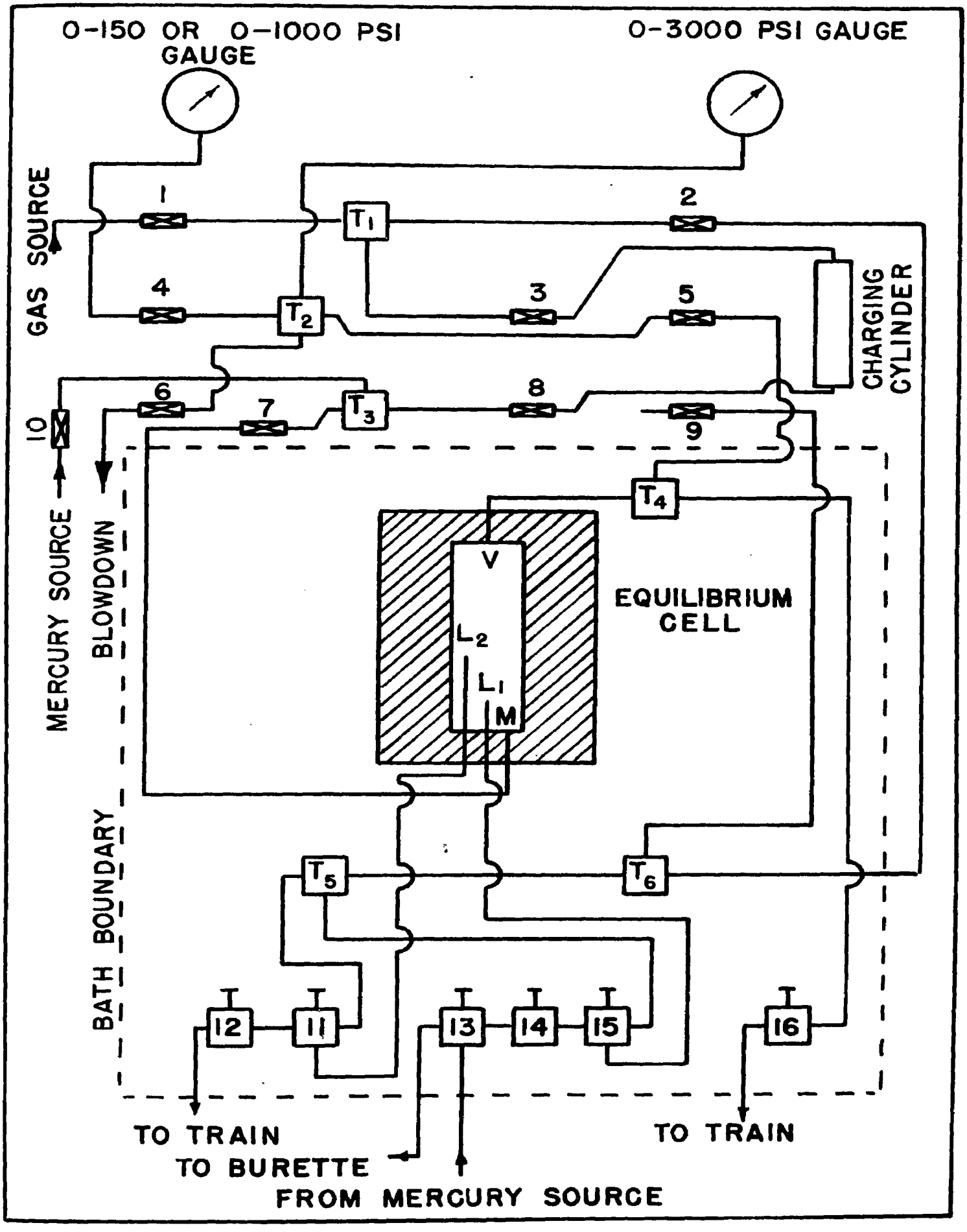


FIGURE 25 FLOW SHEET OF THE VAPOR-LIQUID EQUILIBRIA APPARATUS

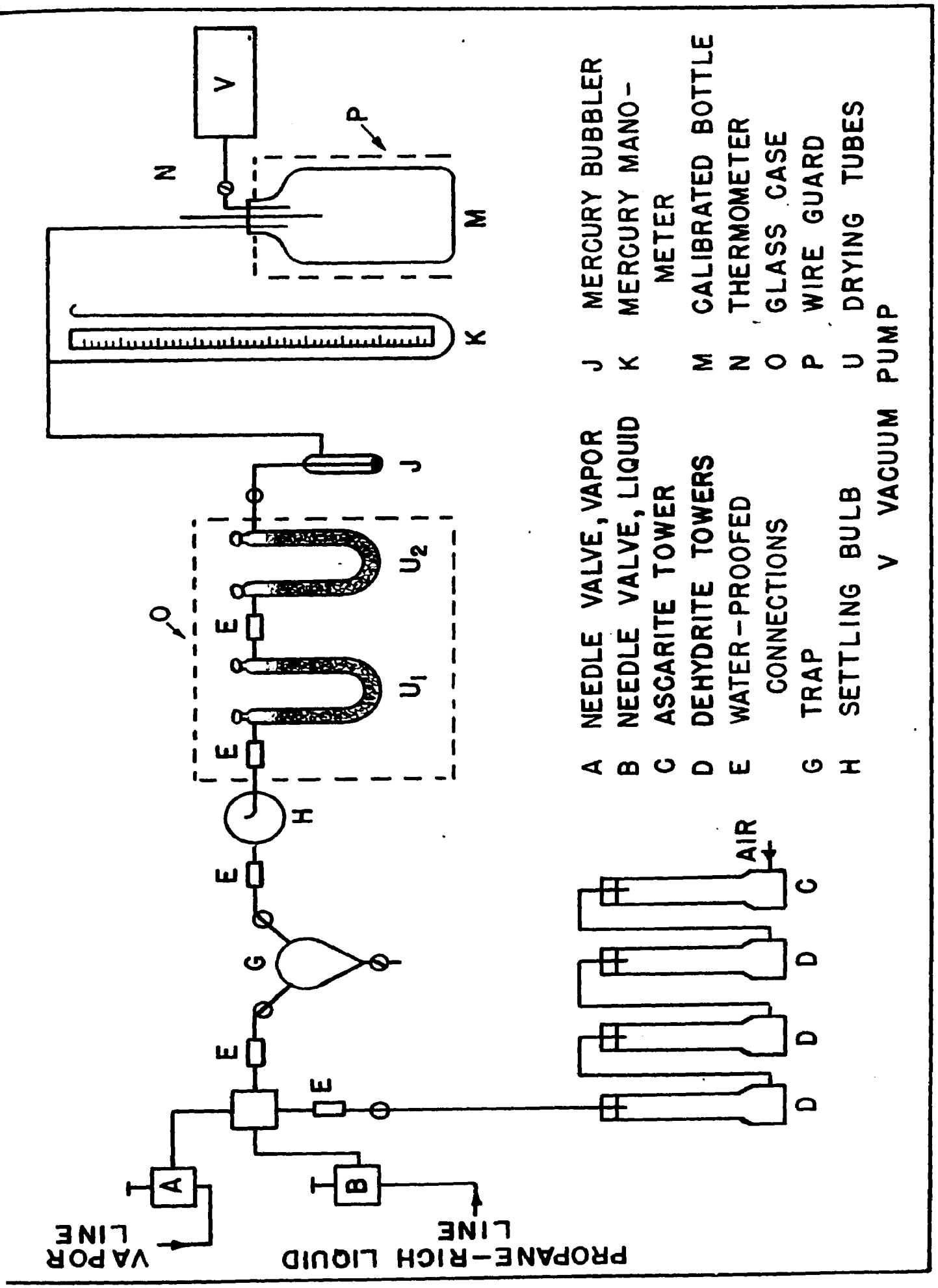
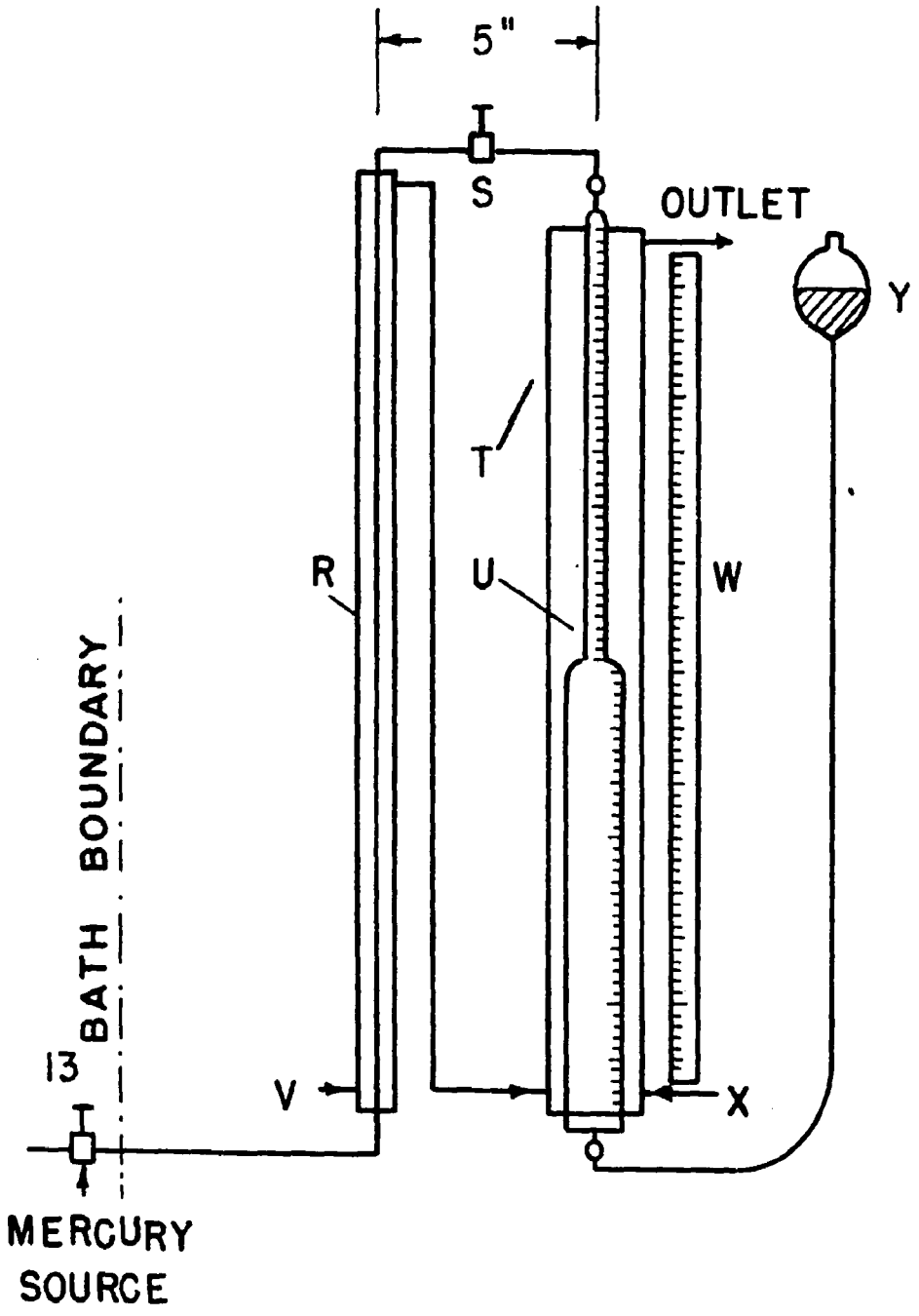


FIGURE 26 ANALYTICAL TRAIN FOR THE ANALYSIS OF THE HYDROCARBON-RICH PHASES



R CONCENTRIC-TUBE COOLER

S NEEDLE VALVE

T 70 MM. PYREX TUBING

U GAS-WATER BURETTE

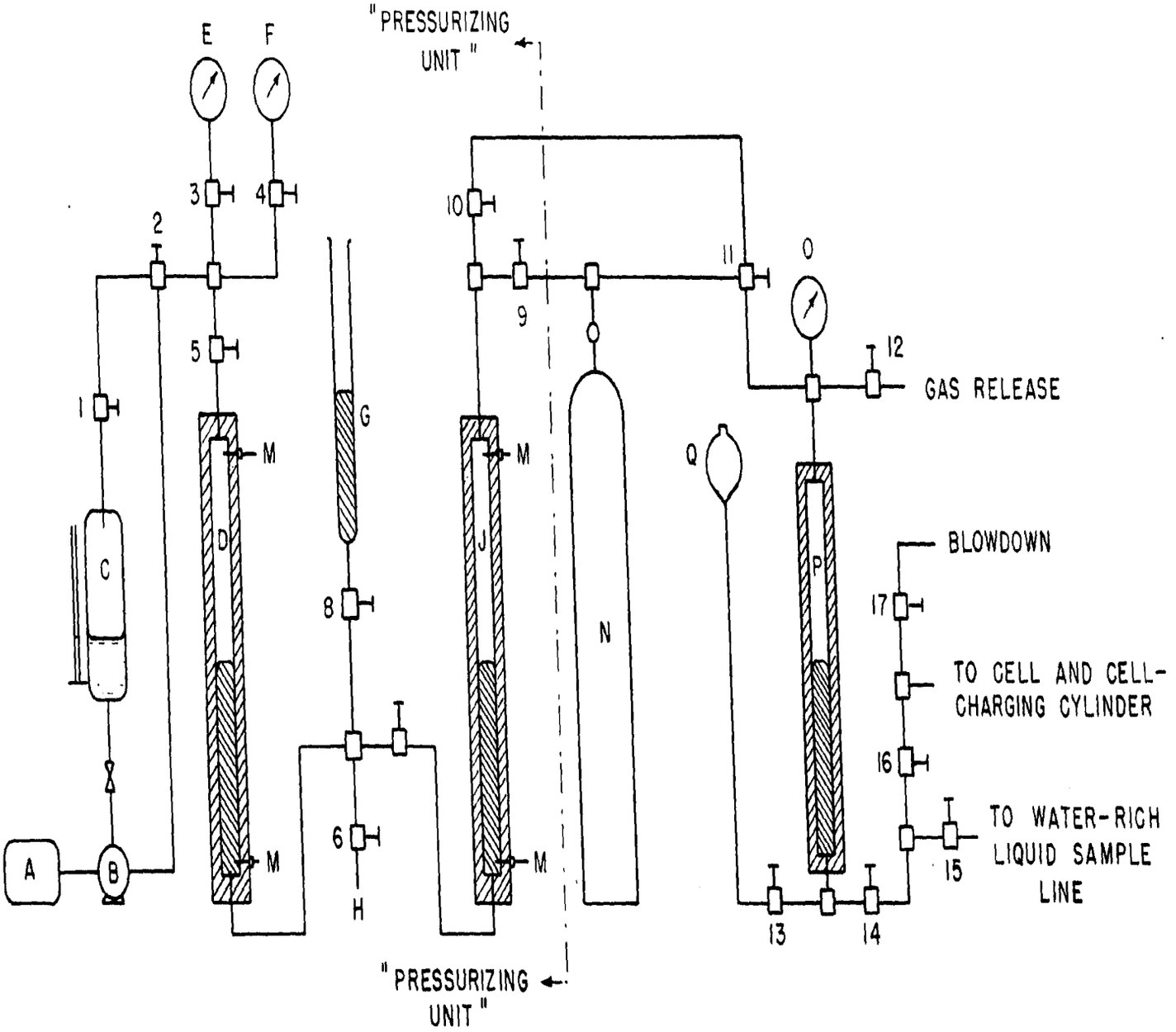
V COOLING WATER

W METRIC SCALE

X AIR INLET

Y MERCURY LEVELLING BULB

FIGURE 27 APPARATUS FOR THE ANALYSIS OF THE WATER-RICH LIQUID PHASE



A VARIABLE SPEED MOTOR
B SIMPLEX OIL PUMP
C OIL RESERVOIR
D OIL-MERCURY CHAMBER
E PRESSURE GAUGE, 0-3000 PSI
F PRESSURE GAUGE, 0-10,000 PSI
G MERCURY CHARGING CYLINDER
H HIGH PRESSURE MERCURY
J MERCURY-GAS CHAMBER
M ELECTRICAL CONNECTORS
N NITROGEN CYLINDER
O PRESSURE GAUGE, 0-5000 PSI
P AUXILIARY MERCURY-GAS CHAMBER
Q MERCURY CHARGING BULB

FIGURE 28 PRESSURIZING AND PRESSURE MAINTENANCE UNIT

EXPERIMENTAL MEASUREMENTS

Temperature Control and Measurement:

The air bath surrounding the equilibrium cell was controlled thermostatically for all temperatures above room temperature. The smaller of two variables load resistance heaters in the air bath was connected to a bimetallic thermoregulator which regulated the temperature at the desired level. For temperatures below room temperature dry ice chips were dropped into the bath to maintain the temperature at a constant value.

The temperature of the cell was measured by means of two calibrated copper-constantan thermocouples inserted well into the walls of the equilibrium cell. The thermocouples were calibrated to 0.1 deg. F in a water bath and in an oil bath with high precision thermometers which are periodically calibrated by the National Bureau of Standards. The temperature of the cell during the course of a run did not vary over 0.3 deg. F up to 200 deg. F and 0.5 deg. F for higher temperatures. The E. M. F.'s of the thermocouples were measured with a Leeds and Northrup High Precision Portable Potentiometer.

Pressure Control and Measurements:

The equilibrium pressures were measured by means of steel tube gauges of the Bourdon type. Gauges of the

following ranges were used: 0–150 psi, 0–1000 psi, and 0–3000 psi. The accuracies are estimated to be: ± 1% of the readings taken with the 0–150 psi gauge, 2/3% of the readings taken with the 0–1000 psi gauge, and 1/2% of the readings taken with the 0–3000 psi gauge.

While equilibrating and sampling, with the aid of the pressurizing and pressure maintenance unit the pressures were maintained, in general, at a given pressure with variations not exceeding the above mentioned accuracies of the gauge readings. For the runs conducted from 2000 to 2800 psi, the pressure during sampling operations was maintained within 2/3% of the equilibrium pressure.

Analytical Weighings:

All analytical weighings were made on Departmental Balance B1–31 using a set of calibrated weights. The weights were calibrated using the method of transposition (49).

Temperature variations in the room were minimized during each run. A counterpoise was used in making the weighings of the U-tube to eliminate, as far as possible, the bouyancy and handling effects. It is believed that the weighings under these conditions were made with an uncertainty not greater than ± 0.2 mg. of the recorded values.

CHEMICALS USED

Propane:

The propane used in this investigation was obtained from the Phillips Petroleum of Bartlesville, Oklahoma. The "Pure Grade Propane" was reported to contain not less than 99 mol % propane. The principle impurities are approximately 0.2% of other hydrocarbons, mainly ethane and isobutane. The sulfur content is probably less than 0.005 wt. % and its vapor pressure at 60 deg. F is 123 psia.

Before charging the propane into the cell, it was run through a high pressure filter consisting of activated carbon, ascarite, sodium hydroxide, and dehydrite.

Distilled Water:

The distilled water, obtained from the departmental source, was boiled several minutes prior to use and injected into the cell while still above 160 deg. F.

Mercury:

Before the mercury removed from the cell was reused, it was cleaned and dried by washing it twice with benzene, then with acetone, and finally by reducing the pressure above the mercury to a few millimeters until all bubbling at its surface ceased. In case the mercury did not present a clean, scum-free surface, it was agitated in the presence

of dilute nitric acid with an air stream for 3 hours. The mercury was then washed with water and dried as before. By a combination of these procedures the mercury was maintained in a clean, dry state.

EXPERIMENTAL PROCEDURE

The experimental procedure was improved and simplified by running each phase completely before going on to the next, both in the 3-phase and the 2-phase regions. The actual order of the determinations was:

(1) 3-phase region:
  (a) vapor phase
  (b) propane-rich liquid phase
  (c) water-rich-liquid phase
(2) 2-phase region:
  (a) propane-rich phases
  (b) water-rich liquid phase

This order was permissible since all the necessary restrictions of the phase rule, constancy of temperature and number of coexisting phases for the 2-phase region, were complied with during each run.

Charging and Equilibrating:

The cell was evacuated and flushed several times with propane gas at the beginning of each series of isothermal runs and whenever the cell was contaminated with other gases. The individual constituents, propane and water, were charged into the cell in such quantities that would satisfy the desired conditions of pressure, temperature, number of phases, and quantity of each phase. The

last requirement was fulfilled so that each phase could be sampled from its assigned port.

Before the beginning of the stirring operation the liquid sampling lines were always filled with clean, dry mercury to displace any liquid present in them and to block off the lines during the agitating period. The water-rich phase sampling line was filled with mercury through valves 13-14-15, Figure 25, and valve S, Figure 27. The propane-rich liquid phase sample line was filled through 1-T_1-2-T_6-T_5-11, Figure 25. The content of the cell was brought to equilibrium under constant conditions of pressure and temperature by the agitation of the stirrer. The period of agitation was from 1-1/2 to 2 hours. Time tests conducted at the outset of the study indicated this to be more than sufficient for attaining equilibrium.

Sampling of the Propane-Rich Phases in the 3-phase Region:

During the sampling operation with 3-phases present, a state of exact equilibrium may not be retained within the cell even though the temperature and pressure are maintained constant. In the 3-phase region changes in the quantities of the phases cannot be detected by pressure measurements. Differential condensation and evaporation can easily take place at constant temperature and pressure while sampling, unless the rate of mercury injection and sampling are precisely equal. Since the two rates could

not be equated with the experimental arrangement used, this difficulty was actually encountered during the 3-phase sampling operations. It was necessary, therefore, to leave the stirrer on continuously while removing the vapor phase from the top of the cell. The vapor-phase sample was removed at the rate of 0.3 moles per hour in the 3-phase region, compared to the general sampling rate of 0.5 moles per hour for the hydrocarbon-rich phases. The rate of stirring was carefully adjusted and the amount of hydrocarbon-rich phase reduced in order to prevent any entrainment of the liquid phases in the vapor sample line. No mercury was injected into the cell while sampling the vapor in the 3-phase region.

A resistance heater was wound around the vapor sampling lines to superheat the vapor leaving the cell. Any condensation of the vapor phase would reduce the carrying capacity of the vapor for water and yield a low concentration for that run. This precaution had to be especially taken in the 3-phase region where condensation can be complete with an undetectable drop below the equilibrium temperature. One heater extended from the top of the cell to the needle valve 16, Figure 25, and another from the latter to the analytical train. The vapor phase was sampled through V and T_4 and expanded down to the pressure of the train at needle valve 16.

In the hydrocarbon-rich liquid phase runs, the amount of water rich phase was reduced and the amount of the former increased. In sampling the hydrocarbon-rich phase mercury was injected into the cell at approximately the same rate that the liquid was being removed in order to minimize the condensation or vaporization taking place within the cell. The quantity of liquid phase present was increased to make this danger less critical. The mercury was injected into the cell through 10-T_2-7-M and the propane-rich liquid phase sampled through L_2-11-12, Figure 25. At needle valve 12 the propane-rich liquid phase was expanded down to the pressure of the analytical train.

In the 2-phase region, the propane-rich phase was sampled through the vapor port while mercury was injected into the bottom of the equilibrium cell. The vapor sample line was turned on slightly to prevent any loss of water during the passage of the sample through the lines, and to hasten the purging of the lines prior to the removal of the sample. The sample was removed from the cell at the rate of about 0.5 moles per hour and passed through the analytical train.

Analysis of the Hydrocarbon-rich Phases:

Preliminary literature studies (42), (27) and experimental work on dehydrite (magnesium perchlorate)

showed that it could be used as an effective drying agent for the quantitative determination of water in propane gas.

Magnesium perchlorate has been known to decompose violently in the presence of hydrocarbon gases for reasons which are not definitely known. High temperatures and the presence of combustible gases are two factors which increase the tendency for the spontaneous decomposition of magnesium perchlorate. This gave an additional reason for sampling the hydrocarbon phases at a slow rate. It gave the drying tubes sufficient time to lose the heat of absorption to the atmosphere. The drying tubes were also shielded from the experimenter in order to protect against explosion hazards.

The effectiveness of magnesium perchlorate as a drying agent under reduced pressure was studied. No loss in weight of previously used drying tubes could be detected after maintaining the pressure at less than 0.1 mercury pressure for 12 hours. Thus, the absorption of water from the propane gas could be conducted under varying pressure conditions, from 0.1 mm mercury to atmospheric pressure.

Propane vapor which had been passed through a series of absorbents, activated carbon, sodium hydroxide, ascarite, and dehydrite under pressure, was then passed through the dehydrite-filled U-tubes to determine its effect on the weight of the U-tubes. Even after the tubes should have

been well "saturated" with propane, the tubes continued to gain a milligram or so of weight. Many materials were tried for the flexible connections, including all kinds of rubber tubing and tygon tubing.

The gain in weight of the U-tubes was traced to the diffusion of water through the tubing into the gas stream, and the subsequent absorption of the water by the magnesium perchlorate. A satisfactory method of treating rubber to prevent diffusion of water to lower concentrations has been developed by Pregl (31). A good grade of india rubber tubing was cut to the desired lengths, aged in 40-50% potassium hydroxide at 60 deg. C for two hours, and steamed for two more hours. The tubing was dried and then placed in pure molten paraffin wax in a flask evacuated on a boiling water bath. As soon as the contents of the flask ceased to foam, air was readmitted into the flask to force the molten paraffin into the interstices of the rubber. Successive evacuations and readmissions of air were made until bubbles were no longer seen on the surface of the tubing. The tubes were drained while warm, wiped on the outside, and on the inside by means of a tobacco pipe cleaner. The tubes were wiped on the inside with glycerine on a pipe cleaner and the excess glycerine removed with a dry pipe cleaner. The treated pieces of rubber tube were stored in a desiccator while not in use. During use it was necessary

to remove the excess paraffin from the ends and the bore of the tubes from time to time with a pipe cleaner.

Before each weighing the U-tubes were flushed with dry air, bled to atmospheric pressure, and the glass connecting stems wiped free of any foreign material. The U-tubes were weighed immediately before and after the sampling operations.

Propane vapors equivalent to two to three times the volume of the stagnant hydrocarbon in the sample line was bled slowly through the train, the two U-tubes being substituted by a glass tubing by-pass. The train and lines were first re-evacuated to valve 16 for vapor phase sampling, or valve 12, Figure 25, for the propane-rich liquid phase sampling, then filled with dry air to atmospheric pressure. The U-tubes were inserted into the train, which was then evacuated to 0.1 mm mercury, the sampling valve opened carefully and the gas adjusted to a satisfactory rate by observing the action of the mercury bubbler. The sample sizes were varied in accordance with the accuracy desired and the amount of phase available for sampling. The variation in the sample sizes was from 0.15 gram mols to 0.9 gram mols.

When the desired amount of propane had been passed through the train, valve 16 or valve 12, Figure 25, depending on the phase being sampled, was closed. The train was allowed to fall back to room temperature and the final

temperature and pressure of the gas in the isochoric bottle read on manometer K, Figure 26. The train was then evacuated, and the U-tubes flushed and filled with dry air. The drying tubes were removed from the train, cleansed, bled to the atmosphere, and weighed as before. The gain in weight of the U-tubes represented the water absorbed from the propane gas collected in the train.

Analysis of the Water-Rich Phase:

The water-rich sample was displaced slowly at the equilibrium pressure and temperature through valves 15-14-13, Figure 25, and expanded at valve S, Figure 27, to atmospheric pressure. The flashed gas and liquid were collected in the gas burette, U, Figure 27. The mercury levelling bulb was adjusted continually to maintain the gas pressure in the burette at precisely the pressure of the atmosphere.

Valve 14, Figure 25, was closed when the desired amount of sample was displaced from the cell, and the sample in the lead lines from valve 14, Figure 25, to valve S, Figure 27, allowed to cool to room temperature. Then valve S was opened slowly to allow the liquid in the lead lines to expand to atmospheric pressure. Finally, mercury was introduced through valve 13, Figure 27, to displace all the liquid and gas in the lead lines into

the burette. In this way, any gas leaving the water-rich phase before valve S, was ultimately caught in the gas-water burette. The magnitude of the error caused by the neglect of this procedure was found to be quite appreciable for any runs conducted above or below room temperature, especially those at high temperatures.

PART III

APPENDIX

LABORATORY DATA AND SAMPLE CALCULATIONS

Propane-Rich Phases:

The data tabulated during the course of a run in the determination of the propane-rich phases were:

1. Cell conditions:
   (a) Equilibrium pressure
   (b) Thermocouple E.M.F. at end of stirring period and at the end of the sampling period
2. Room conditions:
   (a) Barometric pressure
   (b) Room temperature
3. Analytical Train Conditions:
   (a) Initial and final gas pressure
   (b) Initial and final train temperature
   (c) Initial and final U-tube weights
   (d) Analytical train volume

The molecular weight of water was taken to be 18.02. A compressibility factor chart for pure propane gas at several probable values of room temperature up to 800 mm. mercury pressure was prepared and applied to convert pressure-volume-temperature data to moles of propane. Figure 29 shows $Z = PV/nRT$ as a function of pressure for several temperatures.

Corrections or conversion factors applied to the tabulated data were as follows:

(1) Gauge readings converted to absolute pressure, psia

(2) Thermocouple E.M.F., millivolts, converted to temperature, deg. F. using Figure 31.

(3) Calibrations applied to thermometer readings

(4) Temperature corrections applied to manometer readings

(5) Weight calibrations applied to U-tube weights

(6) Barometer corrections applied to barometric readings

The Corrected Laboratory Data and Sample Calculations for Run No. 128 is presented below.

Corrected Laboratory Data:

Equilibrium pressure = 823 psia

Equilibrium temperature = 230.1 deg. F

Barometric pressure = 734.1 mm mercury

Room temperature at analytical balance = 84.6 deg. F

Pressure rise in train, ΔP = 734 mm mercury

Train temperature, T, = 547.5 deg. R

Weight of water absorbed = 0.11727 gms

Compressibility factor, Z, = 0.986

Volume of train, V, = 11,950 cc

Gas constant, R, = 34.65 mm mercury, cc. per gm.-mol, deg. R

Calculations:

$$\text{Gm.-mols anhydrous propane} = \frac{P\ V}{Z\ R\ T}$$

$$= \frac{(734)\ (11,950)}{(0.986)(34.65)(547.5)}$$

$$= 0.4689 \text{ mols}$$

Gm.-mols water $= \frac{\text{gms. water}}{18.02}$

$= \frac{0.11727}{18.02}$

$= 0.00651$

Mols water plus propane $= 0.4754$

Mol Fraction water $= 0.01369$

The calculated data for the propane-rich phases in the 2-phase region were corrected for small deviations of the temperature from the exact temperature of the isotherm by evaluating $\left[\frac{dy_1}{dT}\right]_P$ from the unadjusted data and applying it to the calculated points. In the expression above,

y_1 = mol fraction of water in the propane-rich liquid or vapor phase

T = temperature

P = pressure

These adjusted data are termed "Experimental Points" in this work.

Water-Rich Phase:

The data tabulated during the course of a run in the determination of the water-rich phase were:

1. Cell conditions:
   (a) Equilibrium pressure
   (b) Thermocouple E.M.F. at equilibrium and at the end of the sampling period
2. Room conditions:
   (a) Barometric pressure
   (b) Room temperature

3. Analytical Apparatus:

(a) Burette jacket temperature

(b) Final burette reading of water-gas interface

(c) Final burette reading of water-mercury interface

Temperature, pressure, barometric, and burette volume corrections were applied to the tabulated data. The burette volume calibration is given in Figures 32 and 33. The values of Henry's Law constants for propane dissolved in water are plotted over the necessary temperature range on Figures 32 and 33.

The corrected laboratory data and sample calculations for the water-rich phase for Run 232 are given below.

Corrected Laboratory Data:

Equilibrium pressure = 1128 psia

Equilibrium temperature = 230.2 deg. F

Barometric pressure = 736.6 mm mercury

Room temperature = 87.2 deg. F

Burette jacket temperature = 86.6 deg. F

= 546.2 deg. R

Volume of equilibrium flash gas, V_2 = 31.22 cc

Volume of equilibrium flash liquid, V_1 = 67.26 cc

Henry's Law constant, $K = \frac{P}{N} = 28.8 \times 10^6$

where P = partial pressure of propane in mm of mercury

N = mol fraction of propane in water

Compressibility factor, Z, = 0.9865

Partial pressure of water in flash gas at 86.6 deg. F = 32.0 mm mercury

Partial pressure of propane in flash gas, P = 704.6

Density of flash liquid at 86.6 deg. F, ρ = 0.9956 gms/cc

Calculations:

$$\text{Gm.-mols propane in the flash gas} = \frac{P\ V_2}{Z\ R\ T}$$

$$= \frac{(704.6)\ (31.22)}{(.9865)(34.65)(546.2)}$$

$$= 0.001178$$

Mols water in the flash gas is negligible as far as the material balance for water is concerned.

$$\text{Gm.-mols water in flash liquid} = \frac{V_1 \rho}{18.02}$$

$$= \frac{(67.26)(0.9956)}{18.02}$$

$$= 3.716$$

Gm.-mols propane dissolved in flash liquid

$$= (\text{mols flash liquid})\ \frac{P}{K}$$

$$= \frac{(3.716)(704.6)}{(28.8 \times 10^6)}$$

$$= 0.0000909 \text{ mols}$$

$$\text{Mol fraction propane} = \frac{\text{mols propane}}{\text{total mols}}$$

$$= \frac{0.0012589}{3.717}$$

$$= 0.0003417 \text{ mol fraction propane}$$

The calculated data for the water-rich phase in the 2-phase region were corrected for small deviations of the temperature from the exact temperature of the isotherm by evaluating $\left[\frac{dx_2}{dT}\right]_P$ from the unadjusted data and applying it to the calculated points. In the expression above,

x_2 = mol fraction propane in the water-rich phase

T = temperature

P = pressure

These adjusted data are termed "Experimental Points" in this work.

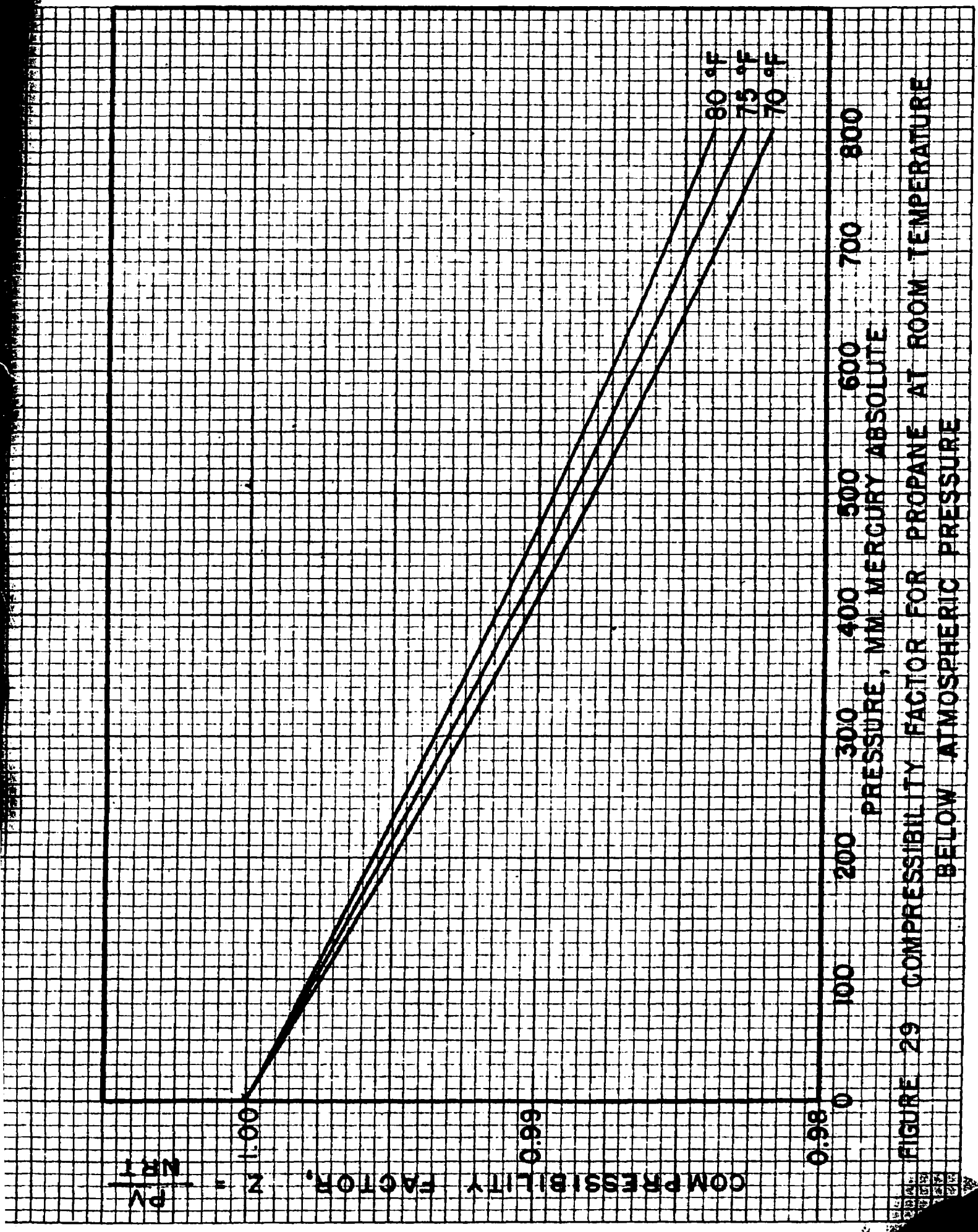


FIGURE 29 COMPRESSIBILITY FACTOR FOR PROPANE AT ROOM TEMPERATURE BELOW ATMOSPHERIC PRESSURE

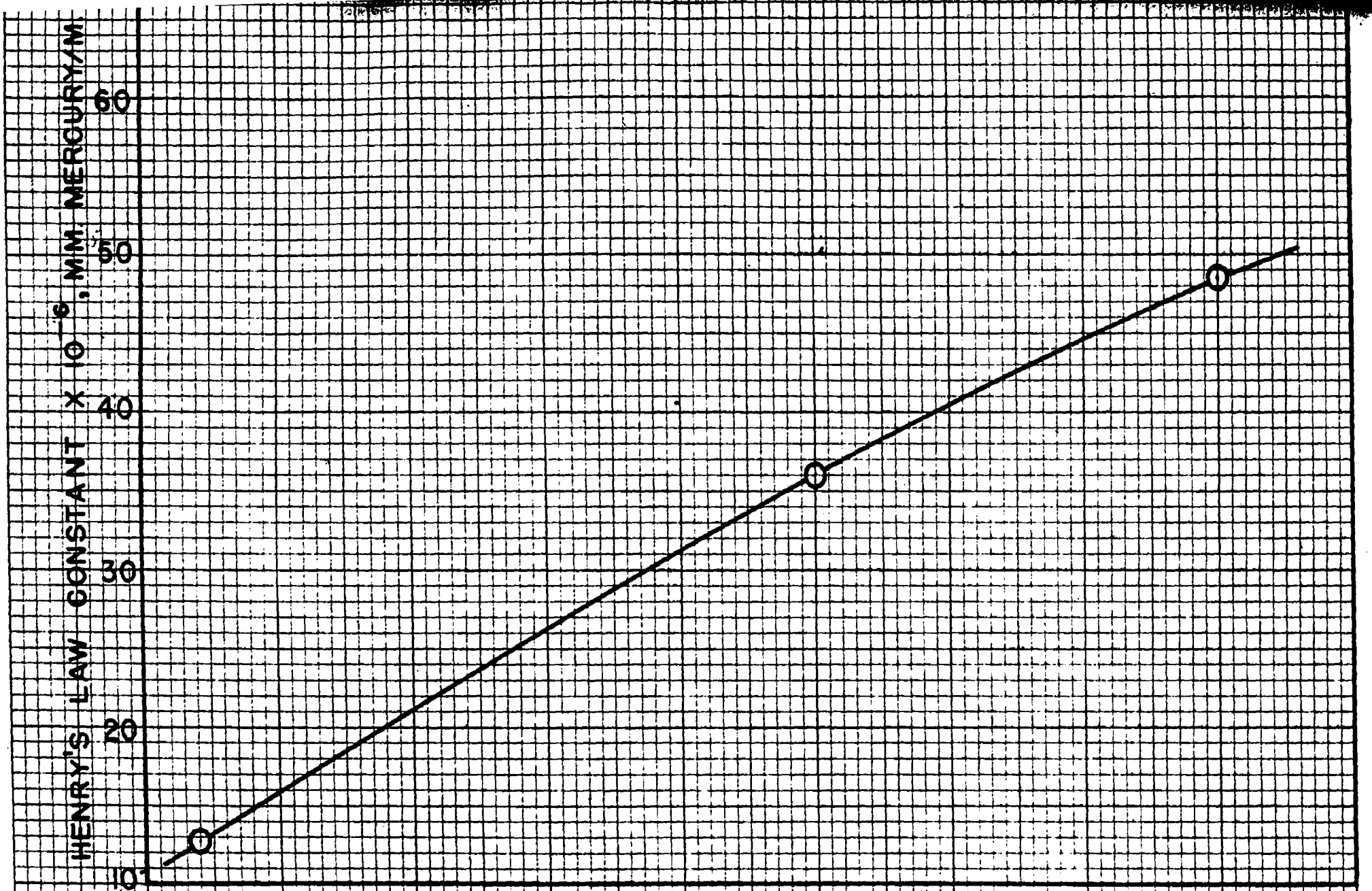


FIGURE 30 HENRY'S LAW CONSTANTS FOR THE SOLUBILITY OF PROPANE IN WATER

CALIBRATIONS

Pressure Gauge Calibrations:

Three steel tube Bourdon pressure gauges were used in this investigation.

Dept. No.	Range
C2-309	0-150 psi
C2-98	0-1000 psi
C2-100	0-3000 psi

The gauges were calibrated at the beginning of the investigation and several times during its course by means of the dead weight tester in the Sohme Precision Laboratory at the University of Michigan.

Thermocouple Calibrations:

Three thermocouples were used in the course of the experimental work. Their locations were as follows:

Thermocouple No.	Position
1	Top right side, in wall of equilibrium cell
2	Vapor phase sample line
3	Bottom left side, in wall of equilibrium cell.

The calibration curves for the copper-constantan thermocouples are presented in Figure 31.

Calibration of Analytical Weights:

The analytical weights used in the fine weighings made in this investigation were calibrated using the method of transposition (49). The calibrations of the weights were made against standard weights in the Sohma Laboratory. The calibrations of the weights are believed to be accurate to 0.05 mg.

Calibration of Gas-Water Burette:

The burette was calibrated by weighing the amount of mercury drained from the burette and taking the corresponding burette readings. The calibration curves for the burette are given in Figures 32 and 33.

Volume Calibration of the Analytical Train for the Analysis of the Hydrocarbon-Rich Phase:

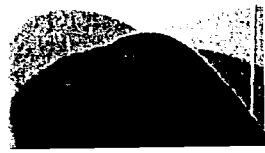
The volume of the train was determined in three sections whose volumes were as follows:

Section	Location	
1	Volume from last needle valve to 1st U-tube	214 cc*
2	Volume of drying tubes filled, bubbler, and lines to bottle	169 cc
3	Volume of bottle in place	11,567 cc
Total Volume		11,950 cc

Sections 1 and 2 were calibrated by noting the pressure change accompanying the expansion of gas in sections 1

*Note: For runs in which the water concentration exceeded 5 mol % water, the volume of the hydrocarbon was taken to be the total train volume minus the volume of water vapor in Section 1.

and/or 2 into a third evacuated chamber of known and comparable volume. A simple pressure-volume-temperature relationship was set up to compute the volume of the unknown sections of the train. Section 3 was calibrated by finding the weight of water contained in the bottle when filled.



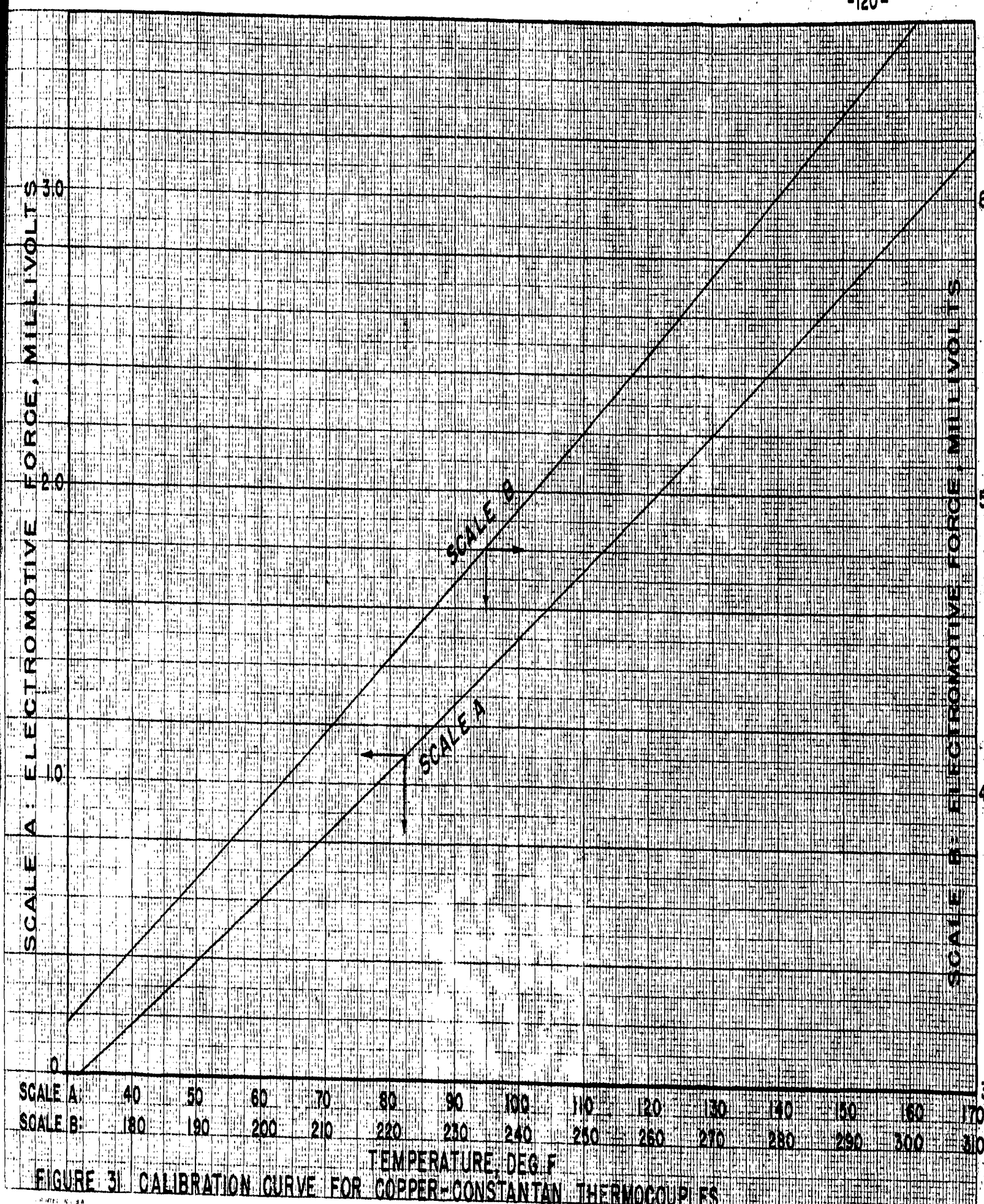


FIGURE 31 CALIBRATION CURVE FOR COPPER-CONSTANTAN THERMOCOUPLES

EUGENE DIETZGEN CO. NO. 346 D

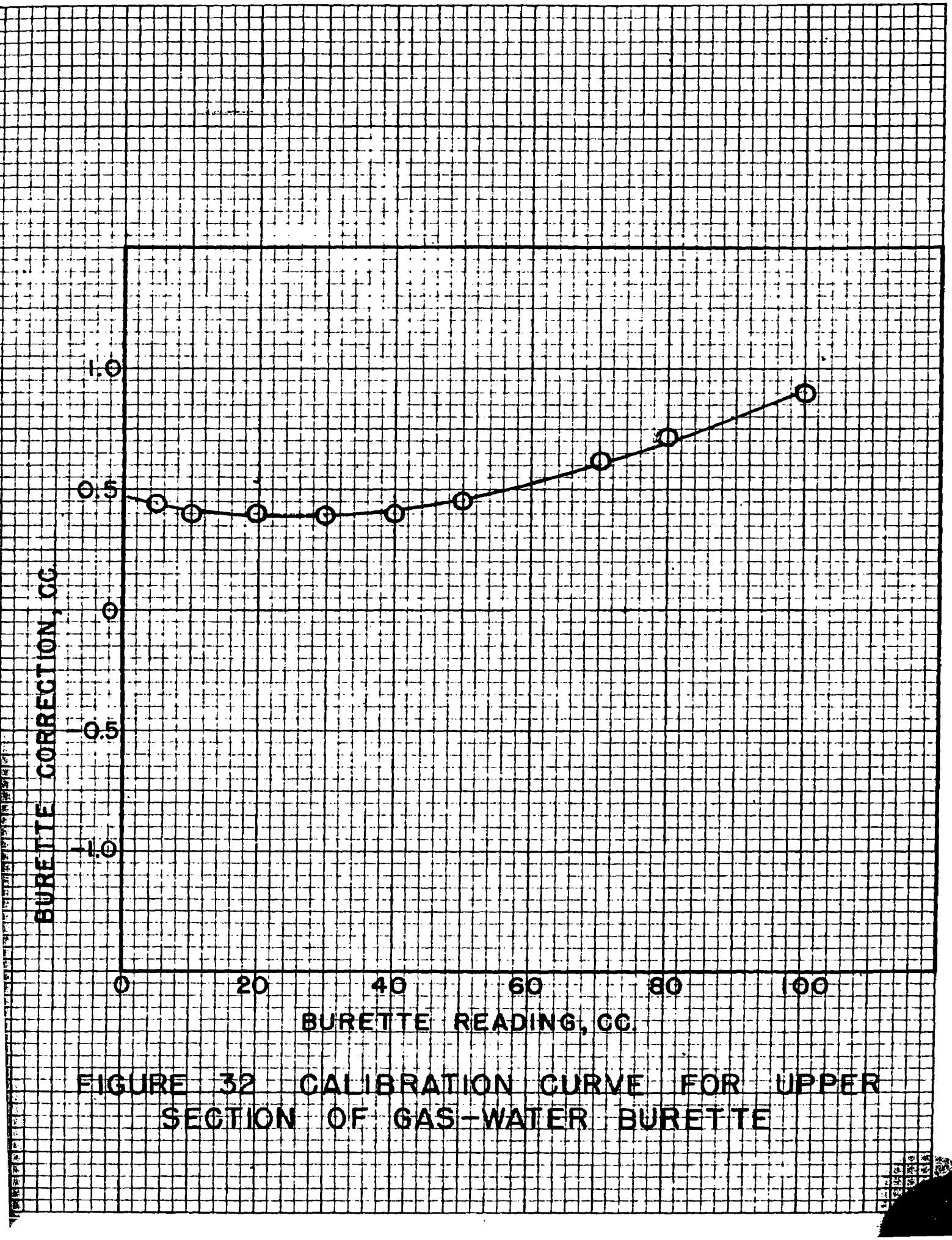


FIGURE 32 CALIBRATION CURVE FOR UPPER SECTION OF GAS-WATER BURETTE

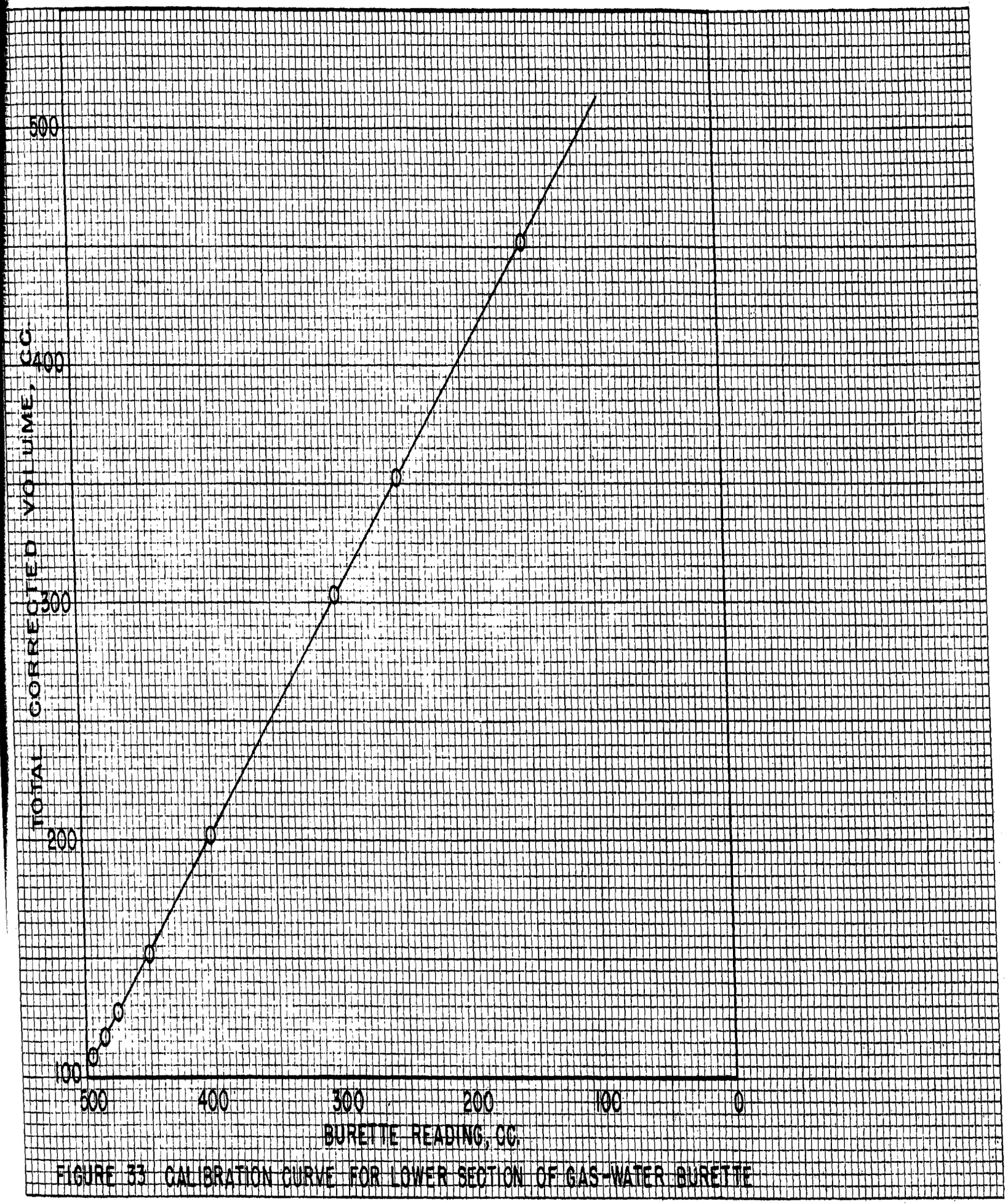


FIGURE 33 CALIBRATION CURVE FOR LOWER SECTION OF GAS-WATER BURETTE

BIBLIOGRAPHY

1. Adams, L.H., J. Am. Chem. Soc. 53, 3769, (1931)
2. Aroyan, H.J., Ph.D. Thesis, Univ. of Michigan (1949)
3. Bartlett, E.P., J. Am. Chem. Soc. 49, 65, (1927)
4. Billman, Sage, and Lacey, A.I.M.E. Trans. 174, 13, (1927).
5. Brown, Katz, Oberfell, and Alden, "Natural Gasoline and the Volatile Hydrocarbons", Section I, Chap. II, Midwest Printing Co., Tulsa, Okla.
6. Carson and Katz, A.I.M.E. Trans. 146, 150, (1942)
7. Chaddock, R.E., Ph.D. Thesis, Univ. of Michigan (1940)
8. Clifford, C.W., Ind. Eng. Chem. 13, 631, (1921)
9. Culberson, Horn, and McKetta, A.I.M.E. Trans. 189, 1, (1950)
10. Culberson and McKetta, A.I.M.E. Trans. 189, 319, (1950)
11. Culberson and McKetta, Private Communications, Univ. of Texas (1950)
12. Deaton and Frost, Am. Gas Assoc. Proc., Nat. Gas Dept., pp 122, (1940)
13. Deaton and Frost, Proc. Am. Gas Assoc. pp. 143, (1941)
14. Dodson and Standing, Proc. A.P.I., Drilling and Prod. Pract., pp. 173, (1944)
15. Dourson, Sage, and Lacey, A.I.M.E. Trans. 151, 206, (1943)
16. Goodman and Krase, Ind. Eng. Chem. 23, 401, (1931)
17. Griswold and Kasch, Ind. Eng. Chem. 34, 804, (1942)
18. Hammerschmidt, E.G., Ind. Eng. Chem. 26, 851, (1934)
19. Hanson, G.H., Ph.D. Thesis, Univ. of Michigan (1942)
20. Krichevsky and Kasarnovsky, J. Am. Chem. Soc. 57, 2168, (1935)

BIBLIOGRAPHY (Cont.)

21. Kuenen, J.P., Proc. Roy. Soc. Edinburgh, 23, 312, (1900)

22. Kuenen, J.P., "Verdampfung and Verflussing von Gemischen", Johann Ambrosius Barth, Leipsig, pp. 82, (1906)

23. Larsen and Black, Ind. Eng. Chem. 17, 714, (1925)

24. Lauhlere and Briscoe, Proc. Pacific Coast Gas Assoc., 30, 121, (1939)

25. Lebeau, Compt. Rend. (de l'institut de France) 140, 1454, 1572, (1905)

26. Lewis and Randall, "Thermodynamics" McGraw Hill Book Co., Inc., N.Y., (1923)

27. McKetta, J.J., Ph.D. Thesis, Univ. of Michigan (1946)

28. McKetta and Katz, A.I.M.E. Trans. 170, 34, (1947)

29. McKetta and Katz, Ind. Eng. Chem. 40, 853, (1948)

30. Olds, Sage and Lacey, Ind. Eng. Chem. 34, 1223, (1942)

31. Pregl (translated by Grant), "Quantitative Organic Microanalysis", pp. 36, The Blakiston Co., Phila. (1946)

32. Reamer, Olds, Sage, and Lacey, Ind. Eng. Chem., 35, 790, (1943)

33. Reamer, Olds, Sage, and Lacey, Ind. Eng. Chem., 36, 381, (1944)

34. Roberts, Brownscombe, and Howe, Oil and Gas Journal, 39, 37, (1940)

35. Russell, Thompson, Vance, and Huntington, A.I.M.E. Trans., 160, 151, (1945).

36. Saddington and Krase, J. Am. Chem. Soc. 56, 353, (1934)

37. Sage, Hicks, and Lacey, A.P.I. Drill. and Prod. Prac. pp. 386, (1938)
Ref. and Nat. Gaso. Mfr. 17, 350, (1938)

BIBLIOGRAPHY (Cont.)

38. Sage and Lacey, A.P.I. Drill. and Prod. Prac., pp. 308, (1941)

39. Sage and Lacey, "Thermodynamic Properties of Hydrocarbons", American Petroleum Institute, New York

40. Scheffer, F.E.C., K. Akad. Wet., Proc. 16, 404, (1913).

41. Scheffer, F.E.C., K. Akad. Wet. Proc. 17, 834, (1914)

42. Smith, G.F. "Dehydration Studies Using Anhydroud Magnesium Perchlorate", a pamphlet by the G.F. Smith Co., Columbus, Ohio

43. Souders, Selheimer, and Brown, Ind. Eng. Chem., 24, 517, (1932)

44. Villard, Compt. rend. 106, 1602, (1888)

45. Wiebe and Gaddy, J. Am. Chem. Soc., 59, 1984, (1937)

46. Wiebe and Gaddy, J. Am. Chem. Soc., 61, 315, (1939)

47. Wiebe and Gaddy, J. Am. Chem. Soc., 62, 815, (1940)

48. Wilcox, Carson, and Katz, Ind. Eng. Chem., 33, 662, (1941)

49. Willard and Furman, "Elementary Quantitative Analysis", pp. 59, D. Van Nostrand Co., Inc., New York, (1940)